

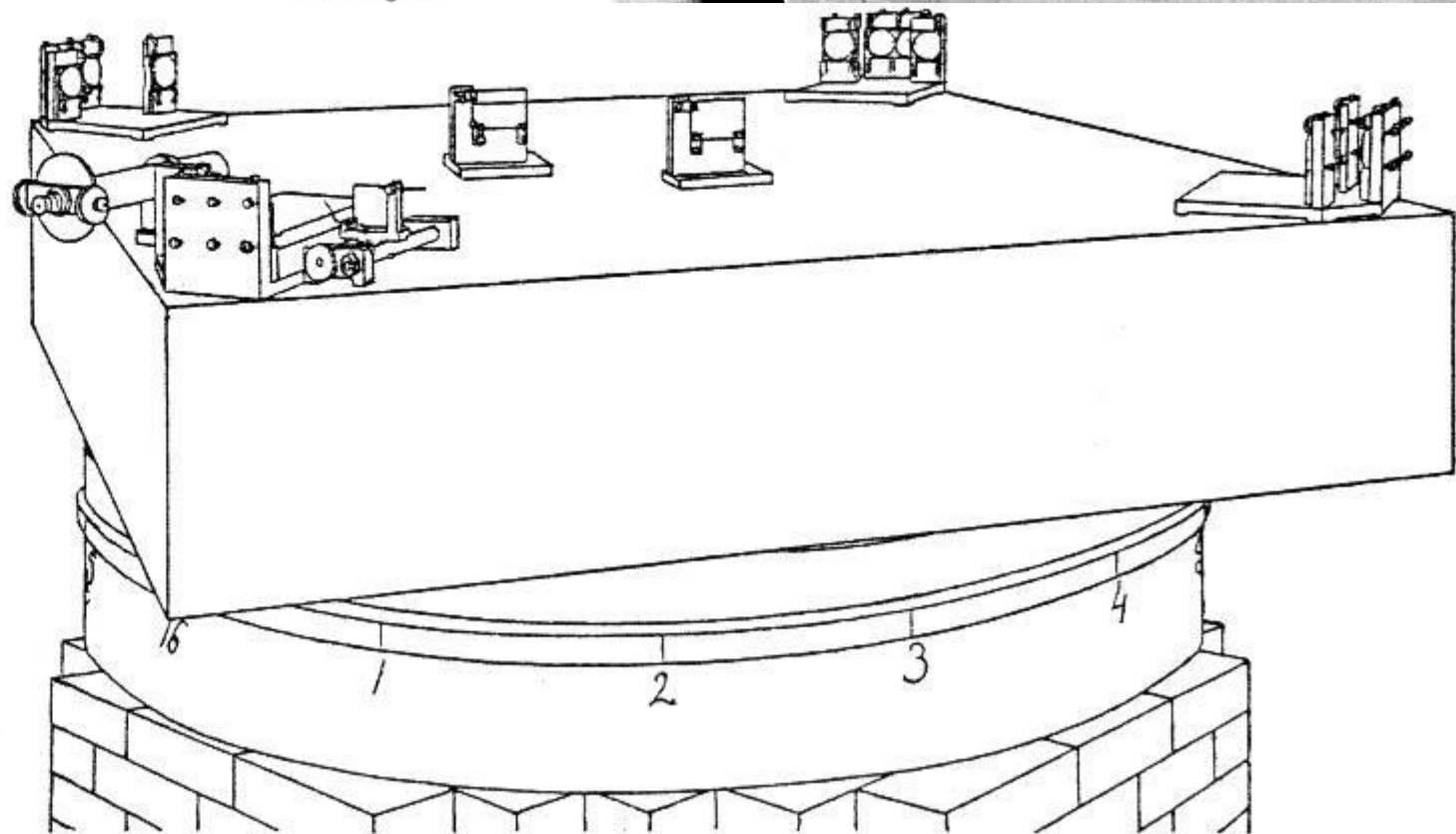
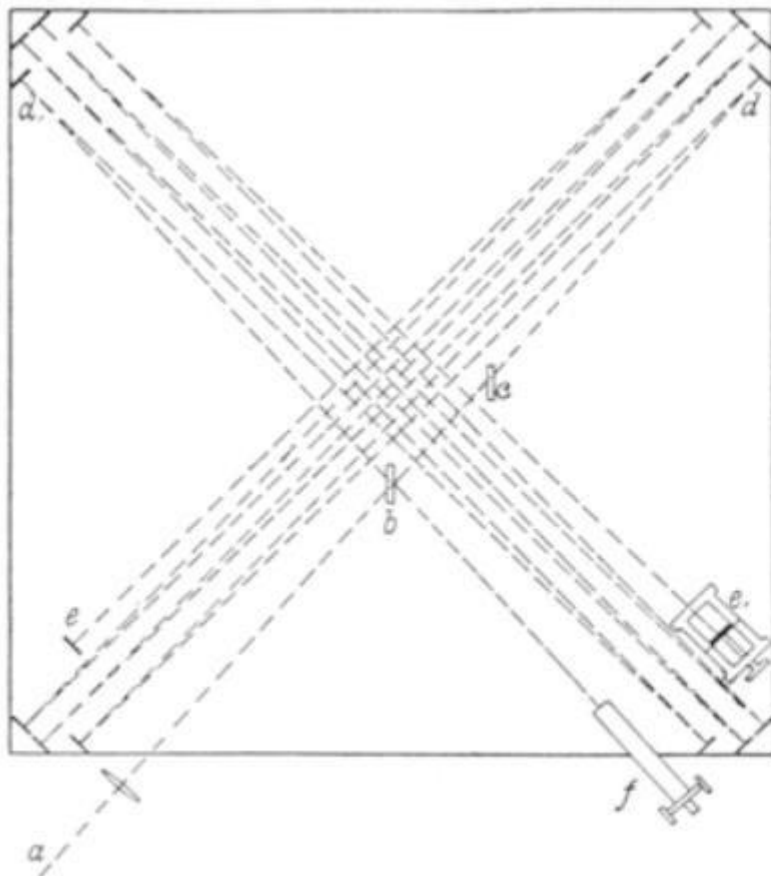
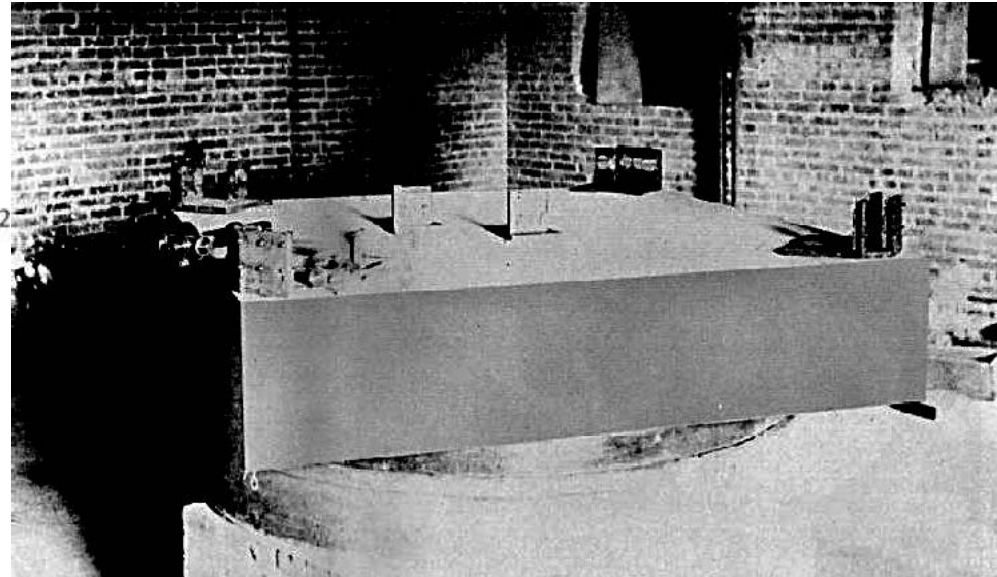
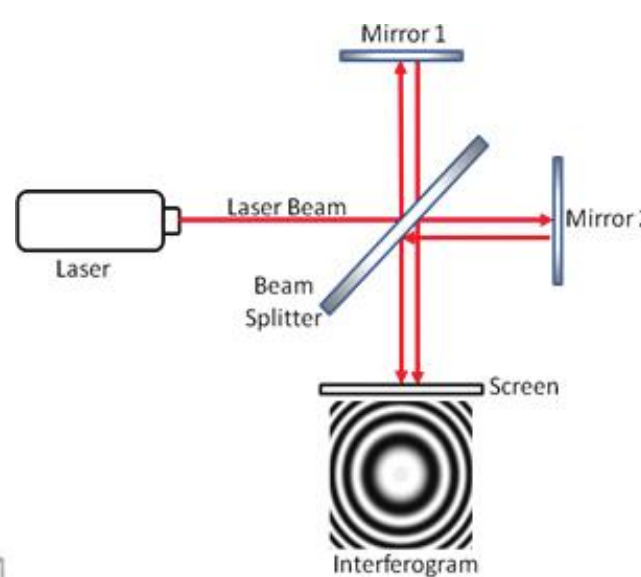
Gravitational wave detection in space: status and outlook

Wei-Tou Ni

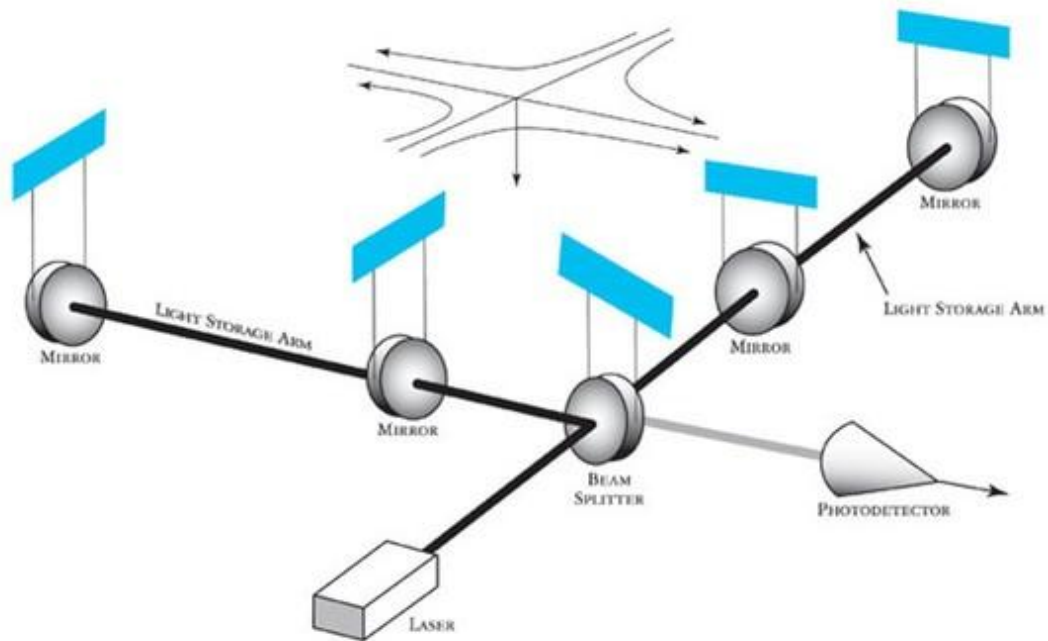
ICTP-AP, UCAS, Beijing 100049, China

Innovation Academy of Precision Measurement Science and Technology (APM), Chinese Academy of Sciences, Wuhan, China

Michelson Interferometry 迈克尔逊干涉



Generalized Michelson Int. 广义的迈克尔逊干涉



Earth-based Fabry-Perot
Michelson Interferometric GW
Detector

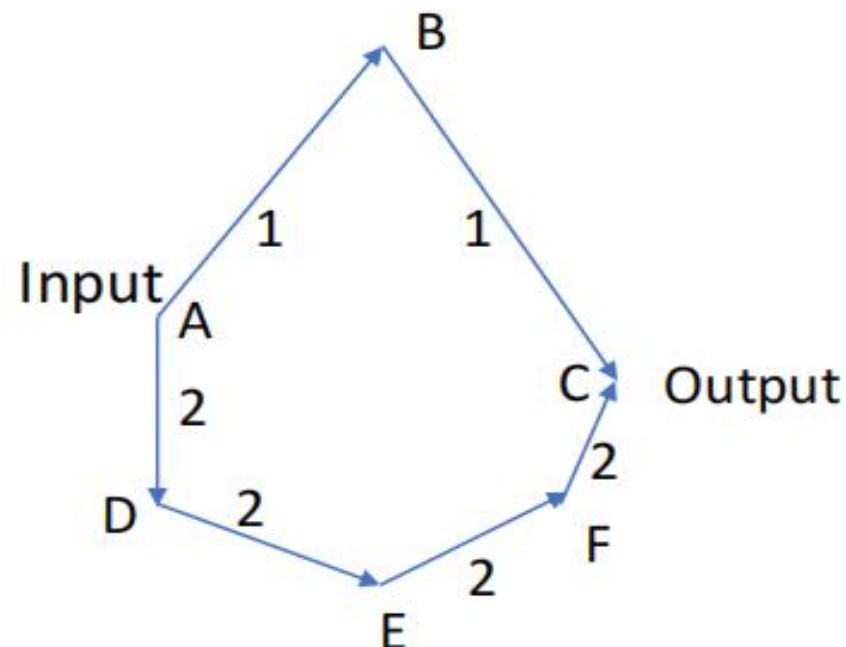
SPACE: Match the Path 1 and Path 2

空间：光路径1, S/C A -->S/C B --> S/C C

光路径2, S/C A -->S/C D --> S/C E

-->S/C F -->S/C C

匹配 光路径 1 和光路径 2 之光程



Master equation for space laser interferometry (1)

- In the **original white-light Michelson interferometry**, the two interferometric **paths (two arms)** must be **almost equal to have fringes** (Michelson 1880s). With light of **very narrow line**, the **match can be relaxed a bit** (e.g., Michelson and Gale 1927).
- For laser light, the interferometry goes further, and **the fringes would manifest for a difference of optical paths within the laser coherent length**. For **Nd:YAG laser of 1 kHz line width**, the **two optical length path can differ by 100 km** and still be coherent to interfere with each other. However, **the closer the path lengths are matched to each other, the clearer the fringes are** (less noise).
- In space, because of large distances involved, at the receiving S/C, we have **to phase lock the local laser oscillator to the weak incoming beam to transmit to another S/C or back**; **the interferometry measures the final phase of interference of the two chosen paths**. The final phase noise $\delta\phi_{\text{interference}}$ of interference at the receiving S/C is
- **$\delta\phi_{\text{interference}} = 2\delta\nu(f)L/c + \text{phase locking noise}(s) + \text{timing noise}(s) + \text{signals \& other noises}$ accrued along the two paths,** (1) -- Master equation

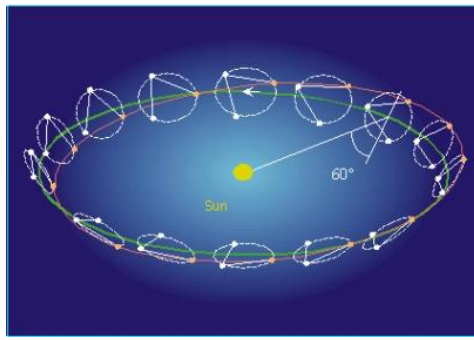
Master equation for space laser interferometry (1)

- where $\delta\nu(f)$ is the frequency noise of the laser source at frequency f , L is the optical pathlength difference of the two chosen paths, and c the light velocity.
- Hence for decreasing the interference phase noise $\delta\phi_{\text{interference}}$, we have to either decrease the frequency noise of the laser source or decrease the pathlength difference, or both.
- After the vast distance travelled, the light received by the telescope in the other S/C is attenuated greatly and needs amplification to go to another S/C. The way of amplification is using a local laser to phase-lock to the incoming weak laser light.
- Hence the phase information is transmitted in contiguous propagation whether in homodyne or with a known frequency offset.
- **The measured phase by the phasemeter is recorded with a time tag for later propagation-identification in the data analysis. This time-tagged tracing after the recording is called time-delay interferometry (TDI).**
- **The first generation Michelson TDI is usually called X, Y and Z TDIs. We call the original (zeroth generation) Michelson topology the X0, Y0 and Z0 TDIs. Both phase-locking and time-tagging contribute noises. TTL (tilt-to-length) noise etc are included in the other noises.**

OUTLINE

- **Introduction – A Brief history, Generalized Michelson Interferometry (GMI)**
- **Space laser GMI Gravitational Wave (GW) Detection**
- **Space low frequency GW detection - mHz & μ Hz**
- **Space middle frequency GW detection - 0.1 Hz to 10 Hz**
- **Research directions**

Introduction



- 1910: discovery of white dwarfs
- Einstein 1916: quadrupole radiation power

$$A = (\kappa/24\pi) \sum_{\alpha\beta} (\partial^3 J_{\alpha\beta} / \partial t^3)^2$$

$J_{\alpha\beta}$ moment of inertia

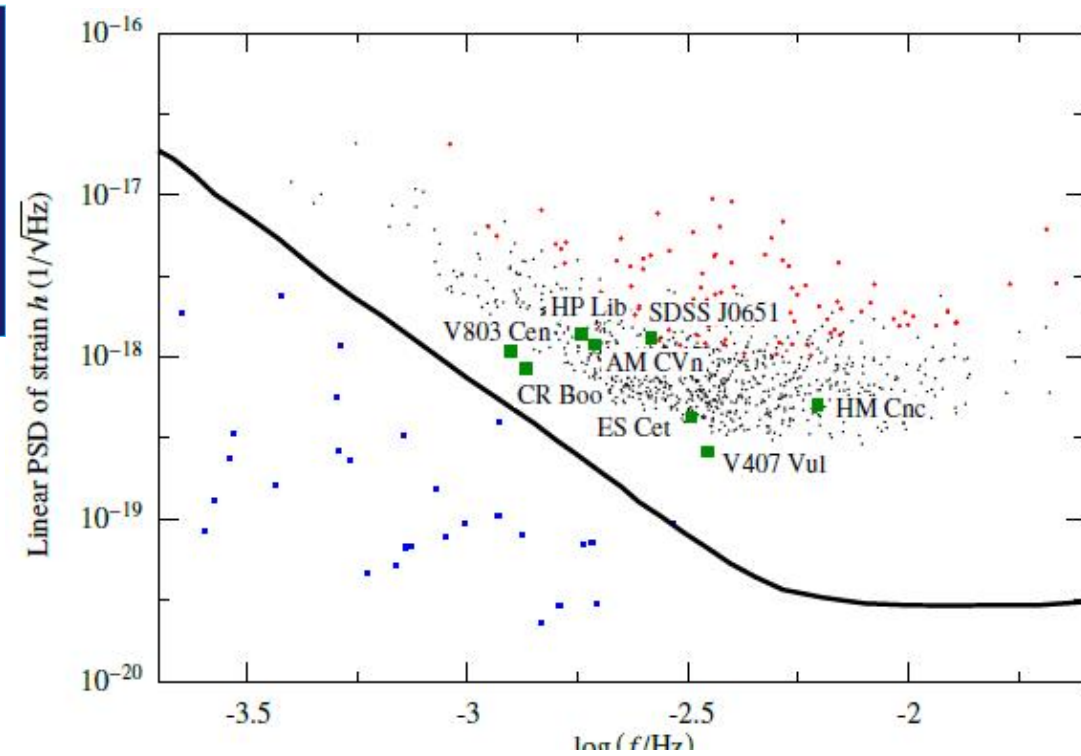
$\kappa = 8\pi G_N$; G_N Newton constant

- Einstein 1918: $J_{\alpha\beta} \rightarrow [J_{\alpha\beta} - (1/3) \text{Tr}(J_{\alpha\beta})]$;
 $\kappa/24\pi \rightarrow \kappa/80\pi$ [i.e., $\times (3/10)$]

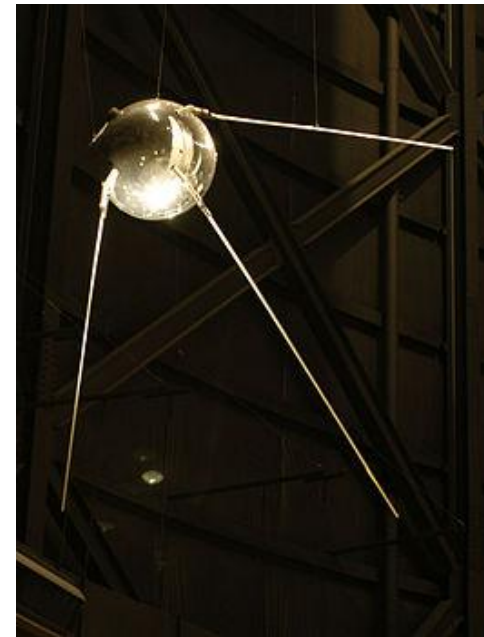
- $\times 2 \rightarrow$ correct quadrupole radiation (e.g., Landau-Lifshitz 1941)
- WDB GW background -- now called also confusion limit.

[close WDB period: 5.4 minutes (HM Cancri) to a few hours]

- first satellite of human kind **Sputnik** 1957 launch.



92 days
1440 orbits
83.60 kg mass



Weber Bar (57 Years ago)

棒状探测器与共振探测

- OBSERVATION OF THE THERMAL FLUCTUATIONS OF A GRAVITATIONAL-WAVE DETECTOR* J. Weber

PRL 1966 (Received 3 October 1966)

Strains as small as a few parts in 10^{16} are observable for a compressional mode of a large cylinder. 改进了10个量级

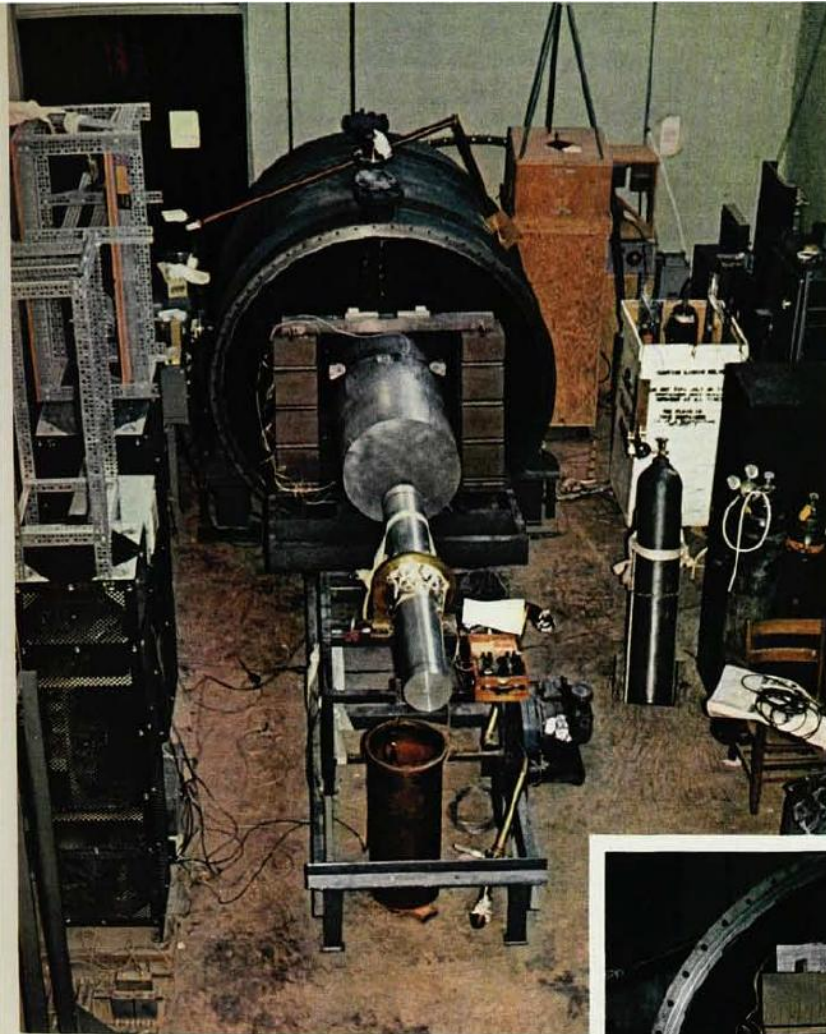
- GRAVITATIONAL RADIATION* J. Weber

PRL 1967 (Received 8 February 1967)

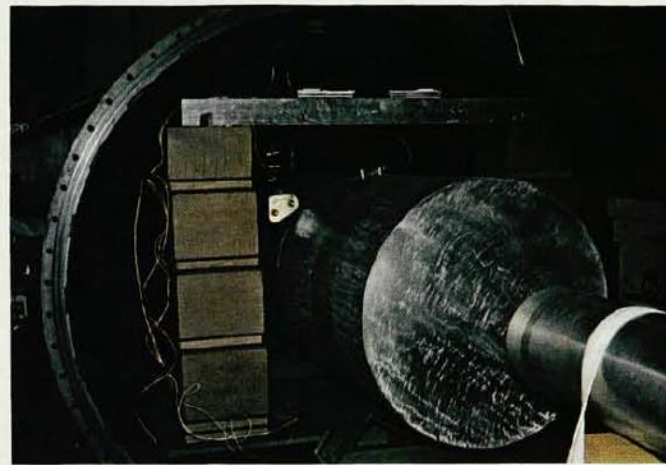
- The results of two years of operation of a 1660-cps gravitational-wave detector are reviewed. The possibility that some gravitational signals may have been observed cannot completely be ruled out. New gravimeter-noise data enable us to place low limits on gravitational radiation in the vicinity of the earth's normal modes near one cycle per hour, implying an energy-density limit over a given detection mode smaller than that needed to provide a closed universe.



UNIVERSITY OF MARYLAND

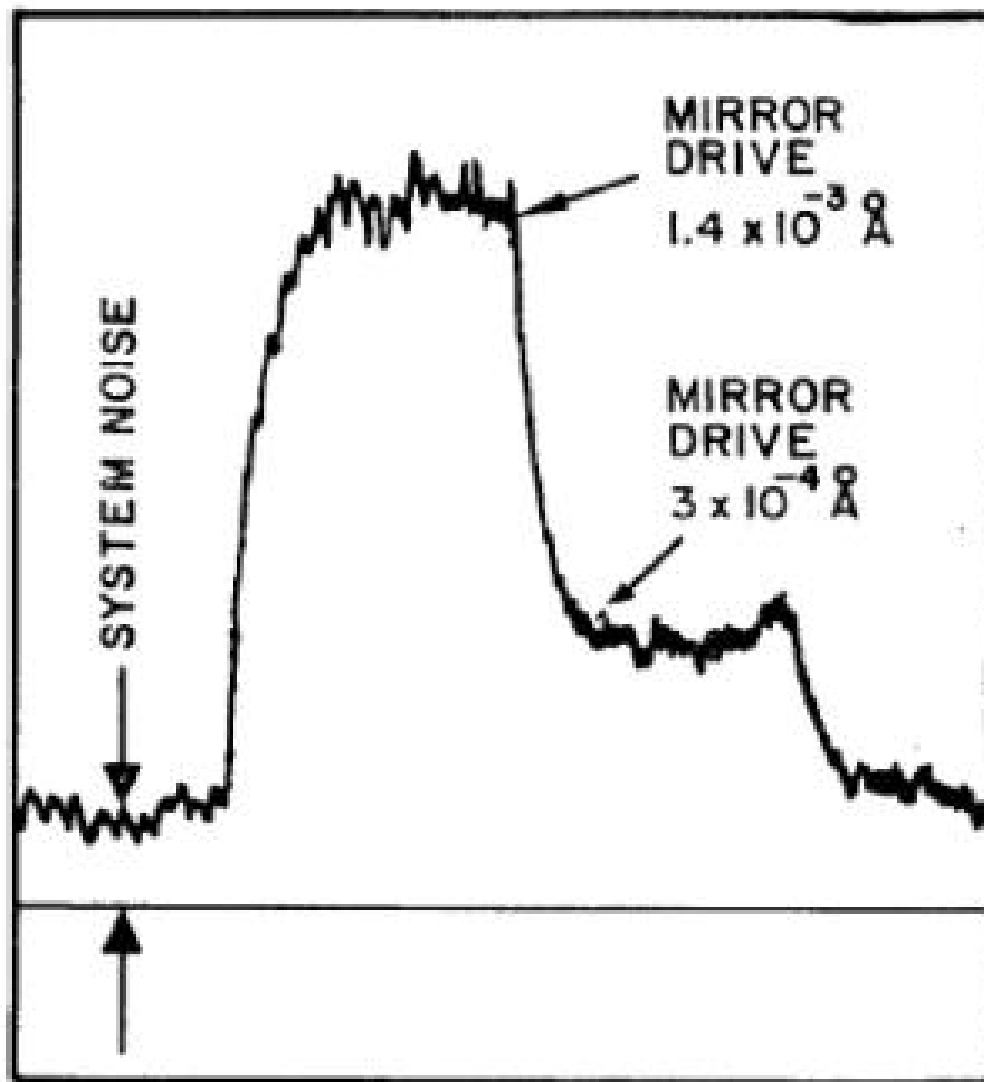


ALUMINUM CYLINDER of 1400-kg mass is suspended by a wire on acoustic filters. Piezoelectric transducers are bonded to the top surface, as shown in the closeup.

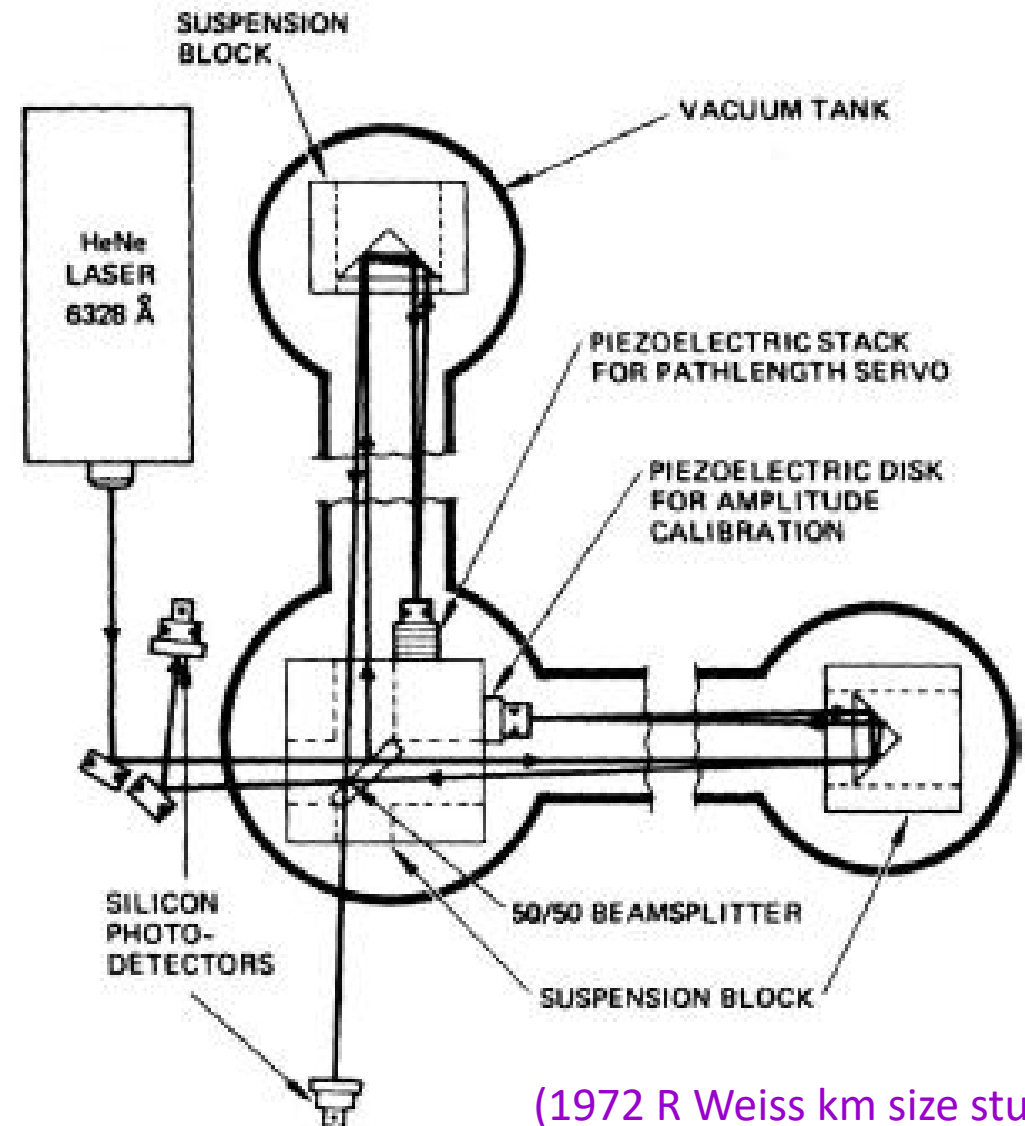


DETECTOR and dynamic gravitational field generator are shown removed from their common vacuum chamber.

noise 1971 at 5 kHz



Malibu laser interferometer 1978

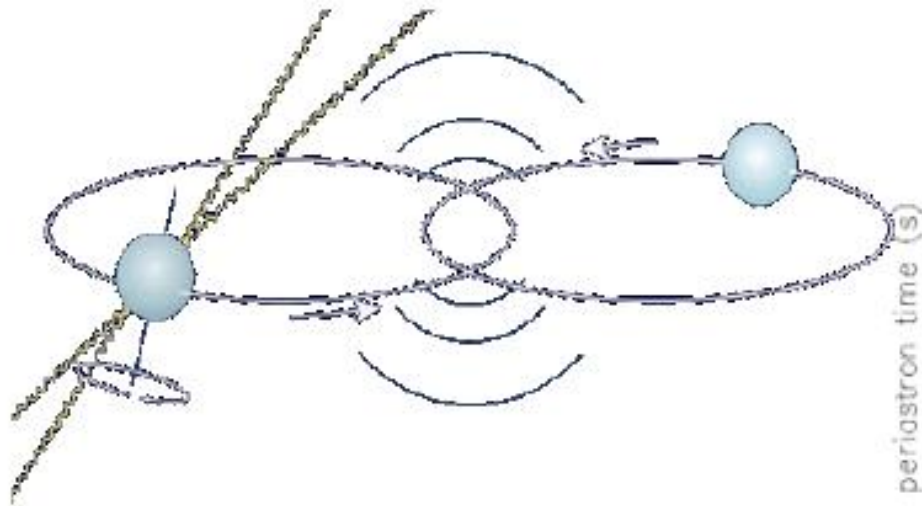


(1972 R Weiss km size study)

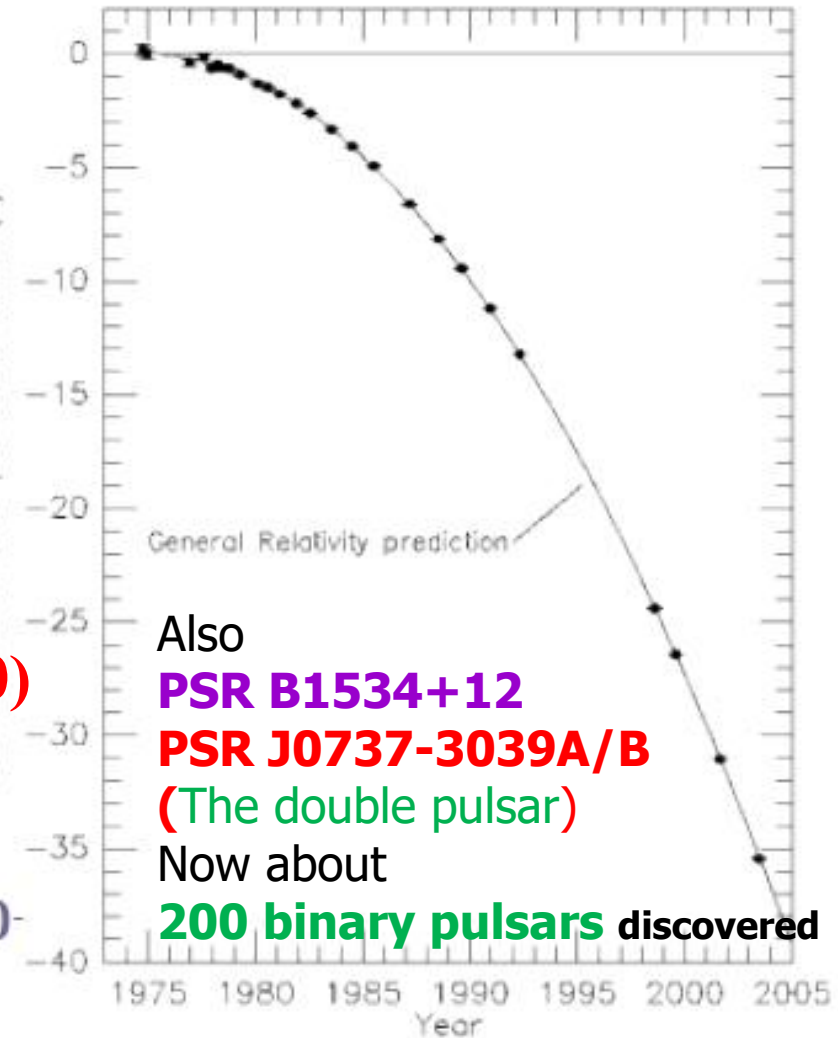
Fig. 5. (left) Interferometer system noise measurement at 5 kHz of Moss, Miller and Forward (1971) [142]; (right) Schematic of Malibu Laser Interferometer CW Antenna (from Forward 1978) [87].

Hulse-Taylor Binary PSR1913+16

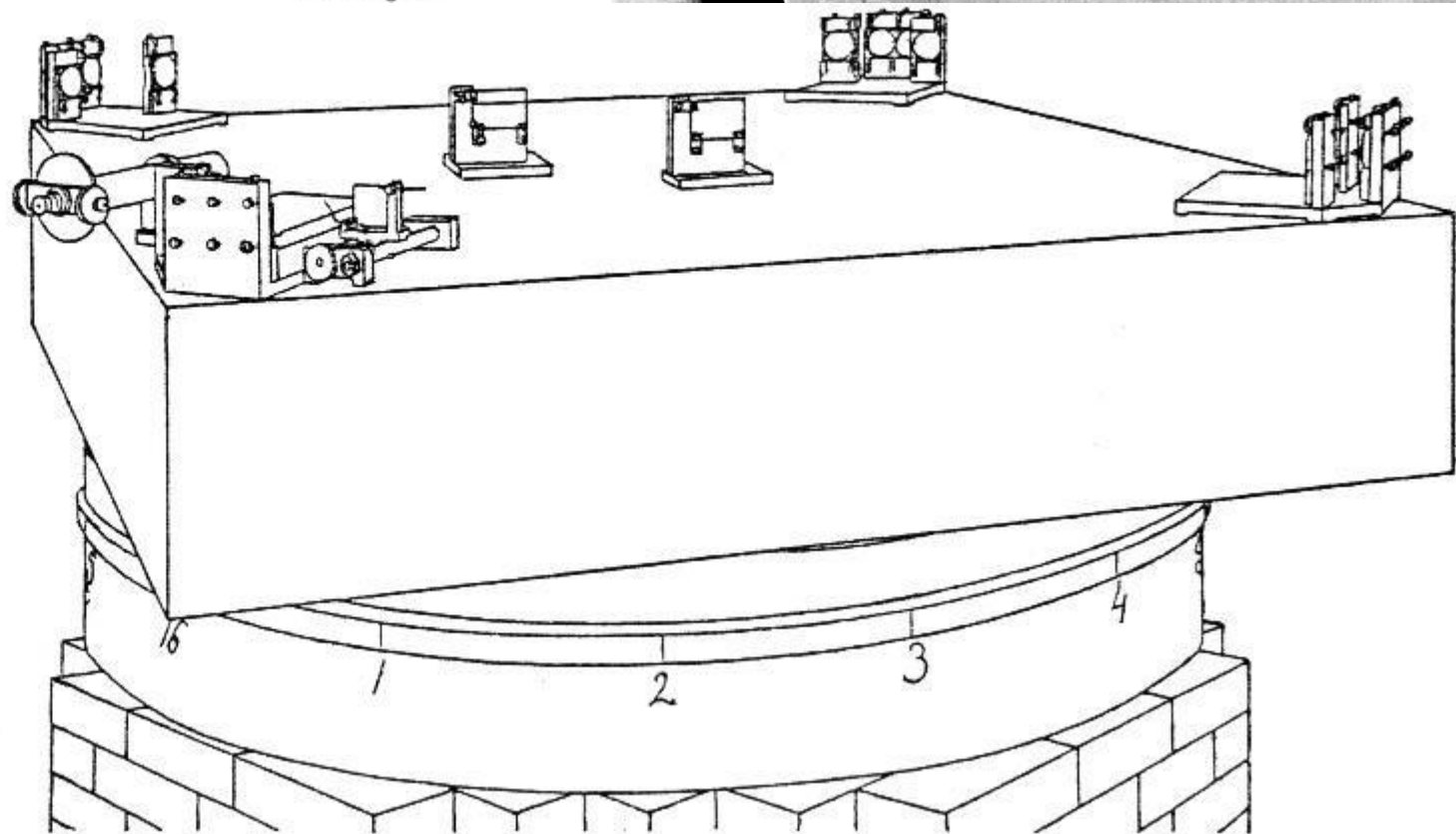
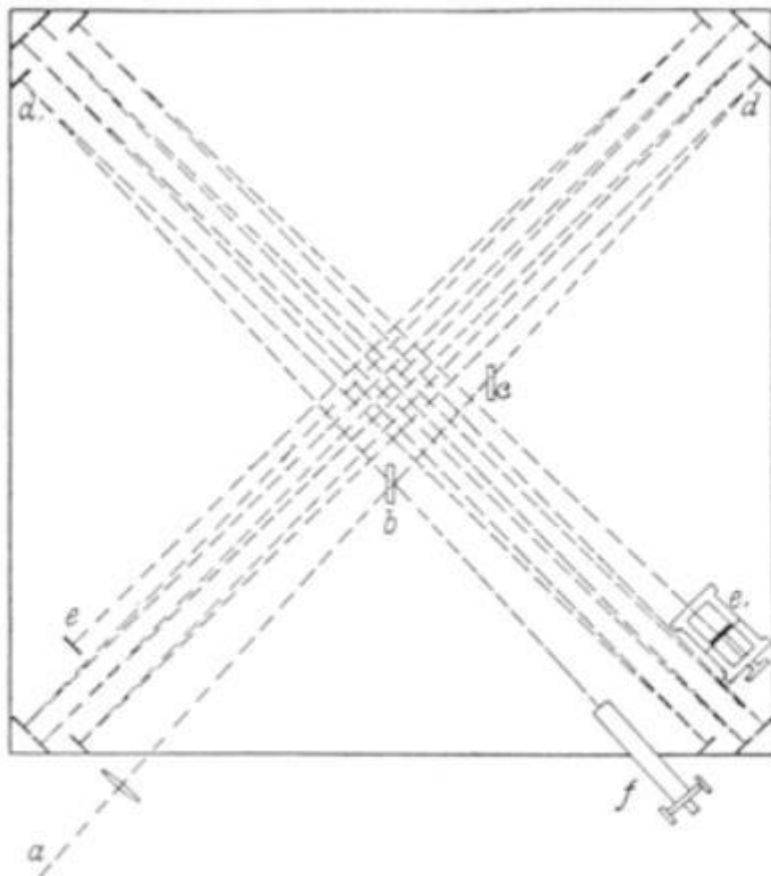
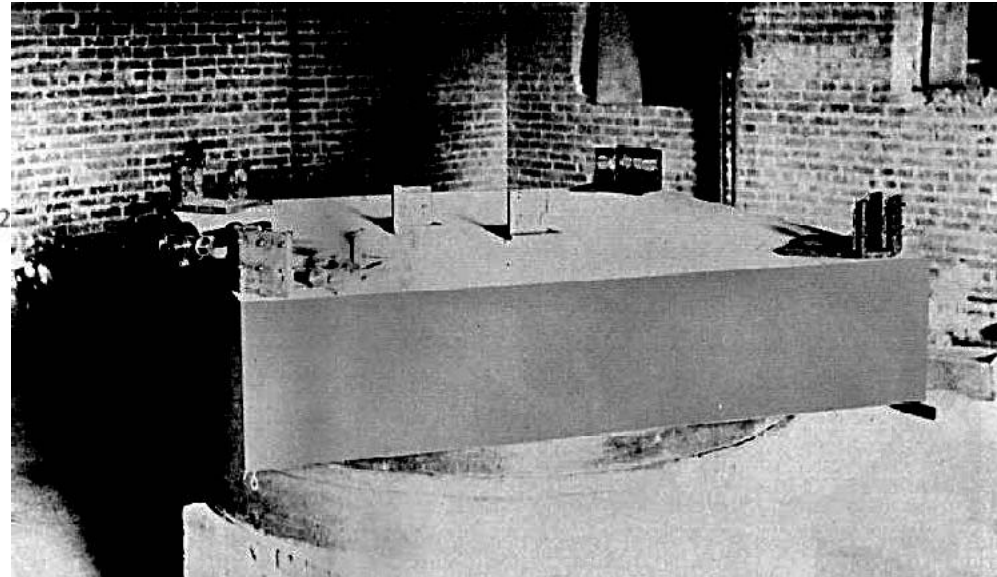
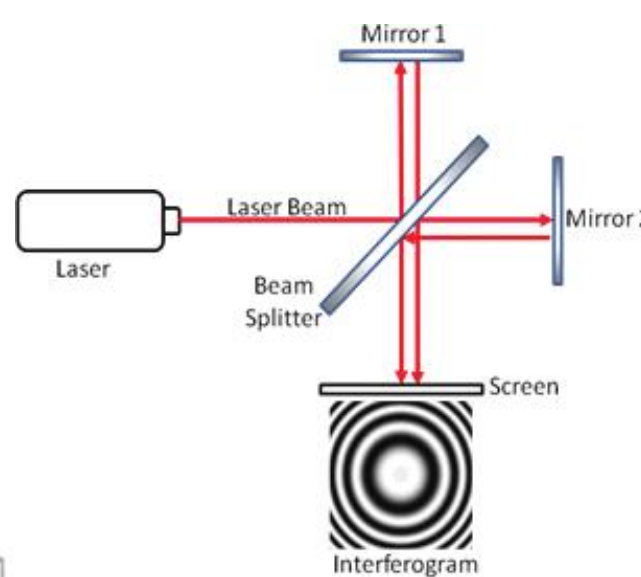
国际暨中德双边激光天文动力学研讨会



- Observed loss of energy matches prediction of GW emission to $(0.13 \pm 0.21)\%$ **$0.997 \pm 0.002 (2010)$**
- Indirect evidence of gravitational waves
- Frequency $70 \mu\text{Hz}$, amplitude 7×10^{-23} \Rightarrow outside detector sensitivity



Michelson Interferometry 迈克尔逊干涉



Ground-based GW detectors 2015

LIGO



VIRGO



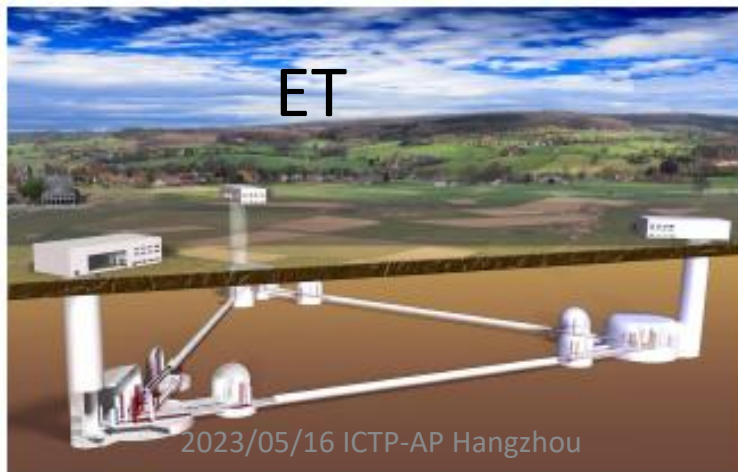
KAGRA



GW detection in space



ET

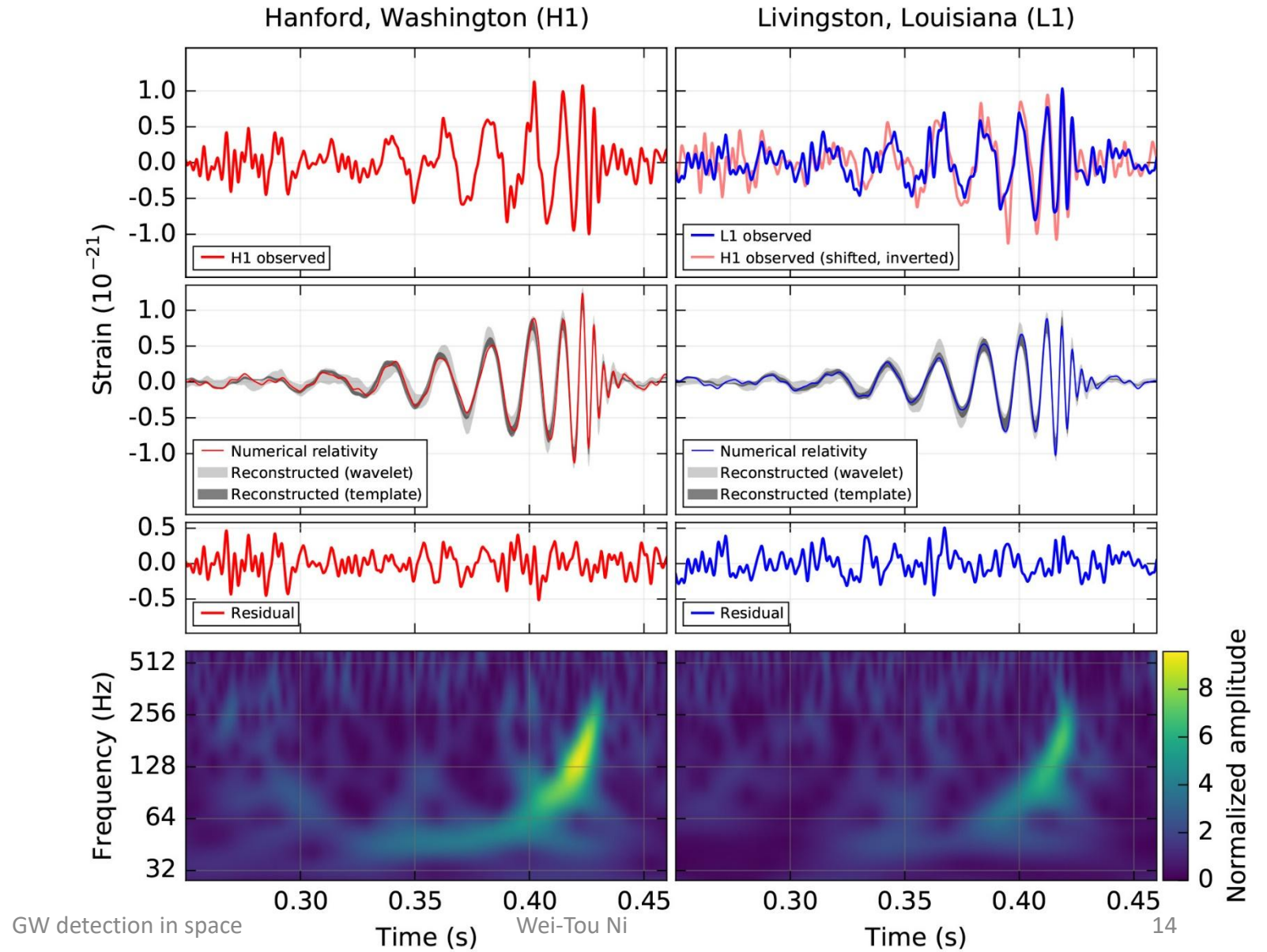
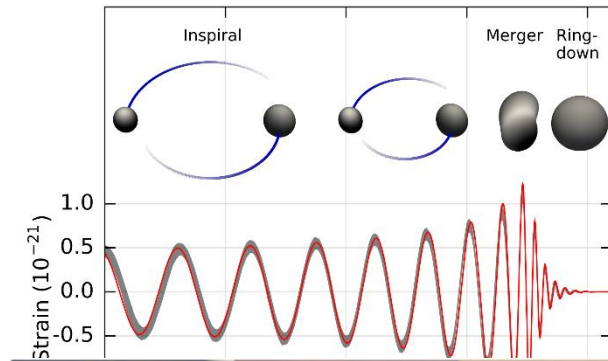
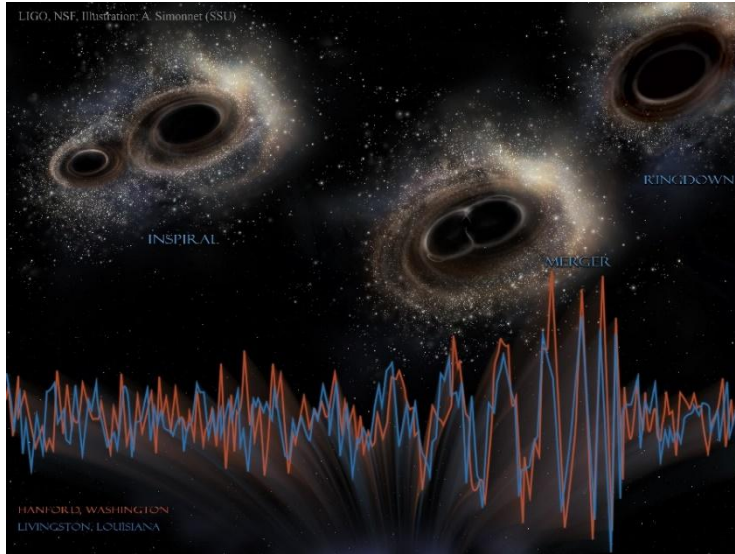


2023/05/16 ICTP-AP Hangzhou



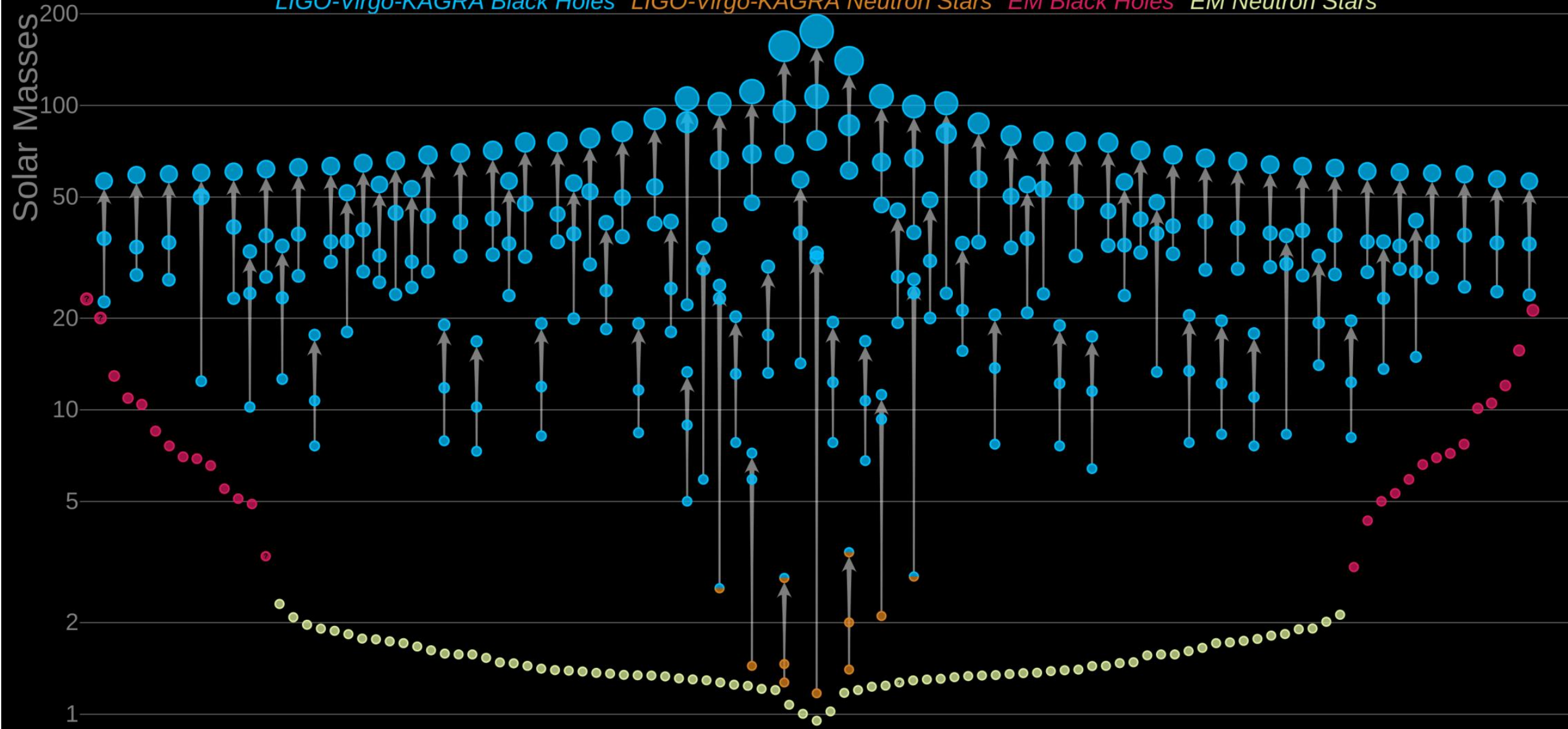
Wei-Tou Ni

2016 February 11 Announcement of first (direct) detection of **Black Holes** and **GWs**



Masses in the Stellar Graveyard

LIGO-Virgo-KAGRA Black Holes *LIGO-Virgo-KAGRA Neutron Stars* *EM Black Holes* *EM Neutron Stars*



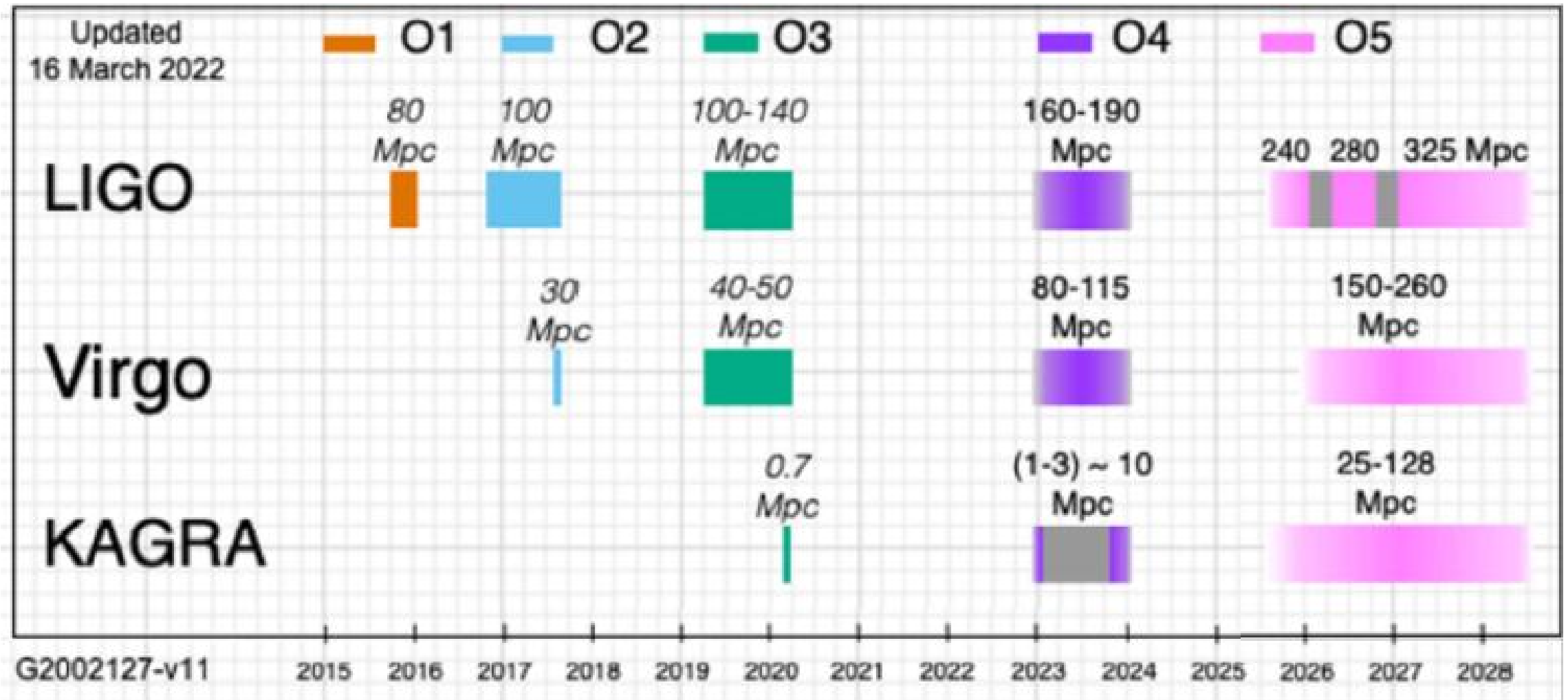
Event Rates

- **Binary Black Holes:** After the detection of GW170104
 - Between $12\text{-}213 \text{ Gpc}^{-3} \text{ y}^{-1}$
 - Including all O1 & O2 events
 - power law distribution
 - $56^{+44}_{-27} \text{ Gpc}^{-3} \text{ y}^{-1}$ (GstLAL)
 - $57^{+47}_{-29} \text{ Gpc}^{-3} \text{ y}^{-1}$ (PyCBC)
 - uniform in log distribution
 - $18.1^{+13.9}_{-8.7} \text{ Gpc}^{-3} \text{ y}^{-1}$ (GstLAL)
 - $19.5^{+15.2}_{-9.7} \text{ Gpc}^{-3} \text{ y}^{-1}$ (PyCBC)
- **Neutron Star Binaries:** (uniform mass set)
 - $662^{+1609}_{-565} \text{ Gpc}^{-3} \text{ y}^{-1}$ (GstLAL)
 - $800^{+1970}_{-680} \text{ Gpc}^{-3} \text{ y}^{-1}$ (PyCBC)

Event Rates from GWTC-3 (76 events of ~ 90)

- Binary Black Holes: After the GW Transient Catalog 3 (GWTC-3)
 - **Between $17.9-44 \text{ Gpc}^{-3} \text{ y}^{-1}$ at a fiducial redshift ($z = 0.2$)**
 - Including all O1 & O2 & O3 events
 -
- **Neutron Star Binaries:** (uniform mass set) **$10-1700 \text{ Gpc}^{-3} \text{ y}^{-1}$**
- **NS-BH merger rate** **$78-140 \text{ Gpc}^{-3} \text{ y}^{-1}$**
- **A broad, relatively flat neutron star mass distribution extending from $1.2^{+0.1}_{-0.2} M_{\text{sun}}$ to $2.0^{+0.3}_{-0.3} M_{\text{sun}}$**

The latest scenario 地基探测



Prototype Einstein Telescope enters building 'black box' in Maastricht

- ET Pathfinder, the test facility for the Einstein Telescope, is housed in the university building at Duboisdomein 30 in Maastricht. **Maastricht University (UM)** had rented the building for **several years**, but with a view to the ET Pathfinder it has now been decided to make a purchase. A team of researchers led by professor **Stefan Hild**, the **UM professor of Gravitational Studies** who **took office on 1 August**, will move into the Dubois domain this month. The construction of the prototype will start early next year.
- ET site choice: **Eurigon, Sardinia**



Astro2020 Science White Paper

The US Program in Ground-Based GW Science: Contribution from the LIGO Lab

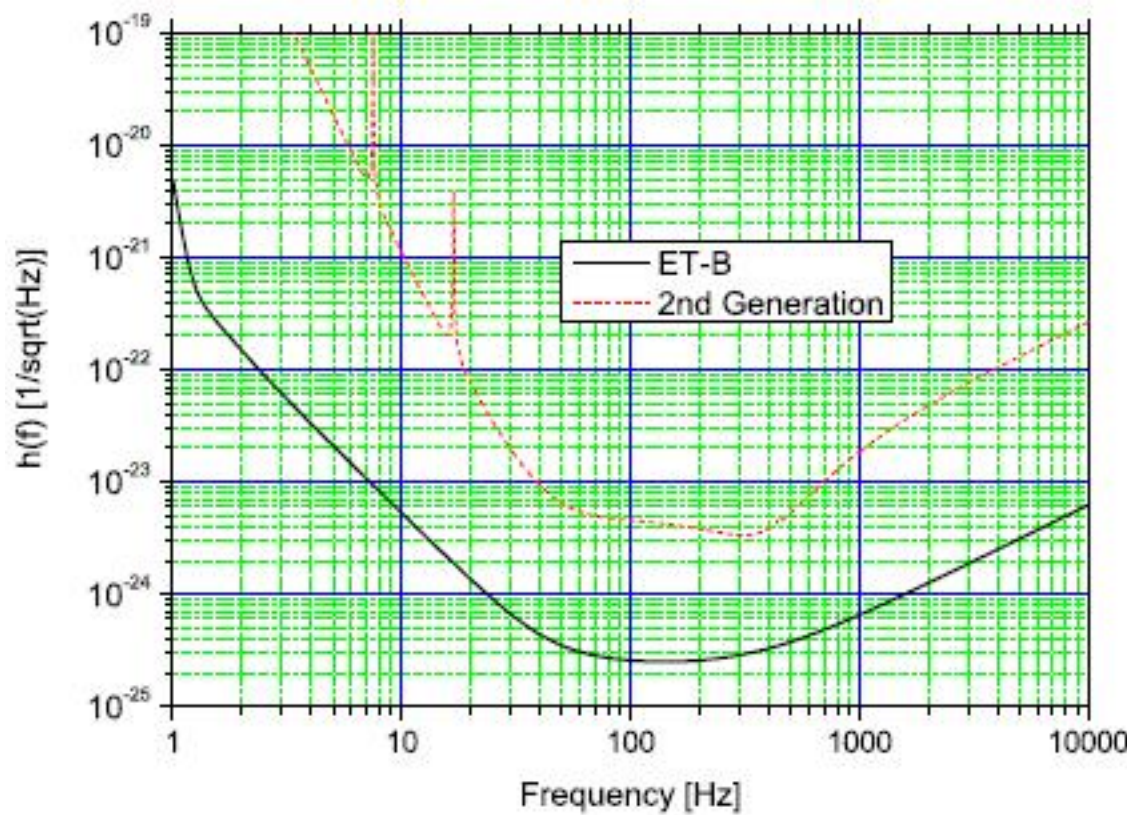
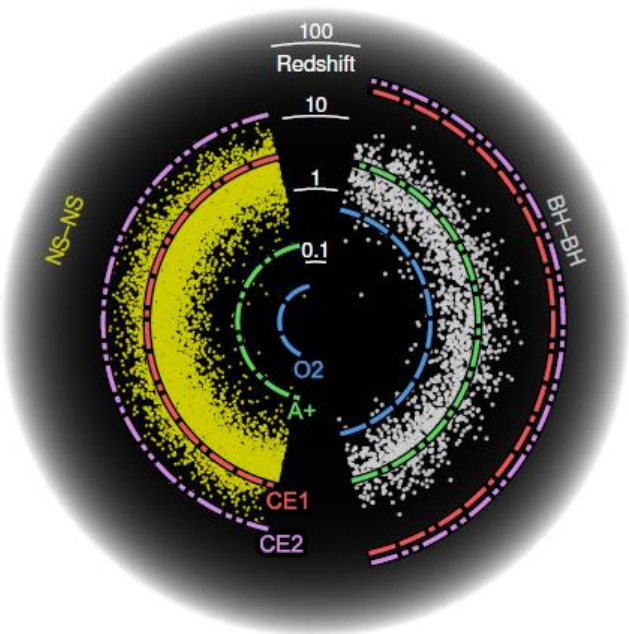
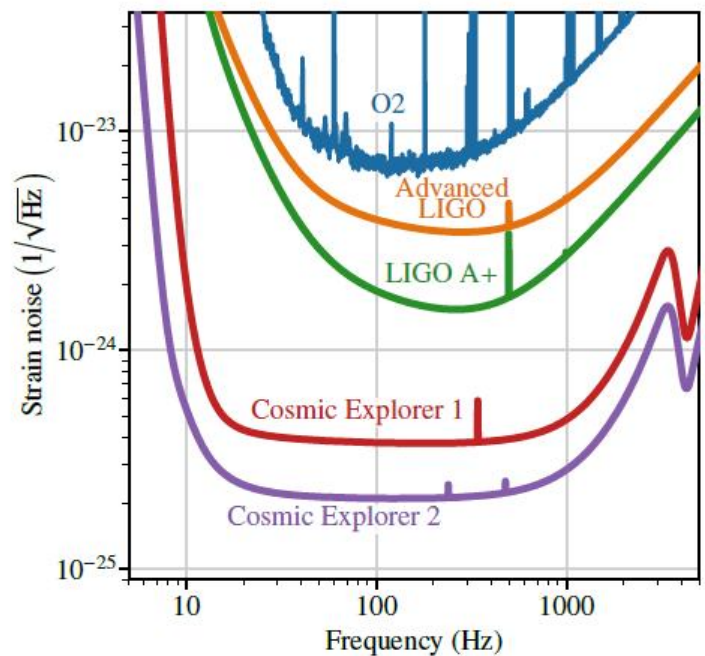
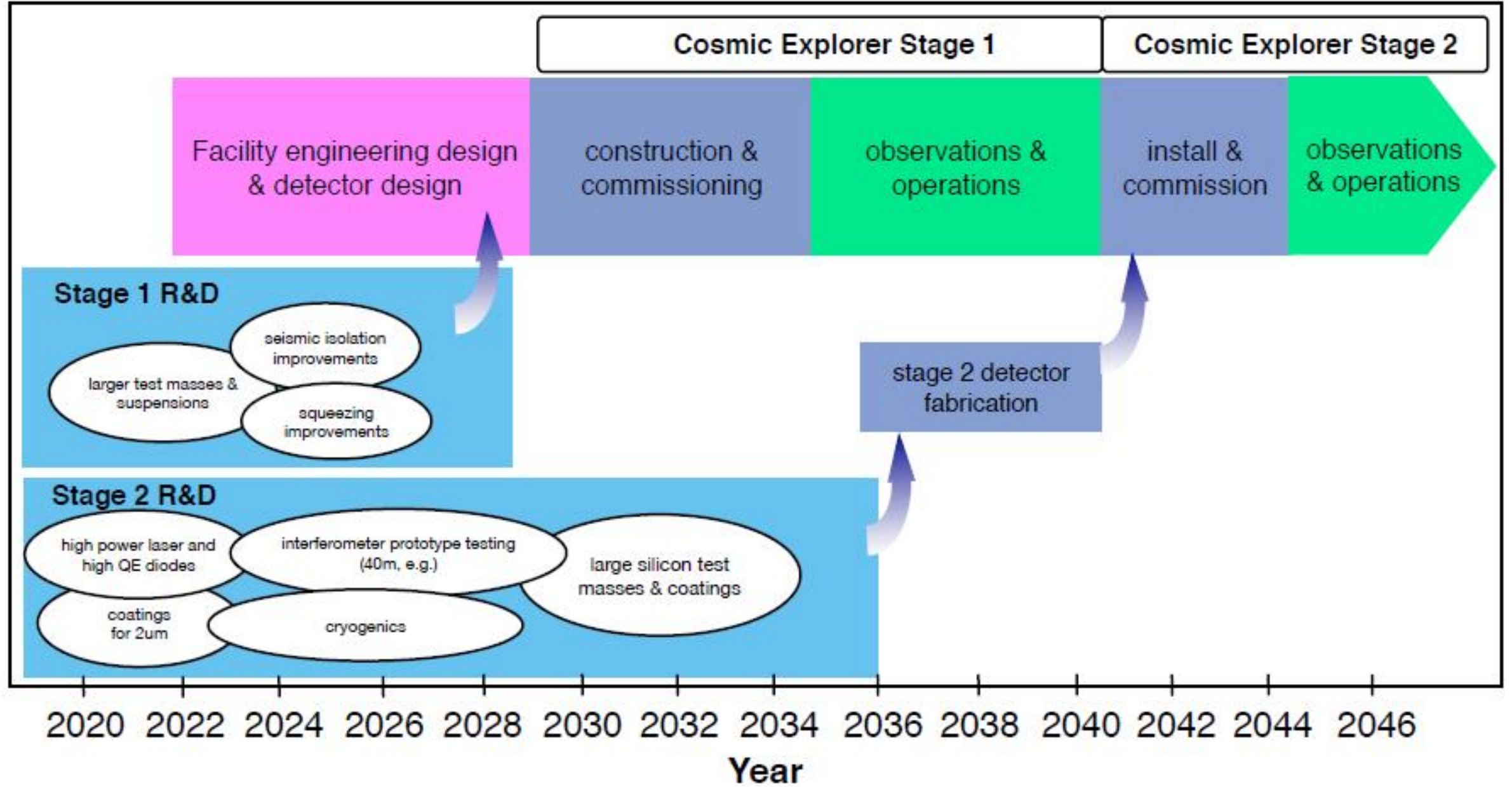


Figure 1: *Left side:* Cosmic Explorer projected strain noise for Stage 1 (during the 2030s) and Stage 2 (2040s), compared with the strain noise achieved by Advanced LIGO during observing run O2, as well as designed noise performance for Advanced LIGO, and LIGO A+. Less strain noise indicates better strain sensitivity. *Right side:* Astrophysical response distance³⁴ of Advanced LIGO at O2 sensitivity, LIGO A+, and Cosmic Explorer (Stages 1 and 2), plotted on top of a population of $1.4\text{--}1.4M_{\odot}$ neutron star mergers (yellow) and $30\text{--}30M_{\odot}$ black hole mergers (gray), assuming a Madau–Dickinson star formation rate³⁵ and a typical merger time of 100 Myr. The radial distribution of points accounts for the detector-frame merger rate per unit redshift.

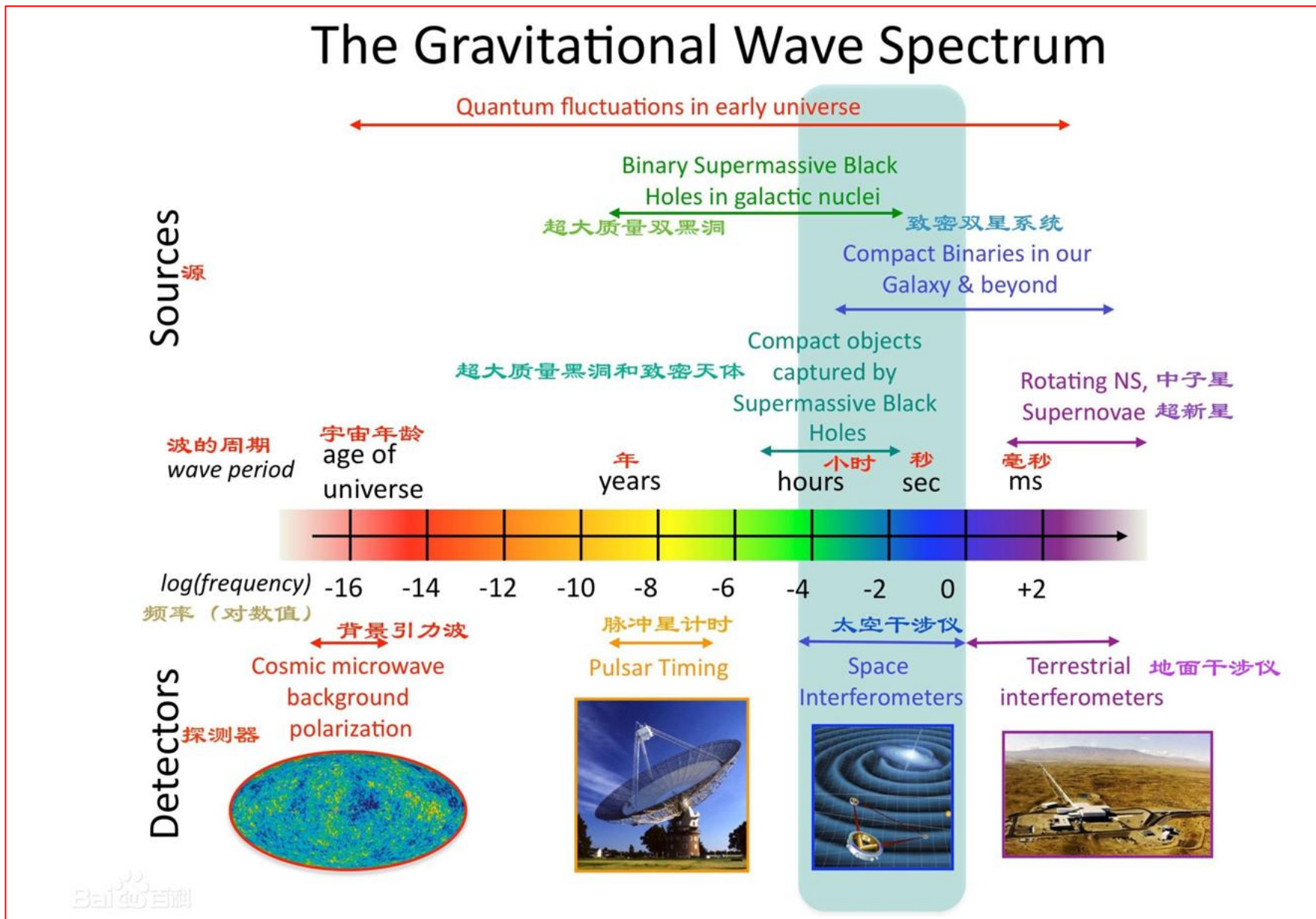
Timeline of a Cosmic Explorer 40km Observatory



2030-2050 the decades of space GW detection

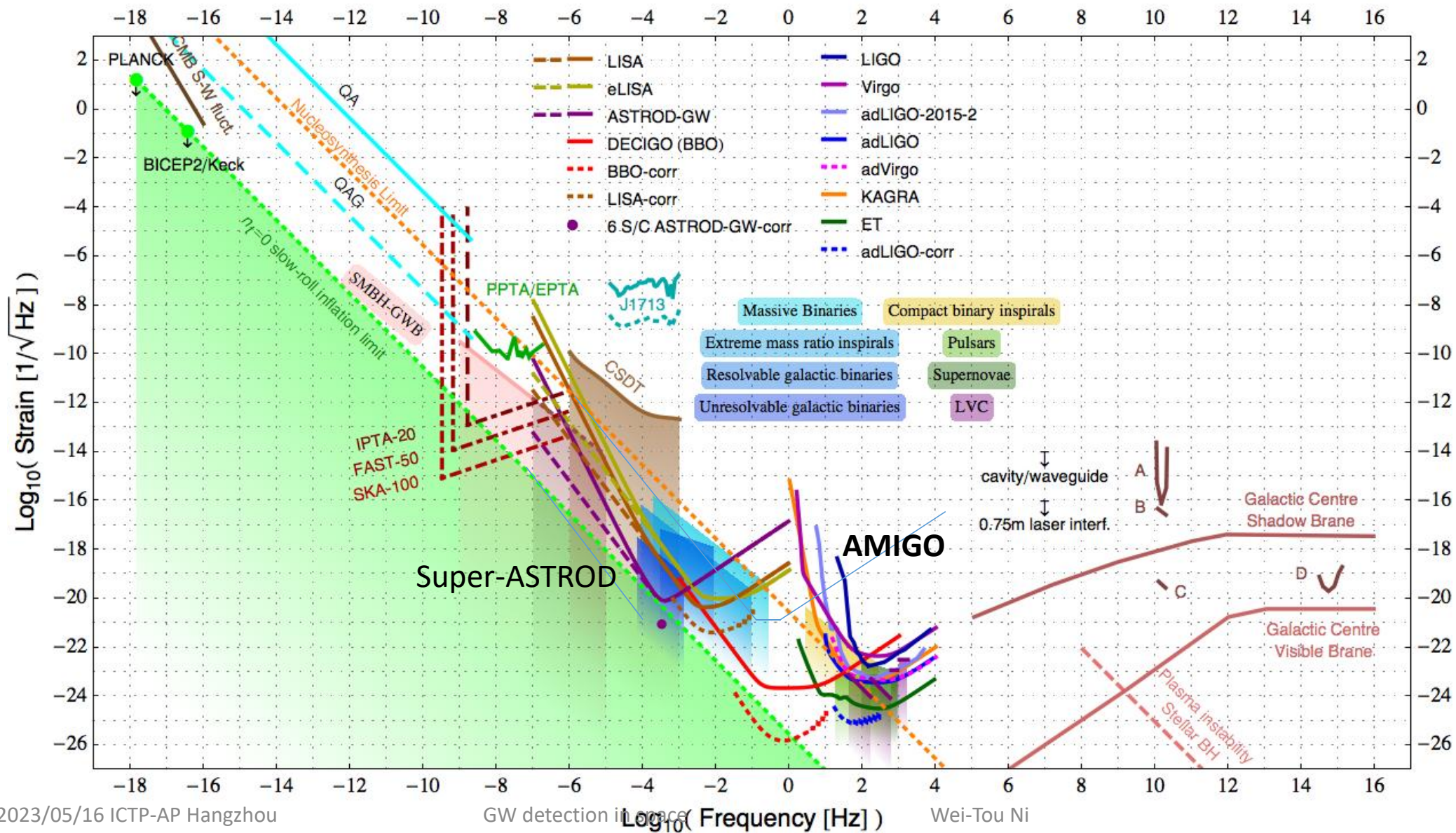
- mHz GWs
- Middle frequency GWs
- μ Hz GWs

Normally (before) people talk about 4 most active detection methods

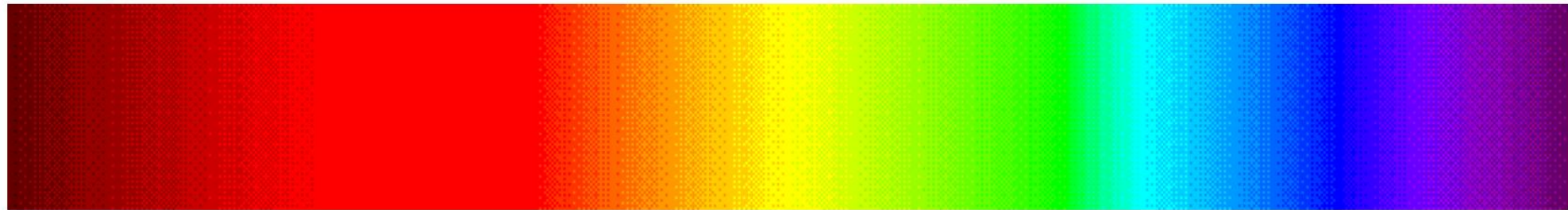
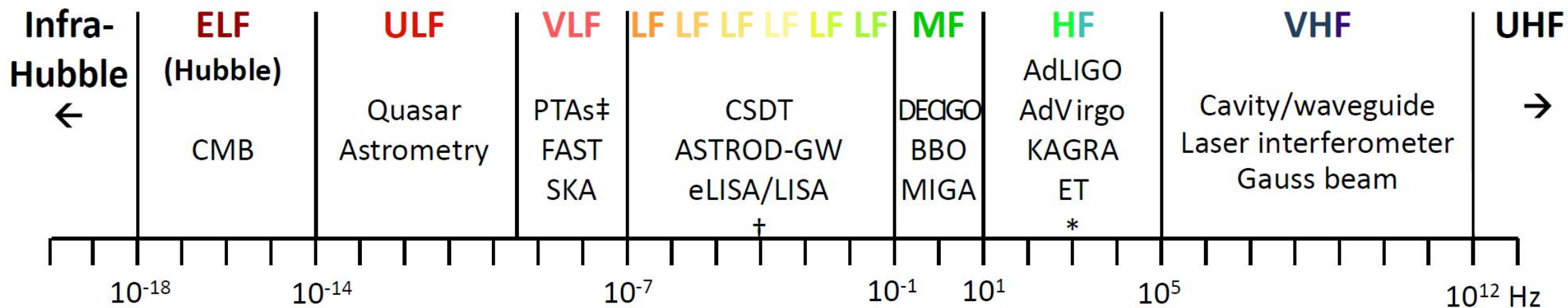


5 Gaps

Strain power spectral density (psd) amplitude vs. frequency for various GW detectors and GW sources



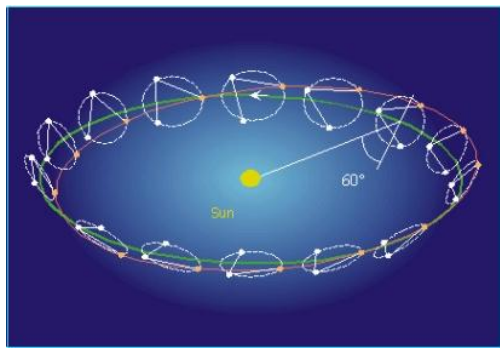
引力波谱分类 The Gravitation-Wave (GW) Spectrum Classification



* AIGO, AURIGA, EXPLORER, GEO, NAUTILUS, MiniGRAIL, Schenberg.

† OMEGA, gLISA/GEOGRAWI, GADFLI, TIANQIN, ASTROD-EM, LAGRANGE, ALIA, ALIA-descope.

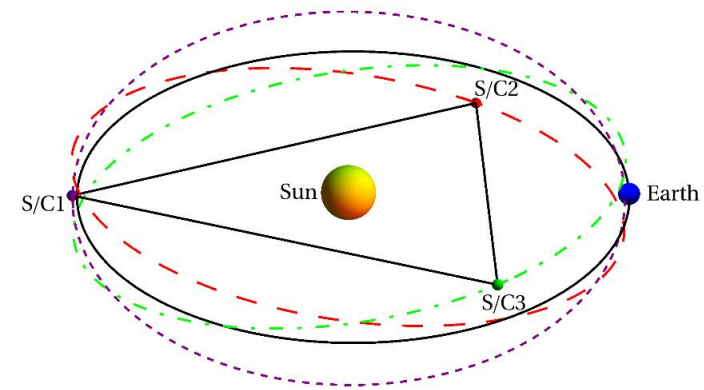
‡ EPTA, NANOGrav, PPTA, IPTA.



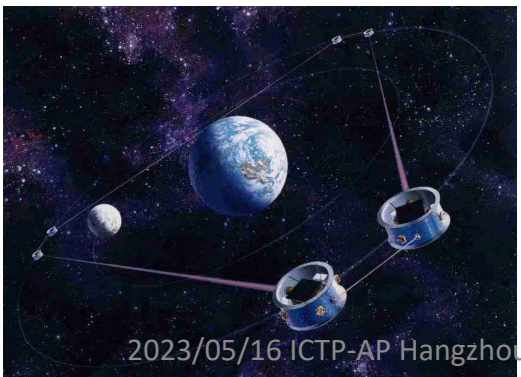
A Compilation of GW Mission Proposals

LISA Pathfinder

Launched on December 3, 2015



Mission Concept	S/C Configuration	Arm length	Orbit Period	S/C #
<i>Solar-Orbit GW Mission Proposals</i>				
LISA ⁶⁵	Earth-like solar orbits with 20° lag	5 Gm	1 year	3
eLISA ⁶⁴	Earth-like solar orbits with 10° lag	1 Gm	1 year	3
ASTROD-GW ⁶⁸	Near Sun-Earth L3, L4, L5 points	260 Gm	1 year	3
Big Bang Observer ⁷³	Earth-like solar orbits	0.05 Gm	1 year	12
DECIGO ⁷²	Earth-like solar orbits	0.001 Gm	1 year	12
ALIA ⁷⁴	Earth-like solar orbits	0.5 Gm	1 year	3
ALIA-descope ⁷⁵	Earth-like solar orbits	3 Gm	1 year	3
Super-ASTROD ⁷¹	Near Sun-Jupiter L3, L4, L5 points (3 S/C), Jupiter-like solar orbit(s)(1-2 S/C)	1300 Gm	11 year	4 or 5
<i>Earth-Orbit GW Mission Proposals</i>				
OMEGA ⁸¹	0.6 Gm height orbit	1 Gm	53.2 days	6
gLISA/GEOGRAWI ⁷⁶⁻⁷⁸	Geostationary orbit	0.073 Gm	24 hours	3
GADFLI ⁷⁹	Geostationary orbit	0.073 Gm	24 hours	3
TIANQIN ⁸²	0.057 Gm height orbit	0.11 Gm	44 hours	3
ASTROD-EM ^{69,70}	Near Earth-Moon L3, L4, L5 points	0.66 Gm	27.3 days	3
LAGRANGE ⁸⁰	Near Earth-Moon L3, L4, L5 points	0.66 Gm	27.3 days	3



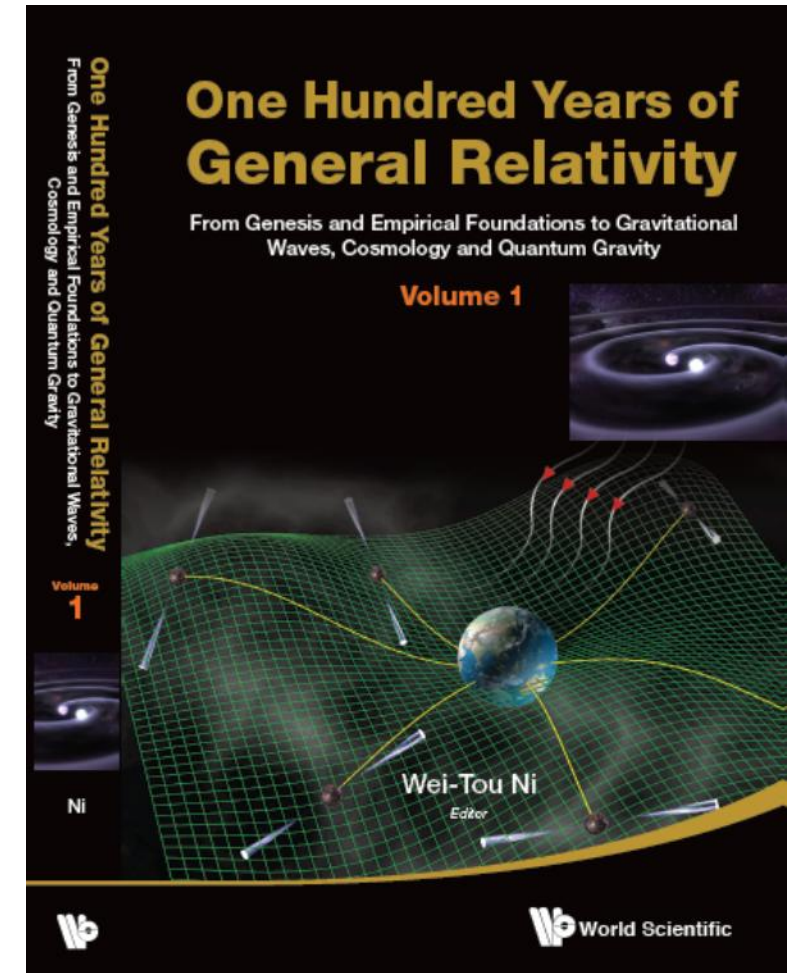
Mission concept	S/C configuration	Arm length	Orbit period	S/C #	Acceleration noise [fm/s ² /Hz ^{1/2}]	Laser metrology noise [pm/Hz ^{1/2}]
<i>Solar-Orbit GW Mission Proposals</i>						
LISA ⁹	Earthlike solar orbits with 20° lag	5 Gm	1 year	3	3	20
eLISA ²¹	Earthlike solar orbits with 10° lag	1 Gm	1 year	3	3	12(10)
ASTROD-GW ^{36–40}	Near Sun–Earth L3, L4, L5 points	260 Gm	1 year	3	3	1000
Big Bang Observer ⁴⁵	Earthlike solar orbits	0.05 Gm	1 year	12	0.03	1.4×10^{-5}
DECIGO ⁴⁴	Earthlike solar orbits	0.001 Gm	1 year	12	0.0004	2×10^{-6}
ALIA ⁴⁷	Earthlike solar orbits	0.5 Gm	1 year	3	0.3	0.6
TAIJI (ALIA-descope) ⁴⁸	Earthlike solar orbits	3 Gm	1 year	3	3	5–8
Super-ASTROD ⁴²	Near Sun–Jupiter L3, L4, L5 points (3 S/C), Jupiterlike solar orbit(s)(1–2 S/C)	1300 Gm	11 year	4 or 5	3	5000
<i>Earth-Orbit GW Mission Proposals</i>						
OMEGA ^{54,55}	0.6 Gm height orbit	1 Gm	53.2 days	6	3	5
gLISA/GEOGRAWI ^{49–51}	Geostationary orbit	0.073 Gm	24 h	3	3, 30	0.3, 10
GADFLI ⁵²	Geostationary orbit	0.073 Gm	24 h	3	0.3, 3, 30	1
TIANQIN ¹⁹	0.057 Gm height orbit	0.11 Gm	44 h	3	1	1
ASTROD-EM ⁴³	Near Earth–Moon L3, L4, L5 points	0.66 Gm	27.3 days	3	1	1
LAGRANGE ⁵³	Earth–Moon L3, L4, L5 points	0.66 Gm	27.3 days	3	3	5

One Hundred Years of General Relativity

From Genesis and Empirical Foundations to Gravitational Waves, Cosmology and Quantum Gravity (Volume 1 & Volume 2)

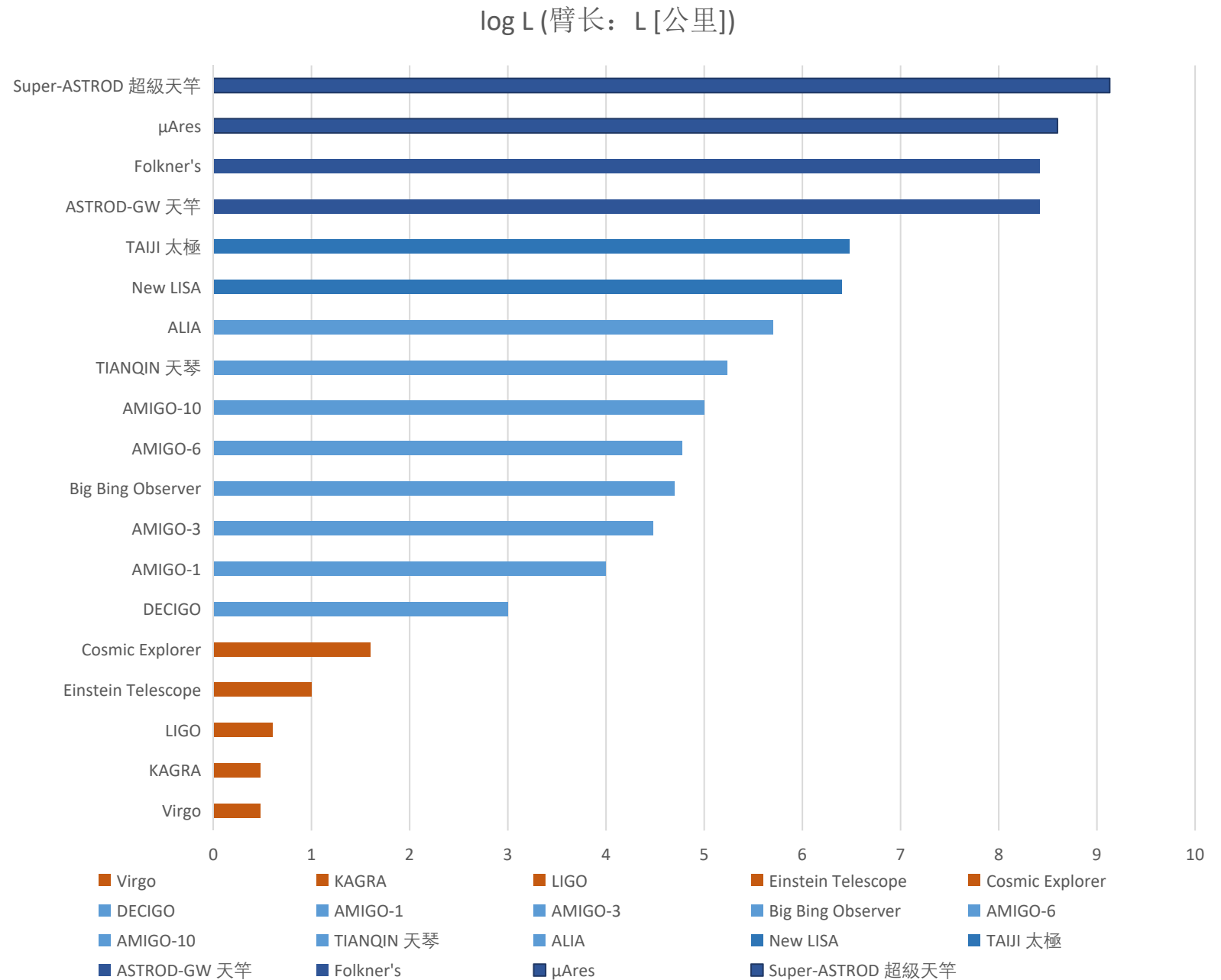
- **OPEN ACCESS**

- <https://www.worldscientific.com/doi/pdf/10.1142/9389-vol1?download=true>
- <https://www.worldscientific.com/doi/pdf/10.1142/9389-vol2?download=true>



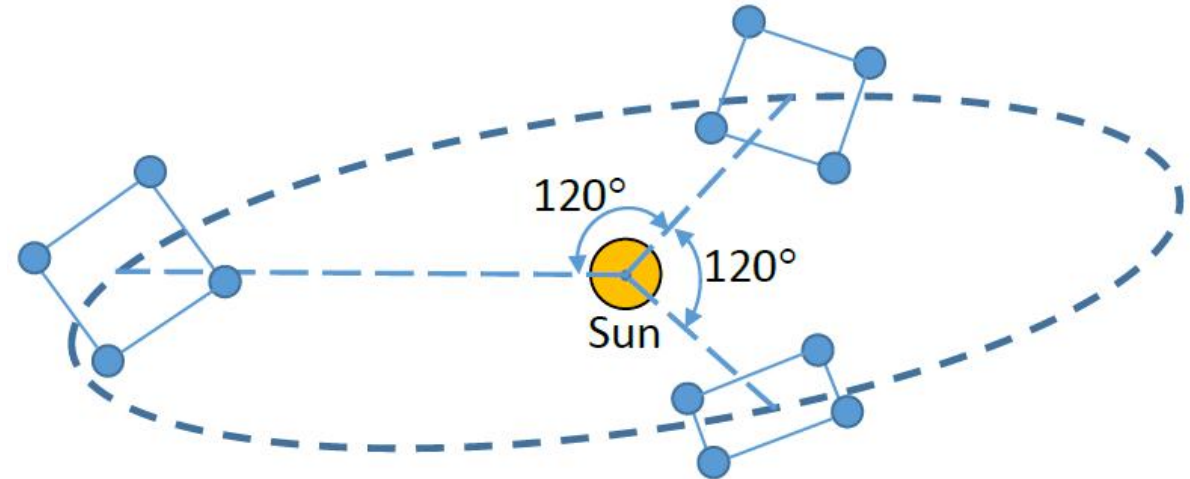
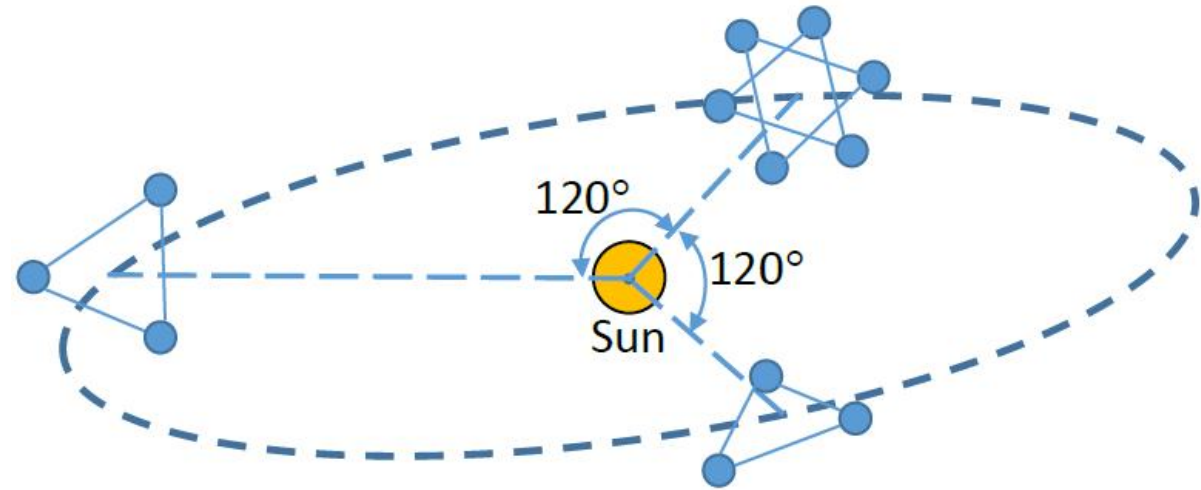
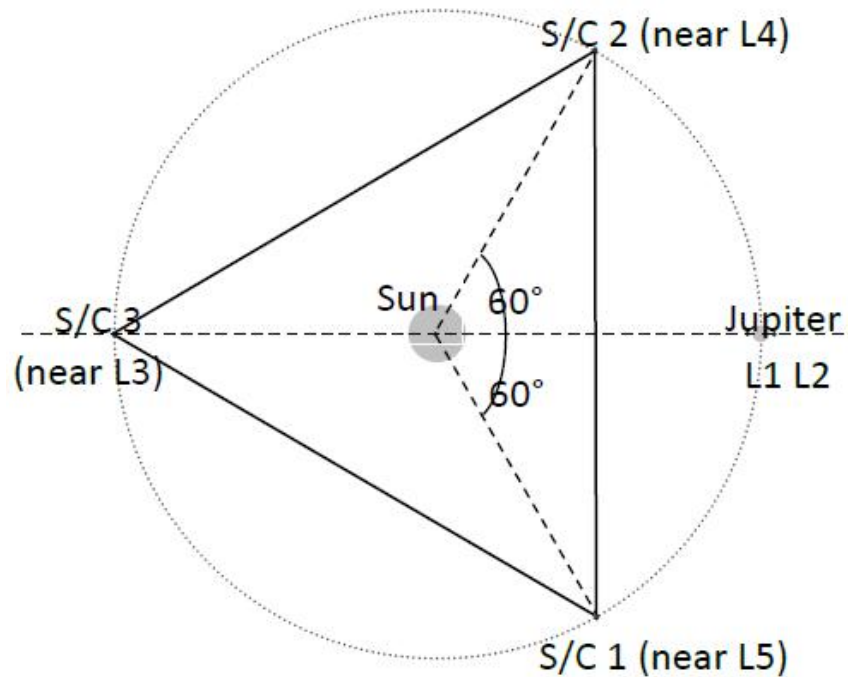
- A list of
 - High-frequency,
 - Middle-frequency
 - Low-frequency
- GW-detectors

According to arm length



Second Generation GW Mission Concepts 2015 review

- DECIGO
- BBO
- Super-ASTROD



Recommended high performance telescope system design for the TianQin project
Capability for detection of GW190521-like binary black holes with TianQin
Science with the TianQin Observatory: Preliminary Results on Stochastic Gravitational-Wave Background
Science with the TianQin Observatory: Preliminary Results on Testing the No-hair Theorem with EMRI
Effects of the space plasma density oscillation on the inter-spacecraft laser ranging for TianQin gravitational wave observatory
Orbital effects on time delay interferometry for TianQin
Eclipse avoidance in TianQin orbit selection
Effect of Earth-Moon's gravity on TianQin's range acceleration noise radii on TianQin constellation stability
Optimizing orbits for TianQin
The TianQin project: current progress on science and technology
Light propagation in the field of the N-body system and the application in the TianQin mission
Science with the TianQin observatory: Preliminary result on extreme-mass-ratio inspirals
Science with the TianQin Observatory: Preliminary results on Galactic double white dwarf binaries
Science with the TianQin observatory: Preliminary results on stellar-mass binary black holes
Analyses of residual accelerations for TianQin based on the global MHD simulation
A preliminary forecast for cosmological parameter estimation with GW standard sirens from TianQin
Science with the TianQin observatory: Prel. results on testing the no-hair theorem with ringdown signals
Science with the TianQin observatory: Preliminary results on massive black hole binaries
Preliminary study on param. estimation accuracy of supermassive black hole binary inspirals for TianQin
Fundamentals of the orbit and response for TianQin
TianQin: a space-borne gravitational wave detector
Fundamentals of the TianQin mission

TianQin

On Detecting Stellar Binary Black Holes via the LISA-Taiji Network

Alternative LISA-TAIJI networks: detectability of the isotropic stochastic GW background

Prospects for detecting exoplanets around double white dwarfs with LISA and Taiji

Unidirectional lasing in nonlinear Taiji micro-ring resonators

Influence of the bus waveguide on the linear and nonlinear response of a taiji microresonator

Alternative LISA-TAIJI networks

Mission Design for the TAIJI mission and Structure Formation in Early Universe

Forecast for cosm. parameter estimation with GW standard sirens from the LISA-Taiji network

Nonlinearity-induced reciprocity breaking in a single non-magnetic Taiji resonator

Taiji: Longest Chain Availability with BFT Fast Confirmation

Measuring Parity Violation in the Stochastic GW Background with the LISA-Taiji network

Hubble parameter estimation via dark sirens with the LISA-Taiji network

Searching anomalous polarization modes of stochastic GW background with LISA and Taiji

Revisiting time delay interferometry for unequal-arm LISA and TAIJI

Constraining gravitational-wave polarizations with Taiji

Numerical simulation of sky localization for LISA-TAIJI joint observation

The LISA-Taiji network

Analytical analysis on the orbits of Taiji spacecrafts to infinite order of the orbital eccentricity

Prospects for improving cosmological parameter estimation with GW standard sirens from Taiji

The LISA-Taiji network: precision localization of massive black hole binaries

Analytical analysis on the orbits of Taiji spacecrafts

Taiji Program: Gravitational-Wave Sources

Hyperunified field theory and Taiji program in space for GWD

Numerical simulation of time delay interferometry for new LISA, TAIJI and other LISA-like missions

TAIJI

Some works has been done in LISA & Taiji

in the following, we just mention briefly the our work on sensitivities and joint observations

1. [arXiv:2105.00746](#) [[pdf](#), [ps](#), [other](#)] **Alternative LISA-TAIJI networks**

[Gang Wang](#), [Wei-Tou Ni](#), [Wen-Biao Han](#), [Peng Xu](#), [Ziren Luo](#)

Journal-ref: Phys. Rev. D 104, 024012 (2021)

2. [arXiv:2010.15544](#) [[pdf](#), [ps](#), [other](#)]

Algorithm for TDI numerical simulation and sensitivity inv

[Gang Wang](#), [Wei-Tou Ni](#), [Wen-Biao Han](#), [Cong-Feng Qiao](#)

Journal-ref: Phys. Rev. D 103, 122006 (2021)

3. [arXiv:2008.05812](#) [[pdf](#), [ps](#), [other](#)]

Revisiting time delay interferometry for unequal-arm LISA

[Gang Wang](#), [Wei-Tou Ni](#), [Wen-Biao Han](#)

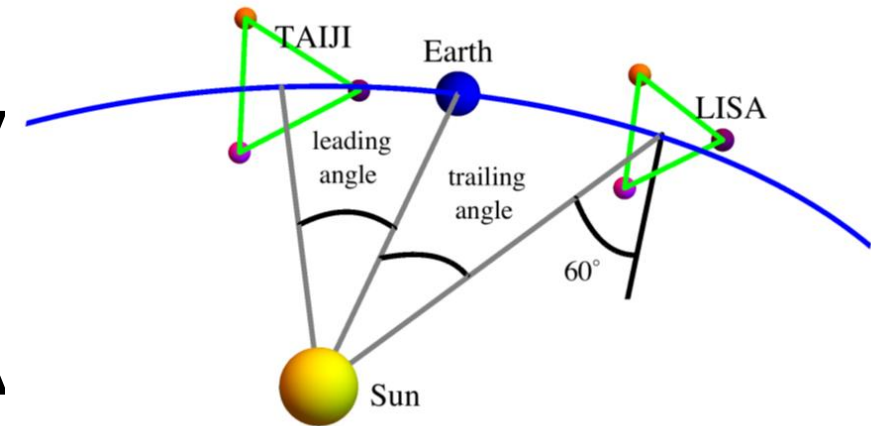
4. [arXiv:2002.12628](#) [[pdf](#), [ps](#), [other](#)]

Numerical simulation of sky localization for LISA-TAIJI joint observation

[Gang Wang](#), [Wei-Tou Ni](#), [Wen-Biao Han](#), [Shu-Cheng Yang](#), [Xing-Yu Zhong](#)

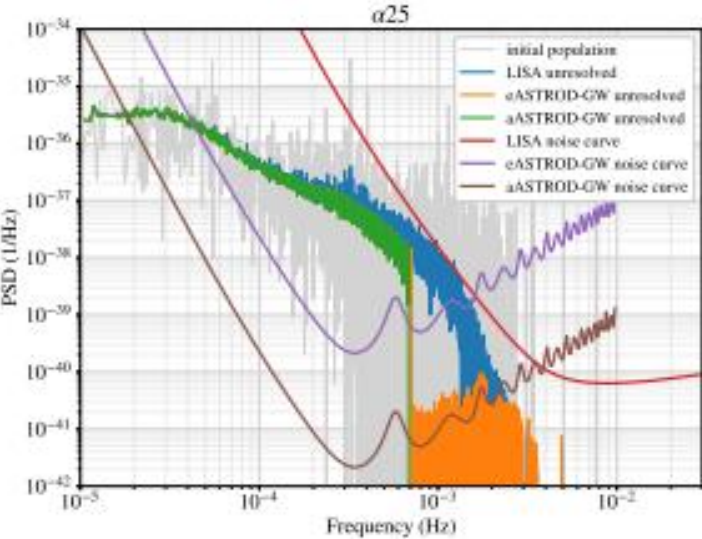
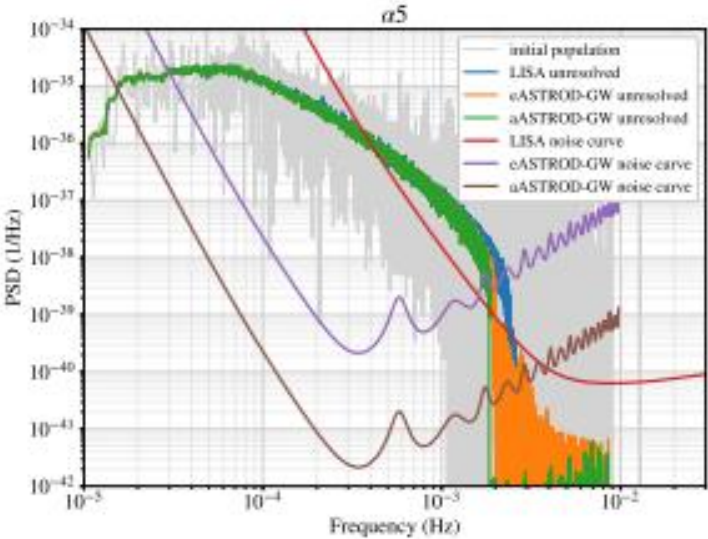
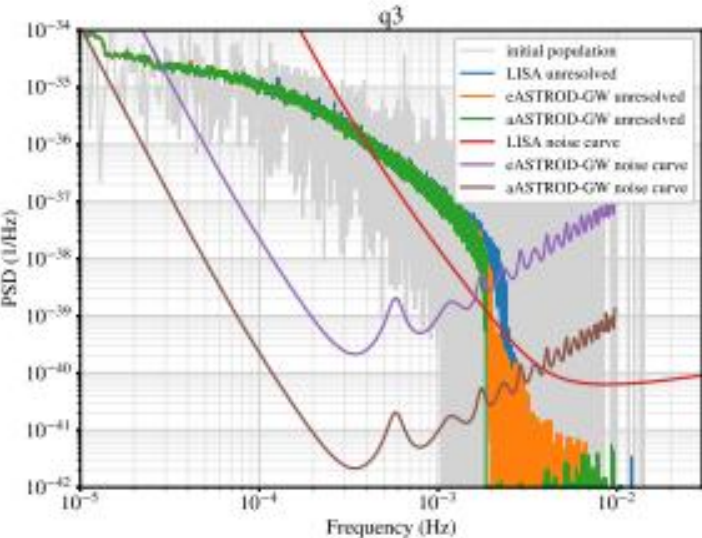
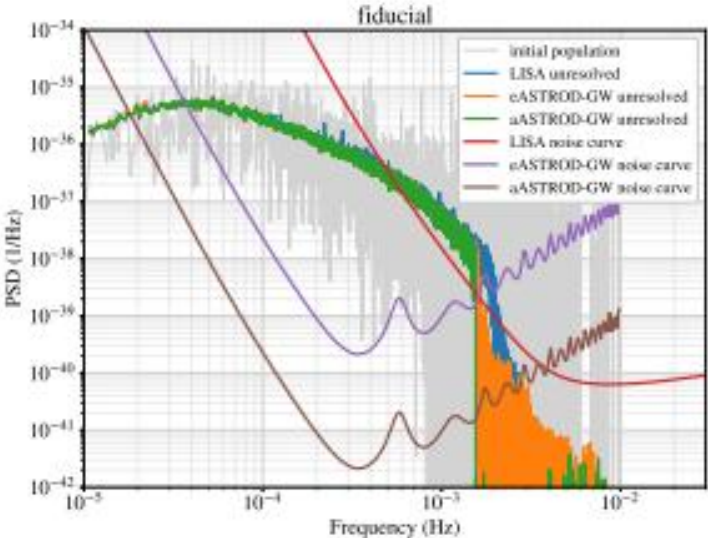
Journal-ref: Phys. Rev. D 102, 024089 (2020)

5. **Numerical simulation of time delay interferometry for new LISA, TAIJI and other LISA-like missions** [Gang Wang](#), [Wei-Tou Ni](#)



The initial DWD population (grey), the unresolved foreground for LISA in 6 years of observation (blue), and the unresolved foreground for eASTROD-GW (orange) or aASTROD-GW (green) in 10 years of observation. The sensitivities of the first-generation TDI Michelson-A for LISA, eASTROD-GW, and aASTROD-GW are shown by red, purple, and brown curves, respectively.

[TAJI confusion limit: YX Liu's (Lanzhou) Group]



- Proposals under active study
- Arm length 100 times longer than LISA
- Arm length 100 times shorter than LISA

Weak-light phase locking and manipulation technology

- Weak-light phase locking is crucial for long-distance space interferometry and for CW laser space communication. For **LISA** of arm length of **5 Gm (million km)** the weak-light phase locking requirement is for **70 pW** laser light to phase-lock with an onboard laser oscillator. For **ASTROD-GW** arm length of **260 Gm (1.73 AU)** the weak-light phase locking requirement is for **100 fW** laser light to lock with an onboard laser oscillator.
- Weak-light phase locking for **2 pW** laser light to **200 μ W** local oscillator is demonstrated in our laboratory in Tsing Hua U.⁶
- **Dick *et al.***⁷ from their phase-locking experiment showed a PLL (Phase Locked Loop) phase-slip rate below one cycle slip per second at powers **as low as 40 femtowatts (fW)**.
- **Shaddock et al: tracking 30 fW free-running laser (2015-2016)**

Arm length 100 times longer than LISA

- **First Generation Technology**
- Inertial Sensor technology: 20 μHz -1 mHz
Demonstrated by LISA Pathfinder
- Weak light demonstrated also
- Long arm shot noise limit needs to be implemented
- A mission can be technologically flown 10 years or even in shorter term after LISA/TAIJI

Primary Thematic Science Area:
Multi-Messenger Astronomy and Astrophysics

Secondary Areas:
Cosmology and Fundamental Physics, Galaxy Evolution,
Formation and Evolution of Compact Objects

Astro2020 APC White Paper

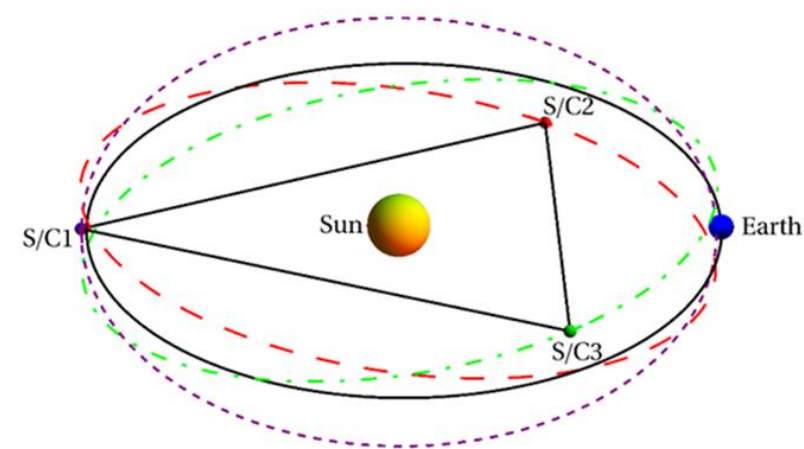
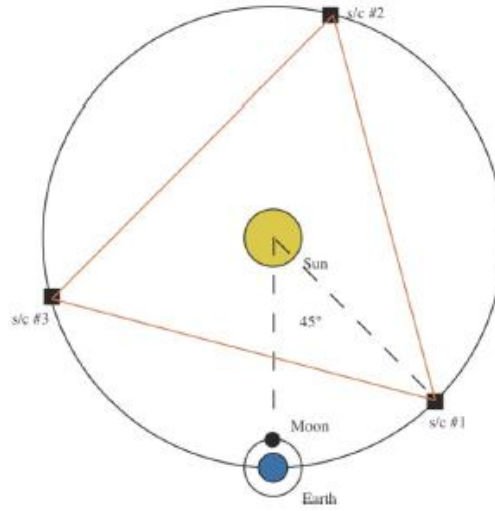
Space Based Gravitational Wave Astronomy Beyond LISA

John Baker,¹ Simon F. Burke,² Peter L. Bender,³ Emanuele Berti,⁴ Robert Caldwell,⁵ John W. Conklin,² Neil Cornish,⁶
Elizabeth C. Ferrara,^{7,8,9} Kelly Holley-Bockelmann,² Brittany Kamai,^{10,9} Shane L. Larson,¹² Jeff Lives,¹ Sean T. McWilliams,¹³
Guido Mueller,² Priyamwada Natarajan,¹¹ Norman Rioux,¹ Shannon R Sankar,⁷ Jeremy Schnittman,¹
Deirdre Shoemaker,¹⁴ Jacob Slutsky,¹ Robin Stebbins,³ Ira Thorpe,¹ and John Ziemer¹⁵

- ¹ NASA Goddard Space Flight Center
- ² University of Florida
- ³ JILA - University of Colorado
- ⁴ Johns Hopkins University
- ⁵ Dartmouth College
- ⁶ Montana State University
- ⁷ University of Maryland, College Park
- ⁸ Center for Research and Exploration in Space Science & Technology (CRESTT)

- ⁹ Vanderbilt University
- ¹⁰ California Institute of Technology
- ¹¹ Yale University
- ¹² Northwestern University
- ¹³ West Virginia University
- ¹⁴ Georgia Institute of Technology
- ¹⁵ Jet Propulsion Laboratory (JPL)

arXiv:1907.11305v1 [astro-ph.IM] 25 Jul 2019

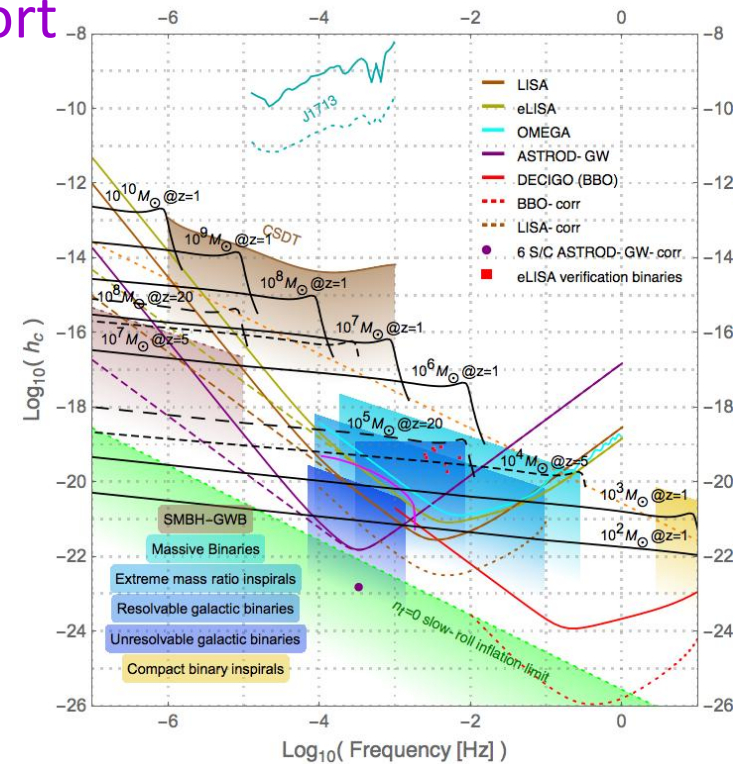
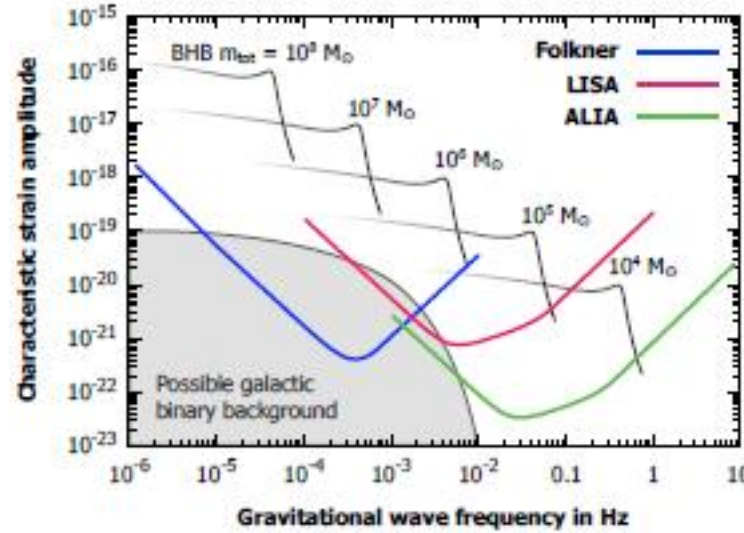


ASTROD GW (2009, 2010)

2016 IJMPD, GR centennial

Folkner's mission 2012 JPL report

2020 Decadal (2019)



ESA Voyage 2050 Science White Paper (GW)

2035-2050 (After LISA) 4 proposals

- The Missing Link in GW Astronomy **DO** (Deci-Hz Obs.)
- Probing the Nature of Black Holes: **ESA AMIGO** (mHz)
- Unveiling the Gravitational Universe at μ -Hz frequencies:

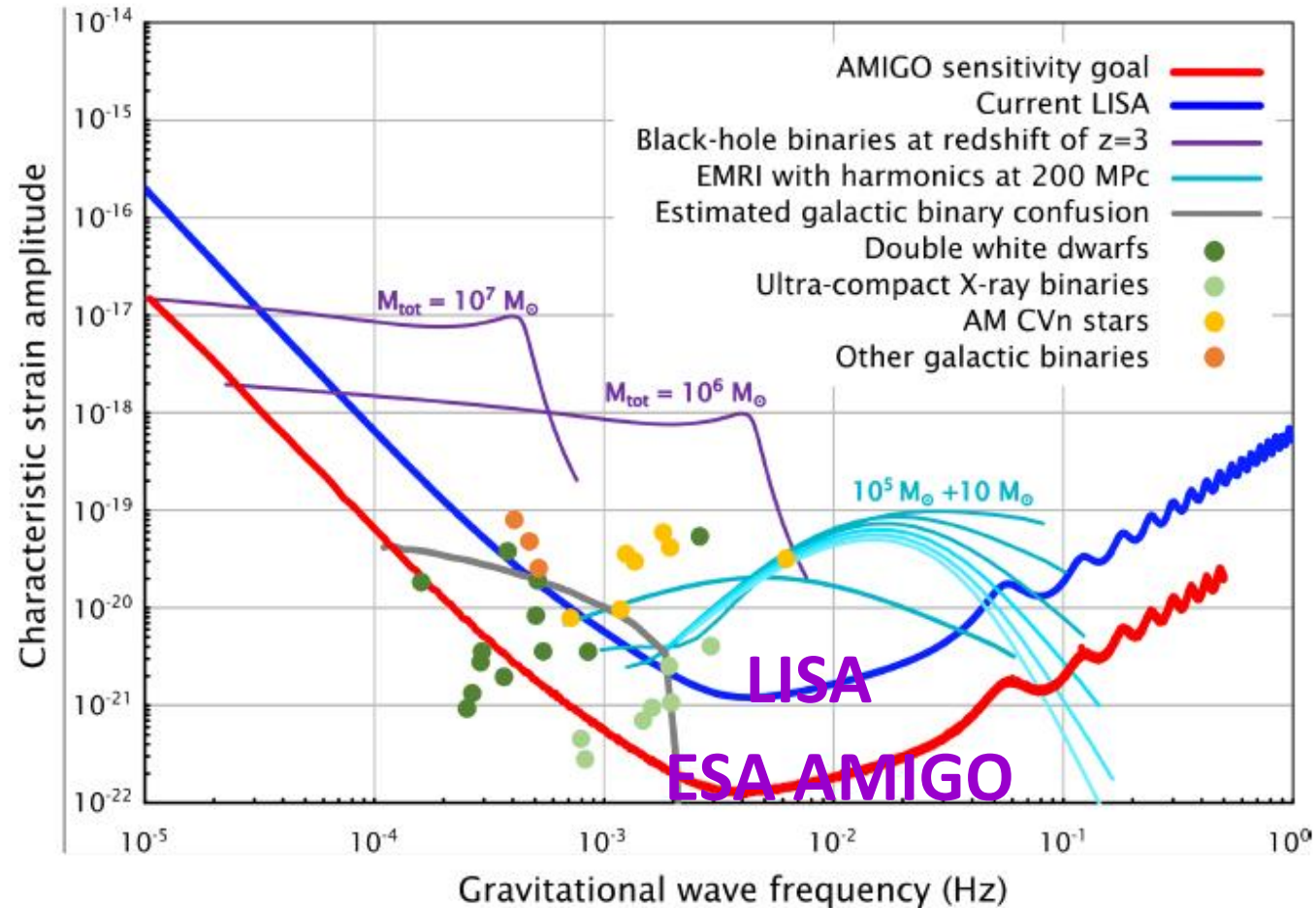
- High angular resolution GW astronomy

- $D \uparrow$ $P \uparrow$ $\lambda \downarrow$

$$h_{\text{SN}} \equiv \frac{\delta L_{\text{SN}}}{L} = \frac{\lambda^{3/2}}{D^2} \sqrt{\frac{\hbar c}{\pi P_{\text{in}}}}$$

- Noise Beyond shot noise:
Stray light

geometric effects that couple spacecraft motion to (apparent) length changes, timing noise in the phasemeter, laser frequency noise, temperature driven optical path length



*Probing the Nature of Black Holes:
Deep in the mHz, Gravitational-Wave Sky*

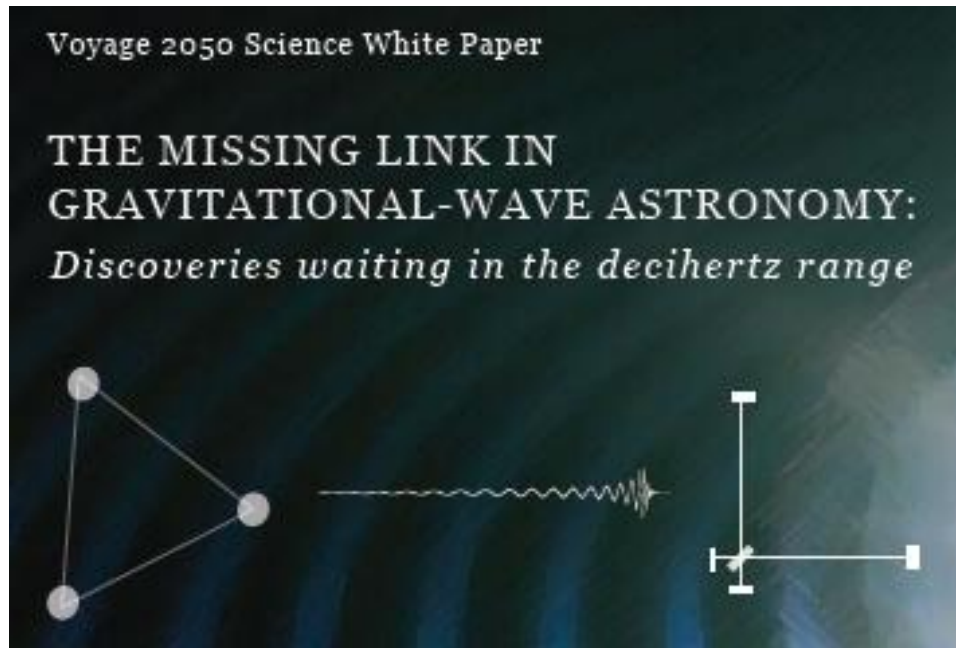
ESA AMIGO

Contact Scientist: Vitor Cardoso
Primary institution and address: CENTRA, Instituto Superior Técnico, Universidade de Lisboa,
Avenida Rovisco Pais 1, 1049 Lisboa, Portugal
Email: vitor.cardoso@tecnico.ulisboa.pt
Phone: 351-218419821

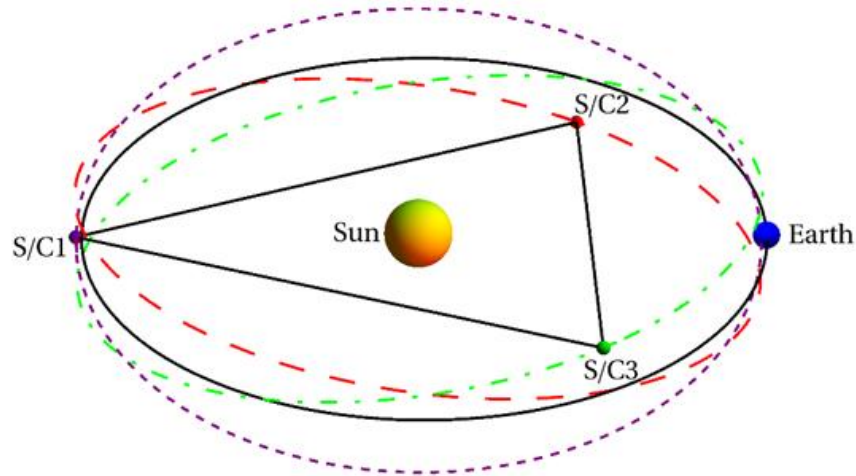
ESA VOYAGE 2050 GW

High angular resolution gravitational
wave astronomy

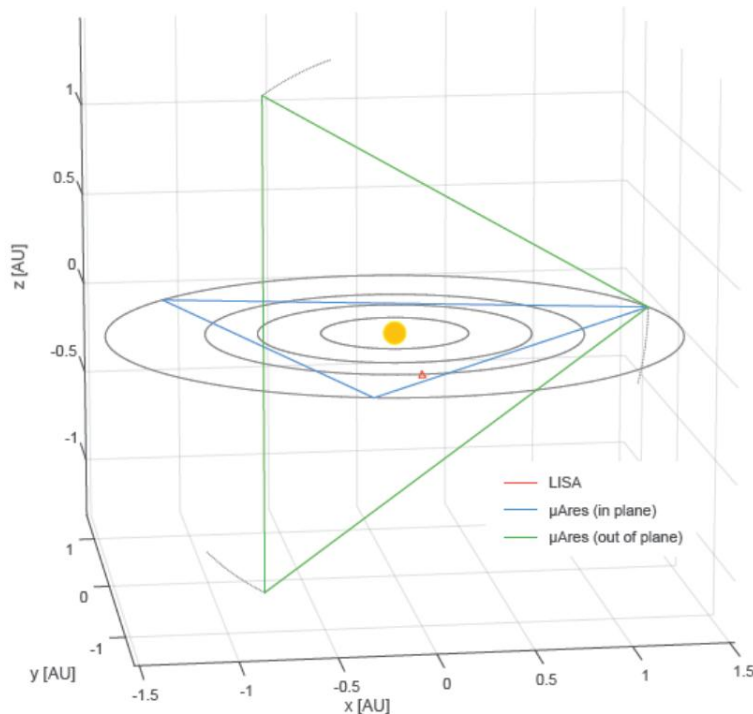
Contact Scientist: Irina Dvorkin



ASTROD-GW and μ Ares (2035-2050)



- ASTROD series proposed 1993 (ASTROD 1993, ASTROD I [Mini-ASTROD 2001], ASTROD-GW 2009, Super-ASTROD 2009)
- ASTROD-GW: 3 S/C near Sun-Earth L3, L4, L5 with inclined orbit formation precessing semi-annually
- Maximum line-of-site velocity in 10 years: 3 m/s (no inclination), 4 m/s (0.5° inclination)
- Arm length 260 million km, 100 times longer than LISA, below 3 mHz to 0.1μ Hz, sensitivity 100 times better than LISA



Average orbit radius	0.7 AU	1.0 AU	1.5 AU
Average arm length	187 million km	259 million km	395 million km
Total arm length variations (in plane constellation)	185,000 km	105,000 km	492,000 km
Total arm length variations (out of plane constellation)	176,000 km	217,000 km	65,700 km
Maximum line-of-sight velocities	6 m/s	4 m/s	12 m/s
Doppler frequencies at 1064 nm	5.5 MHz	4.0 MHz	11.0 MHz

LISAmix: Improving the Gravitational-Wave Sensitivity by Two Orders of Magnitude

W. Martens¹, M. Khan¹, and J.-B. Bayle²

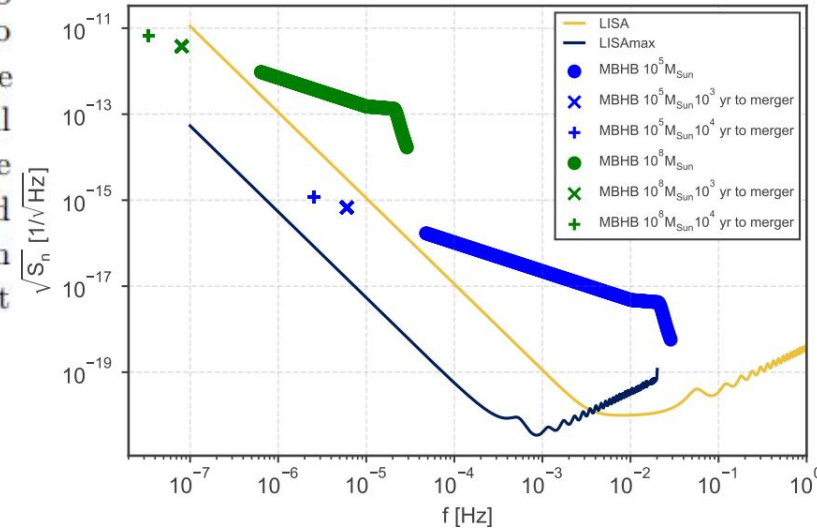
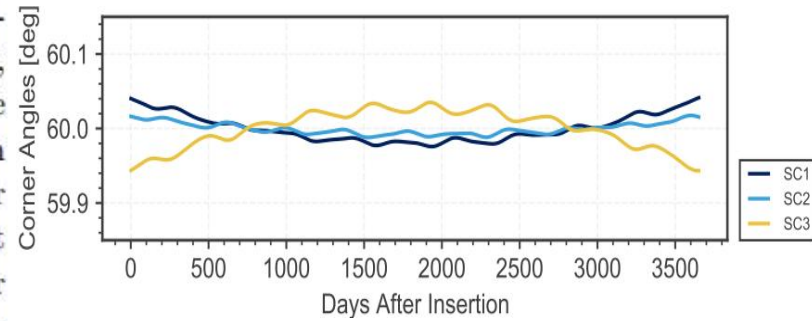
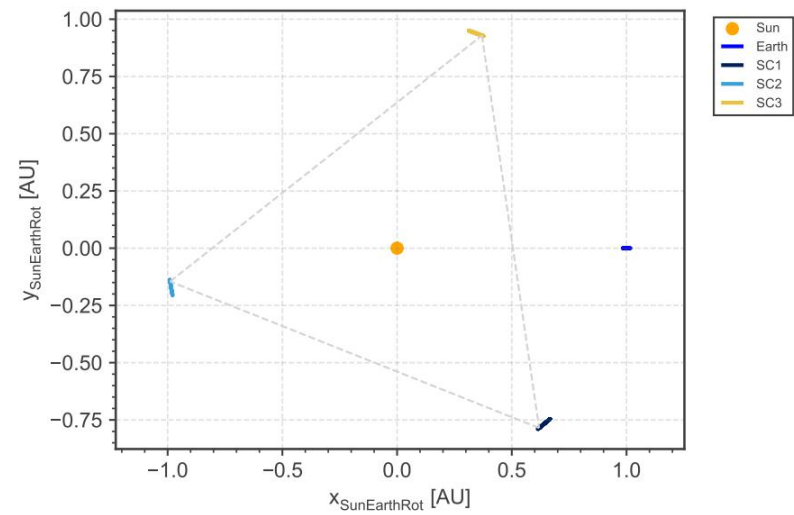
¹Mission Analysis Section, European Space Agency, Darmstadt, Germany

²University of Glasgow, Glasgow G12 8QQ, United Kingdom

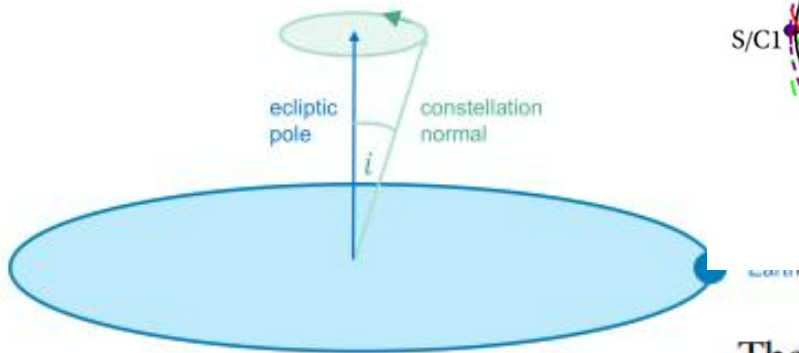
E-mail: waldemar.martens@esa.int

Abstract. Within its Voyage 2050 planning cycle, the European Space Agency (ESA) is considering long-term large class science mission themes. Gravitational-wave astronomy is among the topics under study. This paper presents “LISAmix”, a gravitational-wave interferometer concept consisting of three spacecraft located close to the Sun-Earth libration points L3, L4 and L5, forming a triangular constellation with an arm length of 259 million kilometers (to be compared to LISA’s 2.5 million kilometer arms). This is the largest triangular formation that can be reached from Earth without a major leap in mission complexity and cost. The sensitivity curve of such a detector is at least two orders of magnitude lower in amplitude than that of LISA. Depending on the choice of other instrument parameters, this makes the detector sensitive to gravitational waves in the μHz range and opens a new window for gravitational-wave astronomy, not covered by any other planned detector concept. We analyze in detail the constellation stability for a 10-year mission in the full numerical model and compute the orbit transfers using a European launcher and chemical propulsion. The payload design parameters are assessed, and the expected sensitivity curve is compared with a number of potential gravitational-wave sources. No show stoppers are identified at this point of the analysis.

Keywords: gravitational-wave detector, LISA, Voyage 2050

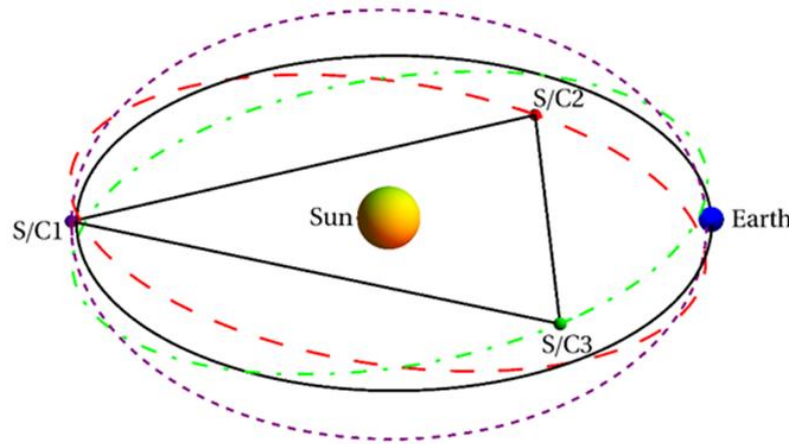


LISAmax: The constellation normal will precess around the ecliptic pole with a period of one year.



2023

LISAmax

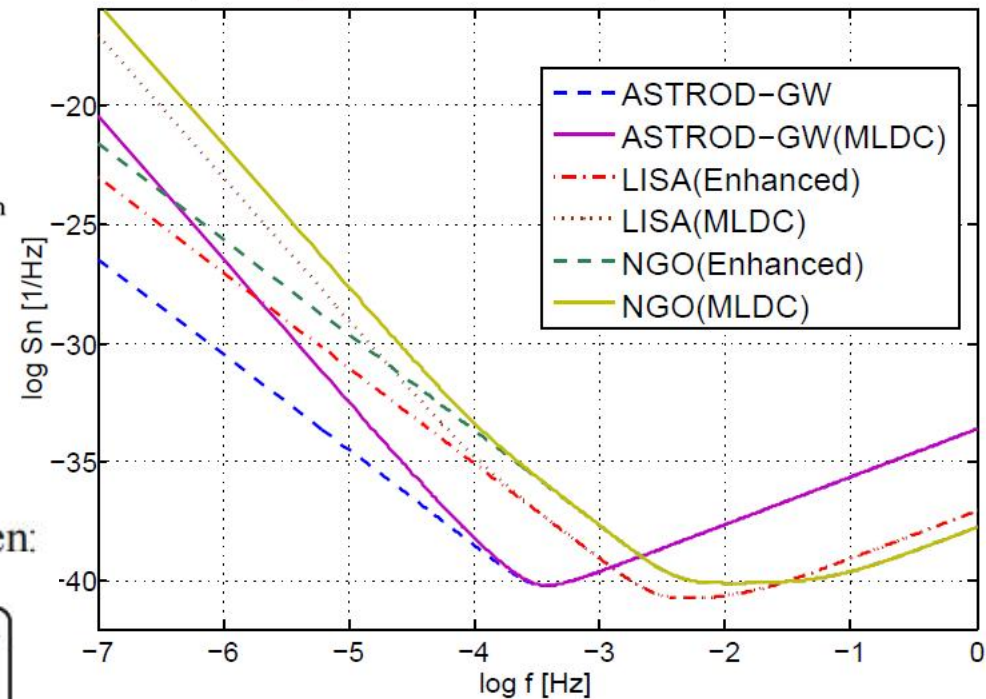


The normalized unit normal vector \underline{n} is then:

$$\underline{n} = [\sin^2 \lambda + (1 - \xi/2)^2]^{1/2} \begin{bmatrix} -\sin \lambda \cos 2\omega t \\ -\sin \lambda \sin 2\omega t \\ (1 - \xi/2) \end{bmatrix}.$$

Precession period: **Half Year**

Noise power spectra of ASTROD-GW, LISA and NGO/eLISA



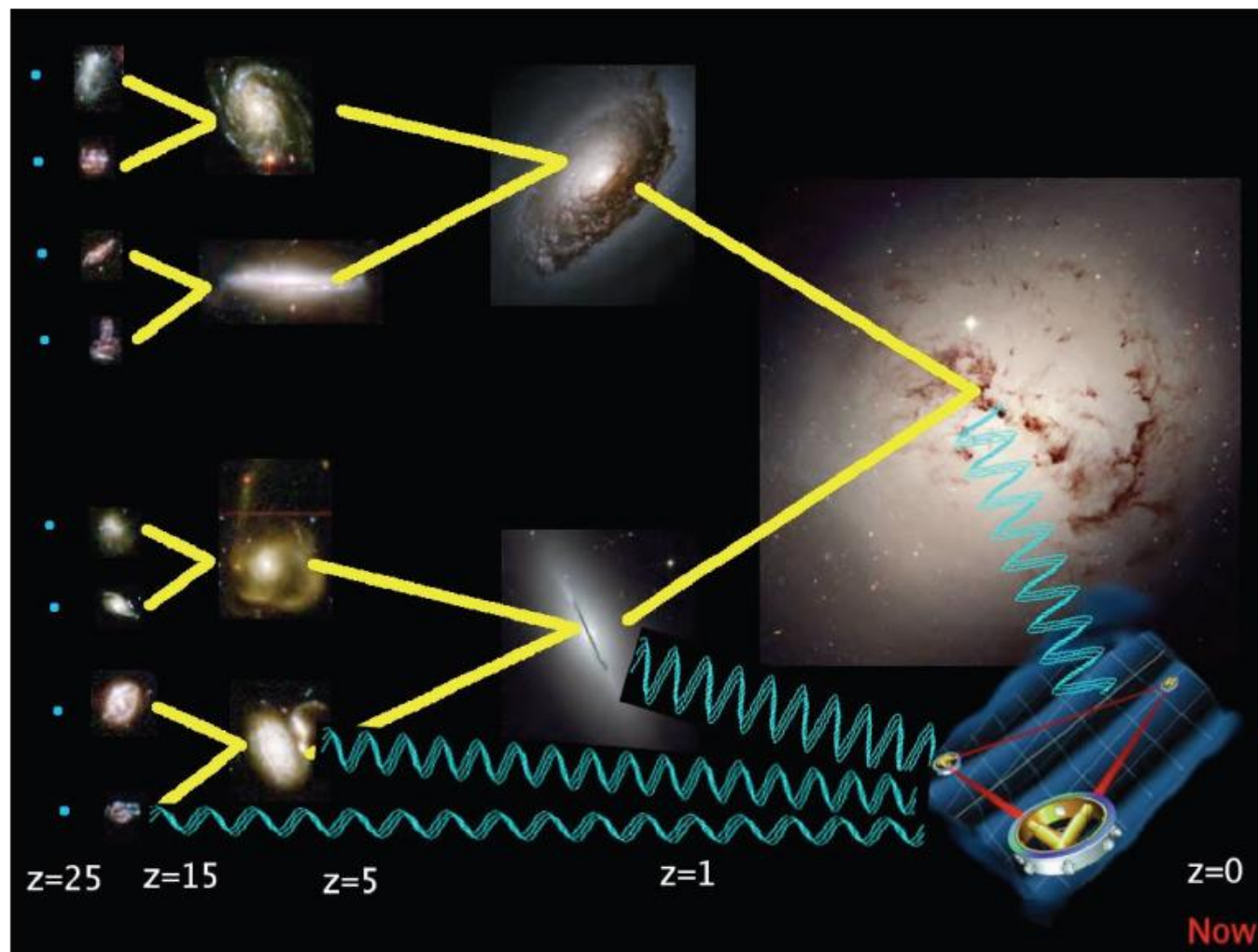
ASTROD-GW
2013 paper

More about ASTROD-GW (G. Wang & WTN)

- Second generation TDI good for Laser Frequency suppression
- Angular resolution: 2 orders better than LISA below 3 mHz

Nominal Orbit Inclination λ	Fractional arm length variation (2 body gravitational field)	Arm length variation (2 body gravitational field)	Doppler velocity variation (2 body gravitational field)	Simulated Doppler velocity variation with planetary perturbations (10 years)	Simulated arm length variation with planetary perturbations (10 years)
0°	0	0	0	3 m/s	6×10^{-4} AU
0.5°	0.19×10^{-4}	0.33×10^{-4} AU	2.0 m/s	4 m/s	6×10^{-4} AU
1°	0.76×10^{-4}	1.32×10^{-4} AU	7.9 m/s	10 m/s	7×10^{-4} AU
1.5°	1.71×10^{-4}	2.97×10^{-4} AU	18 m/s	20 m/s	10×10^{-4} AU
2°	3.04×10^{-4}	5.27×10^{-4} AU	32 m/s	34 m/s	13×10^{-4} AU
2.5°	4.75×10^{-4}	8.23×10^{-4} AU	49 m/s	51 m/s	18×10^{-4} AU
3°	6.84×10^{-4}	11.8×10^{-4} AU	71 m/s	73 m/s	24×10^{-4} AU

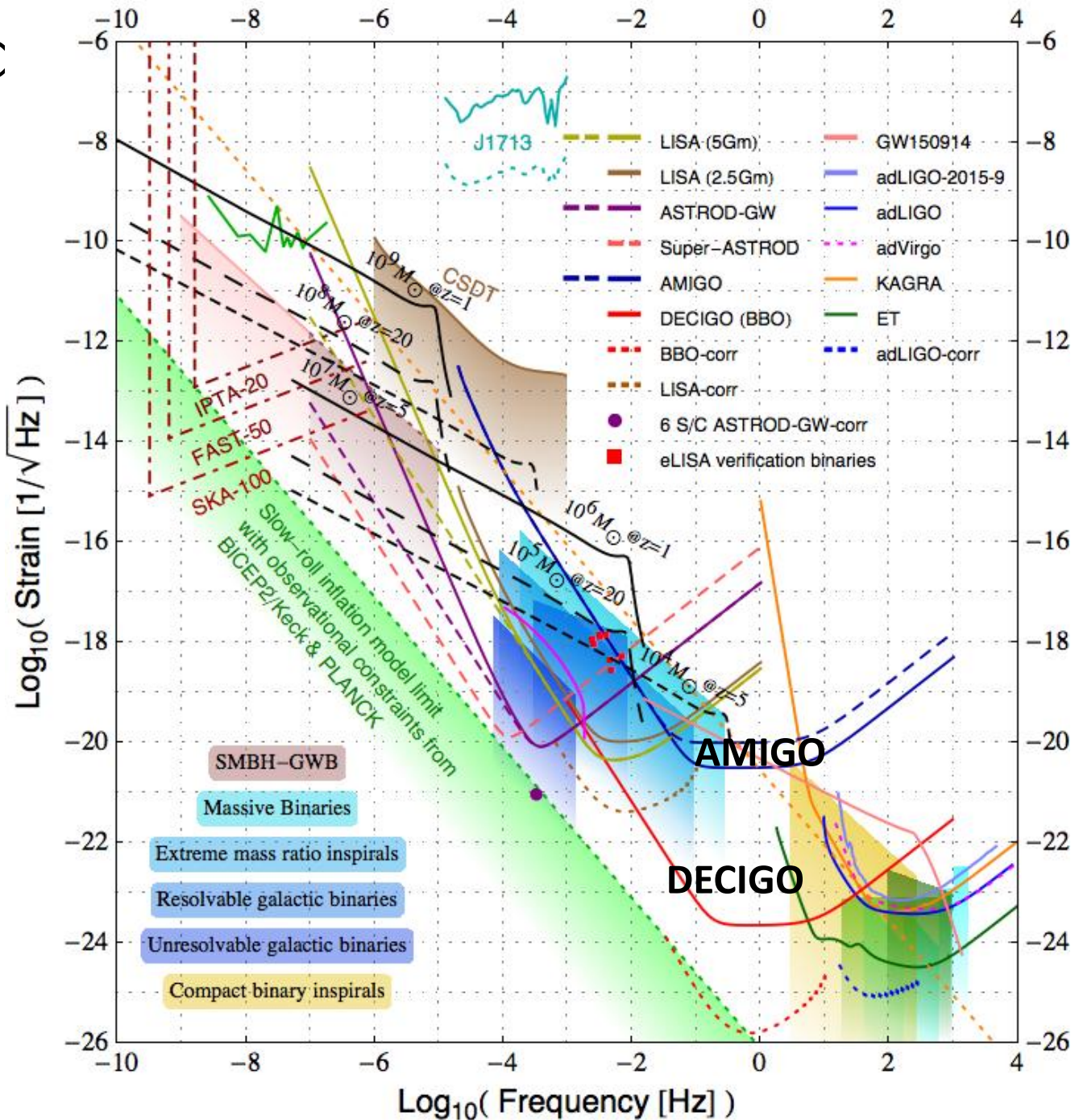
Massive Black Hole Systems: Massive BH Mergers & Extreme Mass Ratio Mergers (EMRIs)



Gap 1 – middle-frequency band

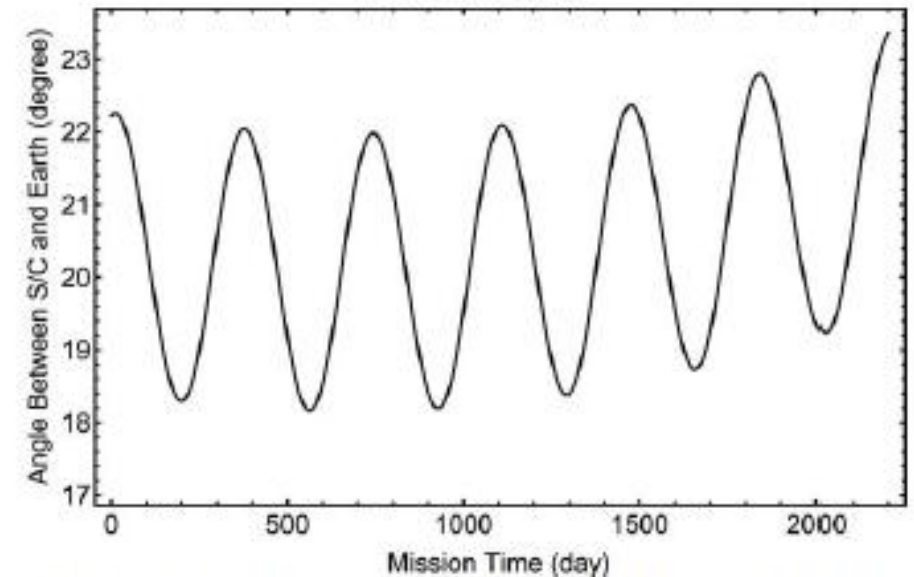
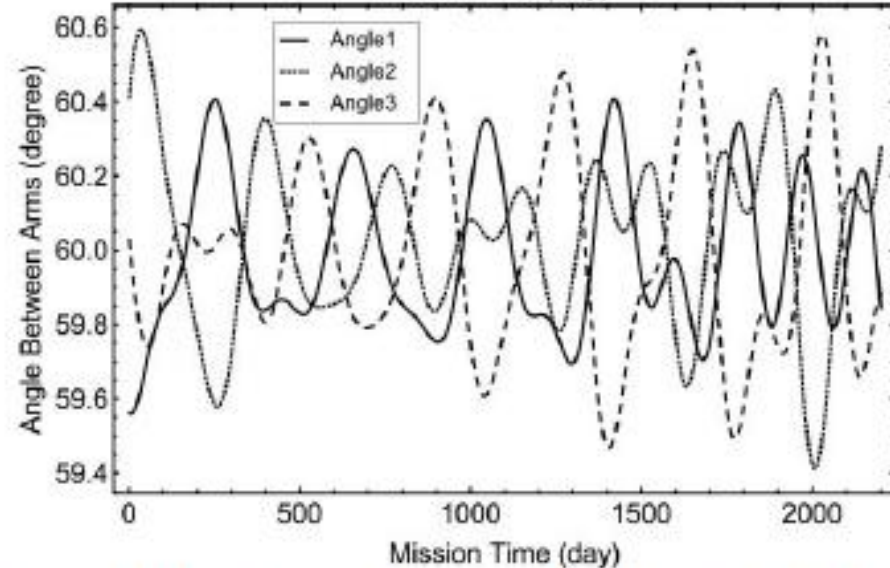
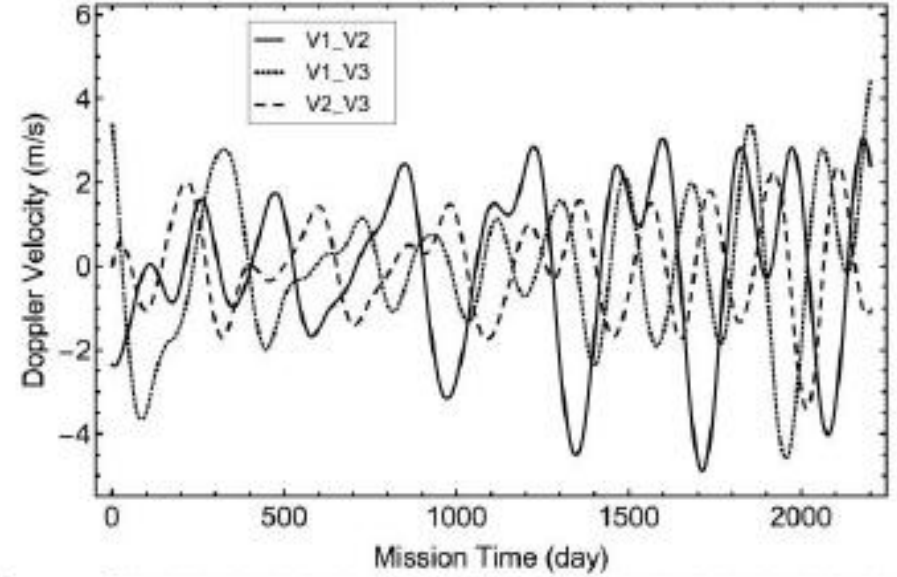
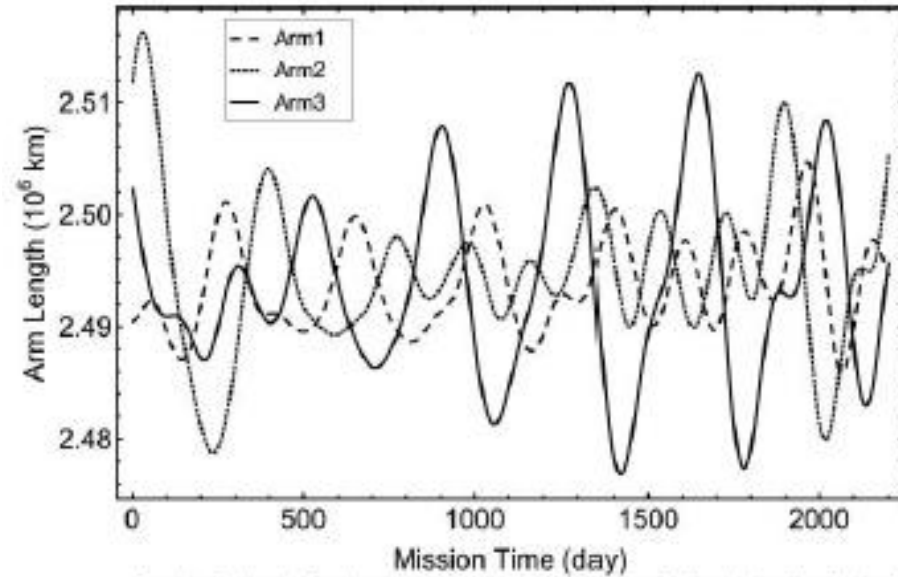
Gap 2 – μHz band

- **Acceleration Noise is local:** Strain is inversely proportional to arm length, hence with the same acceleration noise, the strain noise is decreased toward longer armlength.
- **Antenna limitation:** high frequency sensitivity is restricted by antenna arm length
- **Shot noise:** The shot noise sensitivity in the strain for GW detection is inversely proportional to $P^{1/2}L$ with P the received power and L the distance or arm length. Since P is inversely proportional to L^2 and $P^{1/2}L$ is constant, this sensitivity limit is independent of the distance. For 1-2 W emitting power, the limit is around 10^{-20} – 10^{-21} $\text{Hz}^{-1/2}$ (depending on telescope diameter/laser beam divergence).
- Sometimes, there is a flat region, limited by shot noise



Variations of the arm lengths, velocities in the line-of-sight direction, formation angles and angle between barycenter of the S/Cs and Earth

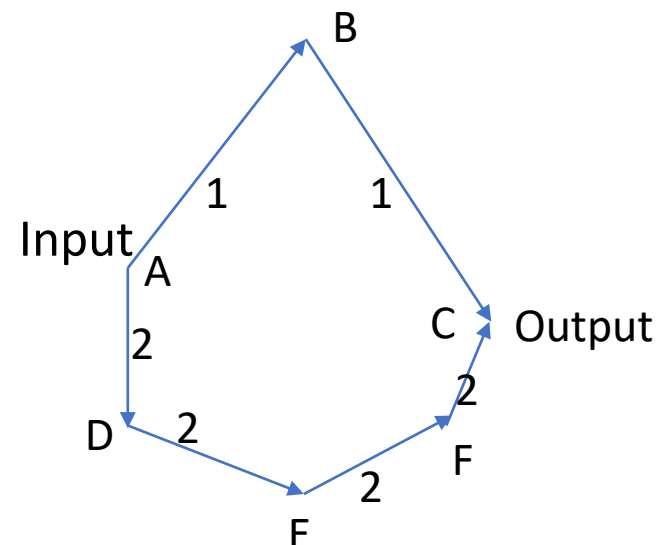
LISA
Orbit
Design
18-22°
behind
the Earth
In
2200 day



有兩種干涉雜訊 (噪聲):

- (I) 1, 2兩臂之光程差所對應的頻率雜訊以及
- (II) 激光在 1臂和2 臂傳播過程中和其間 (A, B, C, D, E, F)

探測/鎖相放大過程中所嵌入的雜訊



第一種雜訊可以利用無拖曳航天器 (或常等臂編隊航天) 軌道的穩定性和激光偽碼訊號的傳遞決定二路徑光程差及二路徑中激光到達各航天器的本地時間。而本地時間和太陽系質心固有時之間的轉換可以用激光偽碼測距和的穩定性決定之。

•激光和激光乘載的偽碼同時抵達各航天器，故激光抵達各航天器和由偽碼定出的時間相同，即各航天器時鐘或超穩定振盪器記錄的時間 (航天器的固有時，亦即航天器的本地時間)。因之，對各航天器時鐘或超穩定振盪器的要求可以寬鬆些。

•偽碼測距可以由 Ka 微波通訊定距，航天器定軌以及行星曆檢驗確認。同時，這些數據也可用來改良行星曆

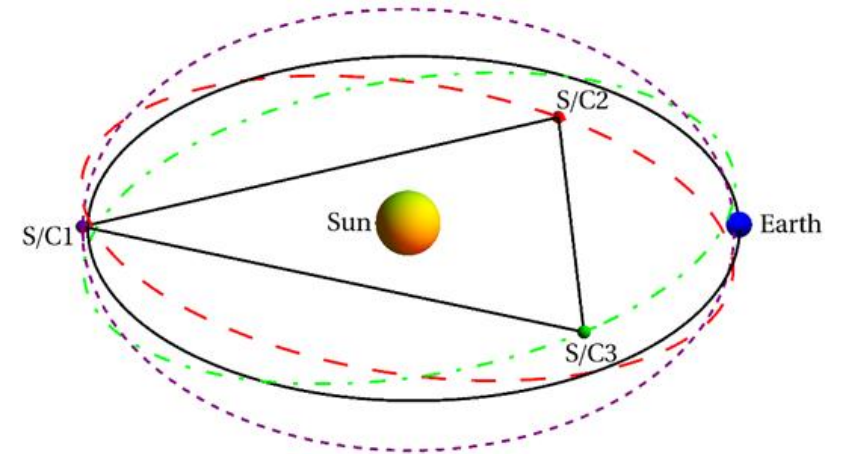
Frequency Noise

- The laser frequency noise can be treated as the white noise and has a one-sided (square root) spectral density of $30 \text{ Hz}/\sqrt{\text{Hz}}$ corresponding to
- the power spectrum density $|C(f)| \approx 1 \times 10^{-13} \text{ Hz}^{-1/2}$ for relevant GW frequency, i.e. $10^{-5} - 1 \text{ Hz}$, i.e. the laser frequency stability in this frequency range is $1 \times 10^{-13} \text{ Hz}^{-1/2}$
- For a path length difference of 30 meters, the noise is $30 \times 10^{-13} \text{ mHz}^{-1/2}$, i.e. the strain noise is $1 \times 10^{-21} \text{ Hz}^{-1/2}$

Time Delay Interferometry (TDI)

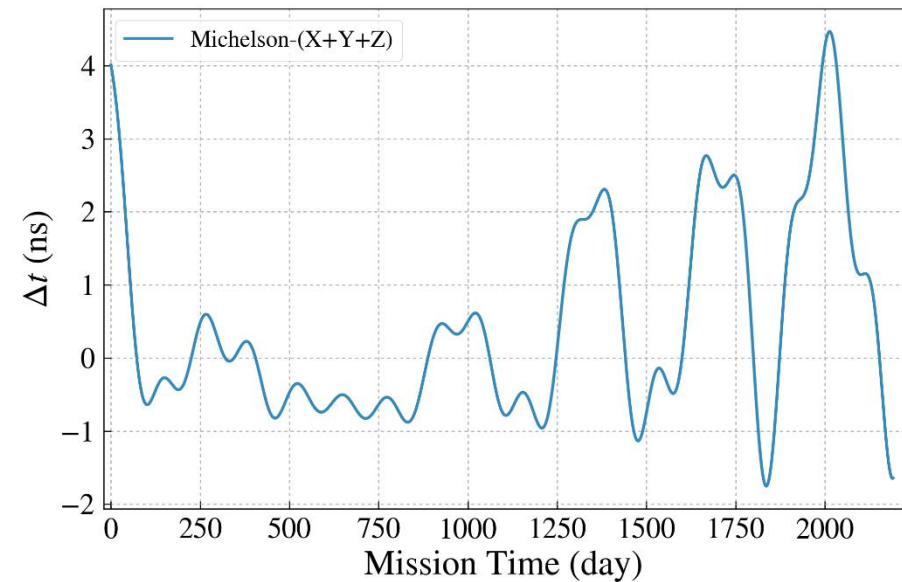
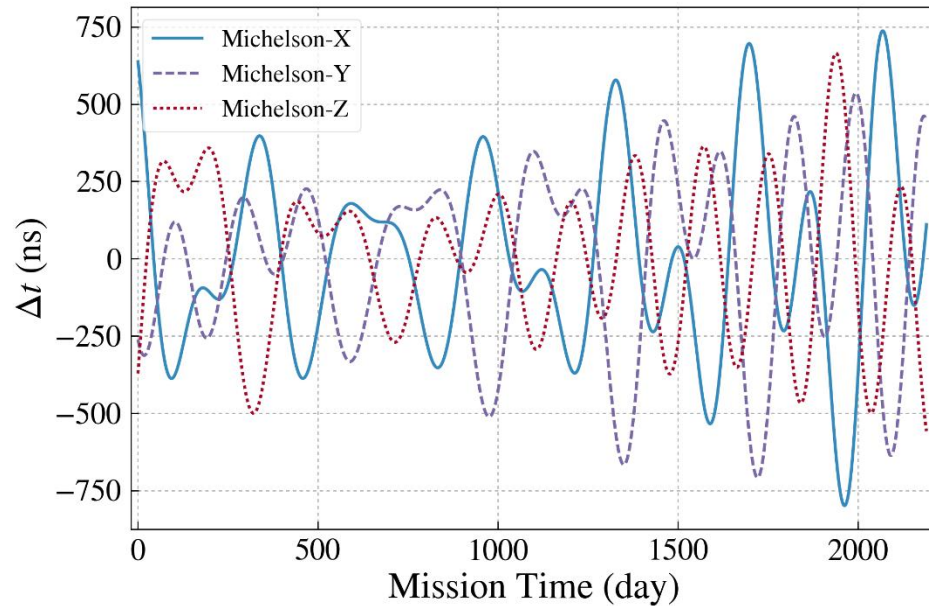
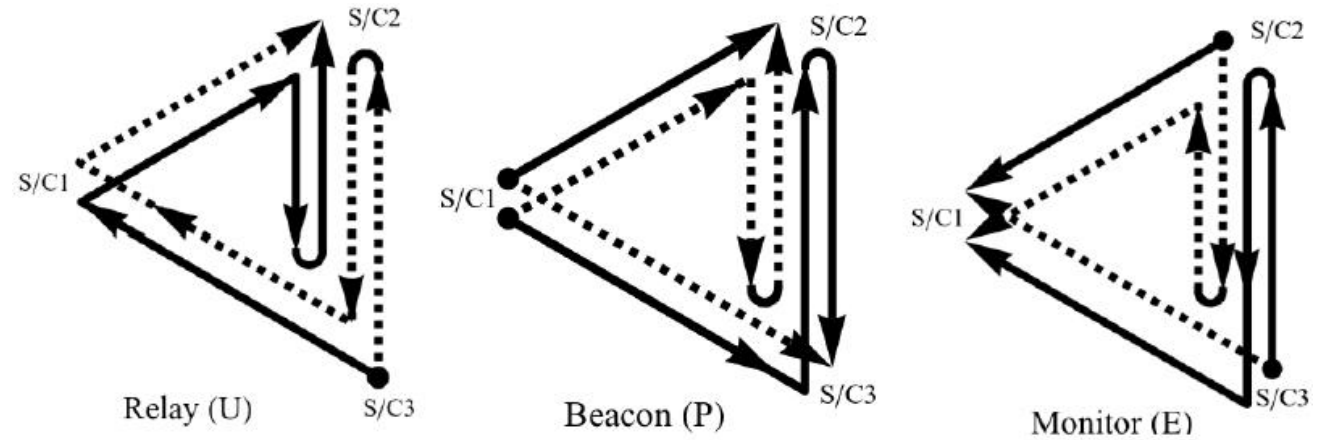
first used in the study of ASTROD mission concept in the 1990s (Ni *et al.* 1997a, 1997b), two TDI configurations were used during the study of ASTROD interferometry and the path length differences were numerically obtained using Newtonian dynamics

- These two TDI configurations are the unequal arm Michelson TDI configuration and the Sagnac TDI configuration for three spacecraft formation flight. The principle is to have two split laser beams to go to Paths 1 and 2 and interfere at their end path. For unequal arm Michelson TDI configuration, one laser beam starts from spacecraft 1 (S/C1) directed to and received by spacecraft 2 (S/C2), and optical phase locking the local laser in S/C2; the phase locked laser beam is then directed to and received by S/C1, and optical phase locking another local laser in S/C1; and so on to return to S/C1:
- Path 1: S/C1 → S/C2 → S/C1 → S/C3 → S/C1. (1)
- The second laser beam starts from S/C1 also:
- Path 2: S/C1 → S/C3 → S/C1 → S/C2 → S/C1, (2)
- to return to S/C1 and to interfere with the first beam.
- If the two paths has exactly the same optical path length,
- the laser frequency noises cancel out; if the optical path length difference is small, the laser frequency noises cancel to a large extent. In the Sagnac TDI configuration, the two paths are:
- Path 1: S/C1 → S/C2 → S/C3 → S/C1, Path 2: S/C1 → S/C3 → S/C2 → S/C1.



Unequal-arm Michelson X , Y & Z TDIs and its sum $X+Y+Z$ for new LISA

- 1999 Armstrong, Estabrook, Tinto, X , Y & Z TDIs $X+Y+Z$ for LISA
- Vallisneri 2005 (U, P, E)
- Tinto & Dhurandhar review 2014



e

Orbit Design I – the initial choice of initial conditions

- Define X_{fk}, Y_{fk}, Z_{fk} , ($k = 1, 2, 3$) to be

$$X_{fk} = R (\cos \psi_k + e) \cos \varepsilon ,$$

$\psi_k + e \sin \psi_k = \Omega (t - t_0) - 120^\circ(k - 1)$, for $k = 1, 2, 3$.
the eccentric anomaly

$$Y_{fk} = R (1 - e^2)^{1/2} \sin \psi_k ,$$

$$Z_{fk} = R (\cos \psi_k + e) \sin \varepsilon .$$

- Define $X_{f(k)}, Y_{f(k)}, Z_{f(k)}$, ($k = 1, 2, 3$), i.e., $X_{f(1)}, Y_{f(1)}, Z_{f(1)}$; $X_{f(2)}, Y_{f(2)}, Z_{f(2)}$; $X_{f(3)}, Y_{f(3)}, Z_{f(3)}$ to be

$$X_{f(k)} = X_{fk} \cos[120^\circ(k - 1) + \varphi_0] - Y_{fk} \sin[120^\circ(k - 1) + \varphi_0],$$

$$Y_{f(k)} = X_{fk} \sin[120^\circ(k - 1) + \varphi_0] + Y_{fk} \cos[120^\circ(k - 1) + \varphi_0],$$

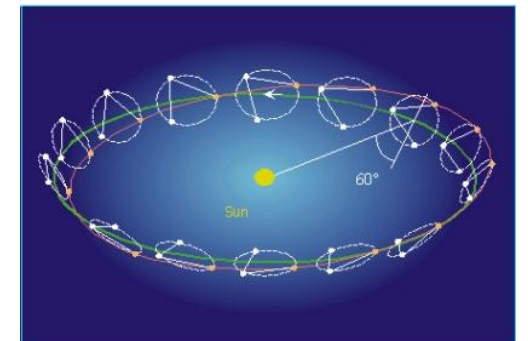
$$Z_{f(k)} = Z_{fk} .$$

- The three S/C orbits are (for one-body central problem) are

$$\mathbf{R}_{S/C1} = (X_{f(1)}, Y_{f(1)}, Z_{f(1)}),$$

$$\mathbf{R}_{S/C2} = (X_{f(2)}, Y_{f(2)}, Z_{f(2)}),$$

$$\mathbf{R}_{S/C3} = (X_{f(3)}, Y_{f(3)}, Z_{f(3)}).$$



Using ephemeris framework for design and TDI numerical calculation

$$\begin{aligned}
 ds^2 = & \left[1 - 2 \sum_i \frac{m_i}{r_i} + 2\beta \left(\sum_i \frac{m_i}{r_i} \right)^2 + (4\beta - 2) \sum_i \frac{m_i}{r_i} \sum_{j \neq i} \frac{m_j}{r_{ij}} \right. \\
 & \left. - c^{-2} \sum_i \frac{m_i}{r_i} \left(2(\gamma + 1) \dot{\mathbf{x}}_i^2 - \mathbf{r}_i \cdot \ddot{\mathbf{x}}_i - \frac{1}{r_i^2} (\mathbf{r}_i \cdot \dot{\mathbf{x}}_i)^2 \right) + \frac{m_1 R_1^2}{r_1^3} J_2 \left(3 \left(\frac{\mathbf{r}_1 \cdot \hat{\mathbf{z}}}{r_1} \right)^2 - 1 \right) \right] c^2 dt^2 \\
 & + 2c^{-1} \sum_i \frac{m_i}{r_i} \left((2\gamma + 2) \dot{\mathbf{x}}_i \right) \cdot d\mathbf{x} c dt - \left[1 + 2\gamma \sum_i \frac{m_i}{r_i} \right] (d\mathbf{x})^2
 \end{aligned} \tag{40}$$

$$\ddot{\mathbf{x}}_i = - \sum_{j \neq i} \frac{GM_j}{r_{ij}^3} \mathbf{r}_{ij} + \sum_{j \neq i} m_j (A_{ij} \mathbf{r}_{ij} + B_{ij} \dot{\mathbf{r}}_{ij}),$$

$$\begin{aligned}
 A_{ij} = & \frac{\dot{\mathbf{x}}_i^2}{r_{ij}^3} - (\gamma + 1) \frac{\dot{\mathbf{r}}_{ij}^2}{r_{ij}^3} + \frac{3}{2r_{ij}^5} (\mathbf{r}_{ij} \cdot \dot{\mathbf{x}}_j)^2 + G \left[(2\gamma + 2\beta + 1) M_i + (2\gamma + 2\beta) M_j \right] \frac{1}{r_{ij}^4} \\
 & + \sum_{k \neq i, j} GM_k \left[(2\gamma + 2\beta) \frac{1}{r_{ij}^3 r_{ik}} + (2\beta - 1) \frac{1}{r_{ij}^3 r_{jk}} + \frac{2(\gamma + 1)}{r_{ij}^3 r_{jk}} - (2\gamma + \frac{3}{2}) \frac{1}{r_{ik} r_{jk}^3} - \frac{1}{2r_{jk}^3} \frac{\mathbf{r}_{ij} \cdot \mathbf{r}_{ik}}{r_{ij}^3} \right],
 \end{aligned}$$

$$B_{ij} = \frac{1}{r_{ij}^3} \left[(2\gamma + 2) (\mathbf{r}_{ij} \cdot \dot{\mathbf{r}}_{ij}) + (\mathbf{r}_{ij} \cdot \dot{\mathbf{x}}_j) \right].$$

3 complete ephemeris + 1 ephemeris framework

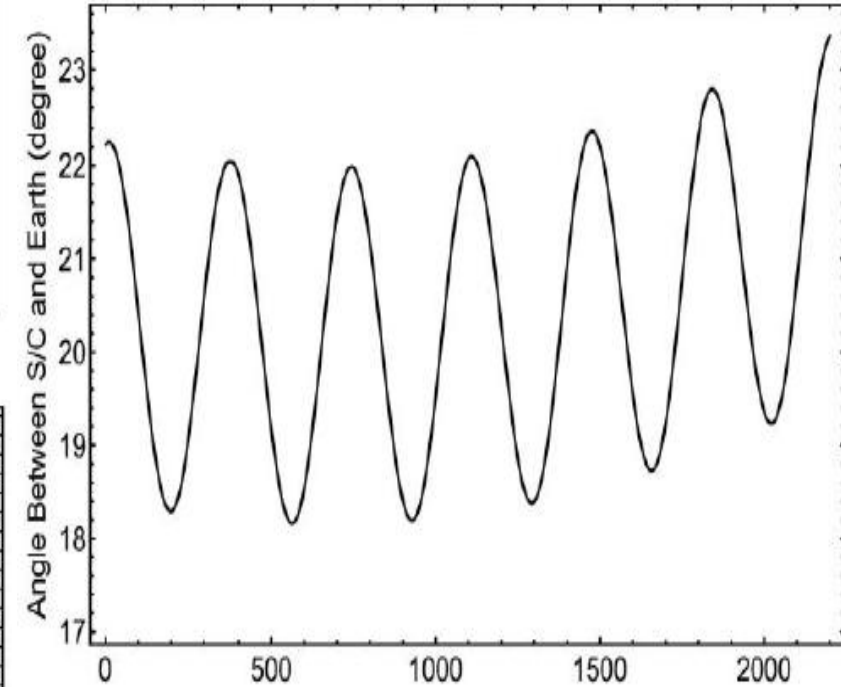
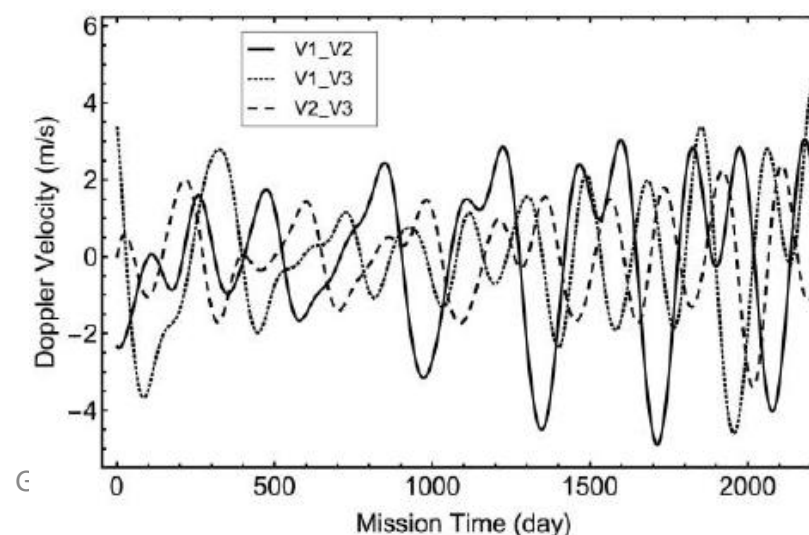
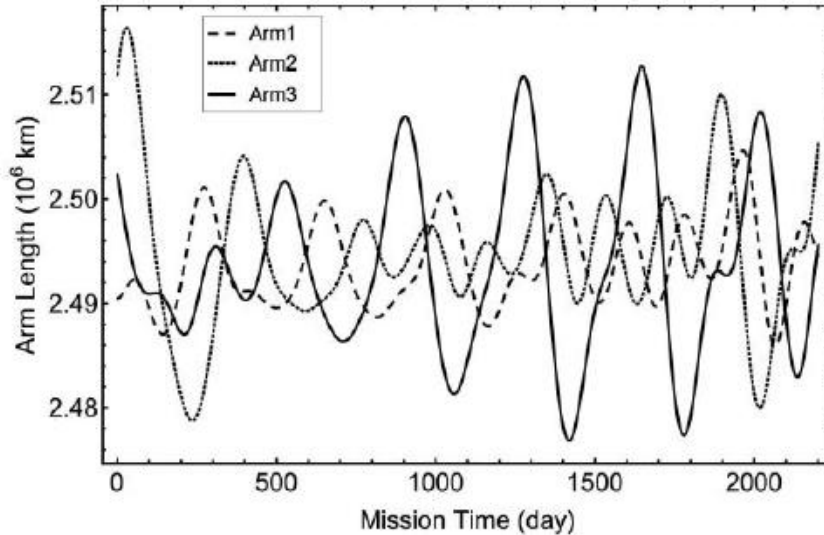
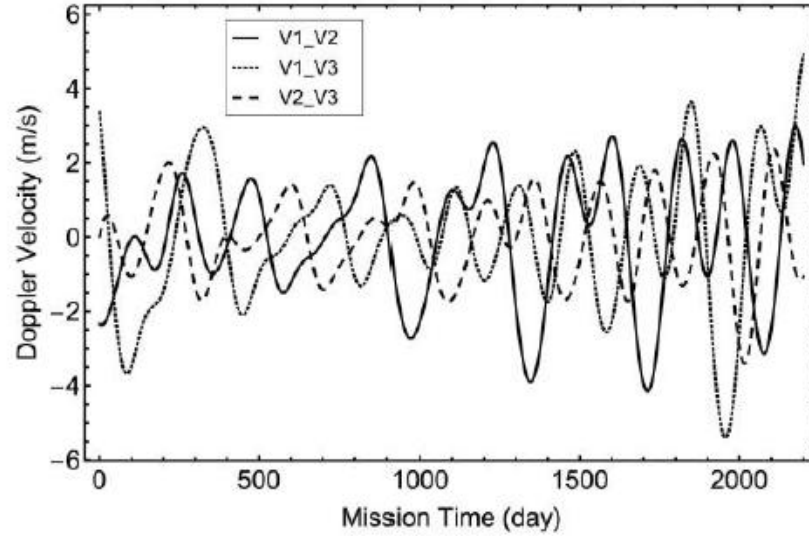
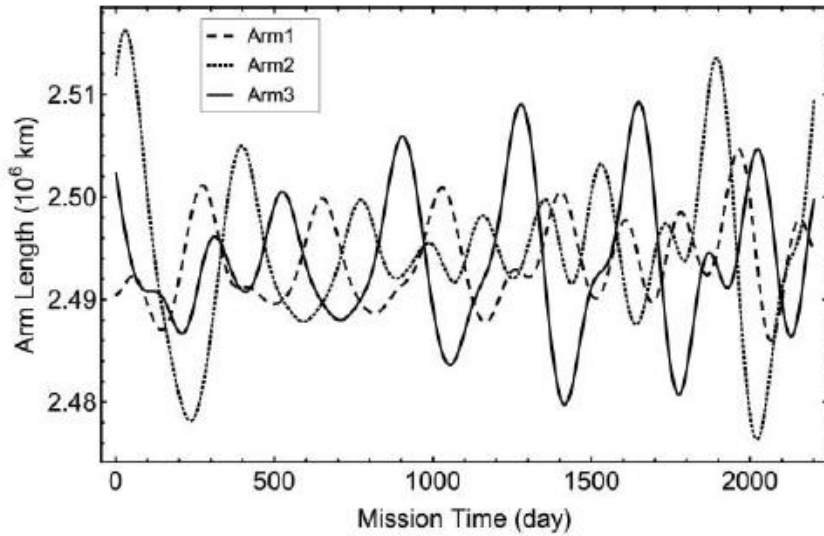
- DE: Development Ephemerides
- EPM: Ephemerides of Planets and Moon
- INPOP: Intégrateur Numérique Planétaire de l'Observatoire de Paris
- CGC: Center for Gravitation and Cosmology Ephemeris Framework

Orbit design for New LISA (arm length 2.5 Gm)

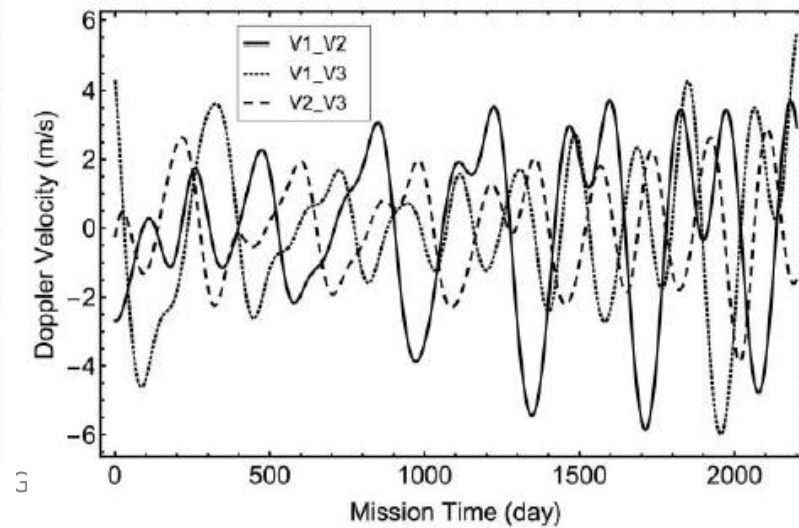
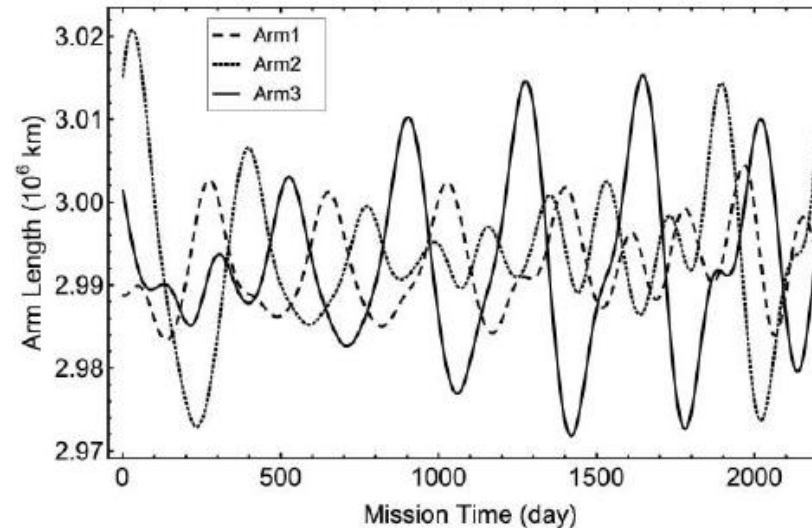
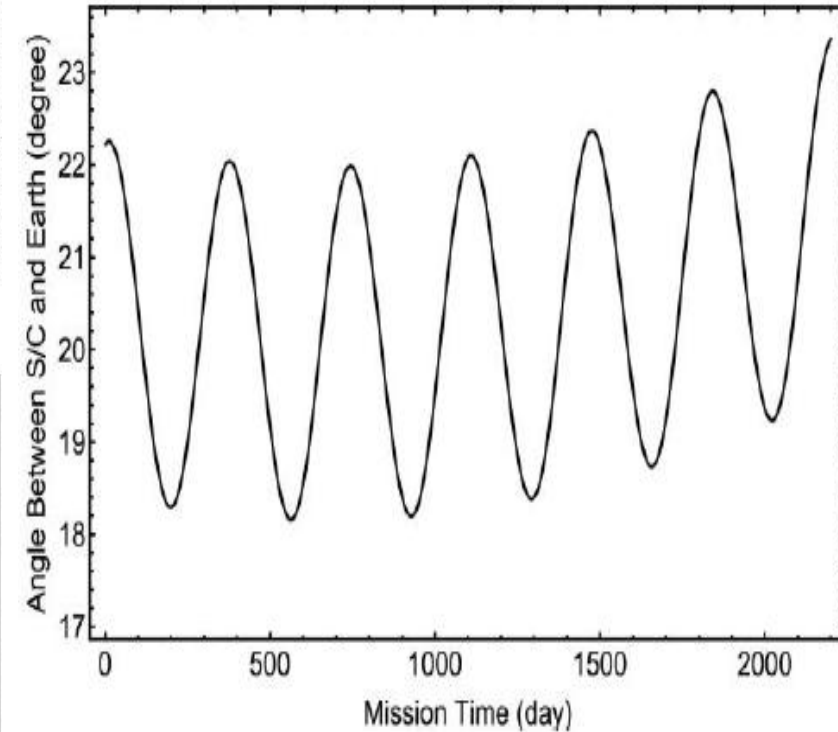
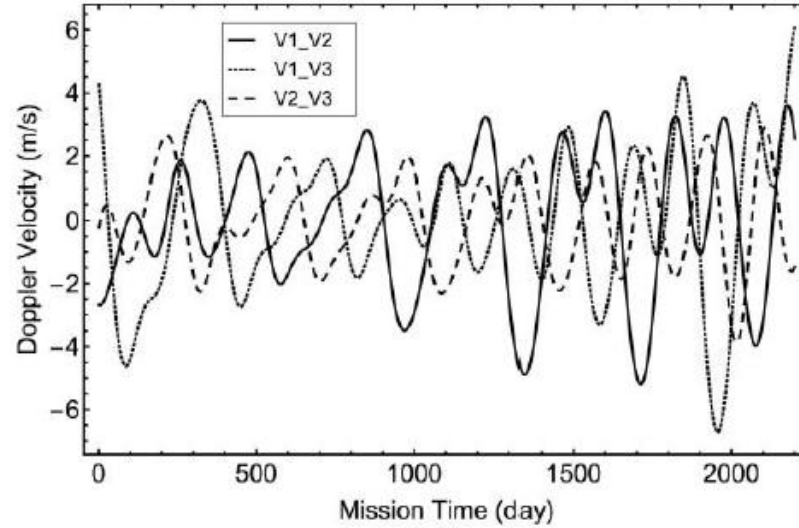
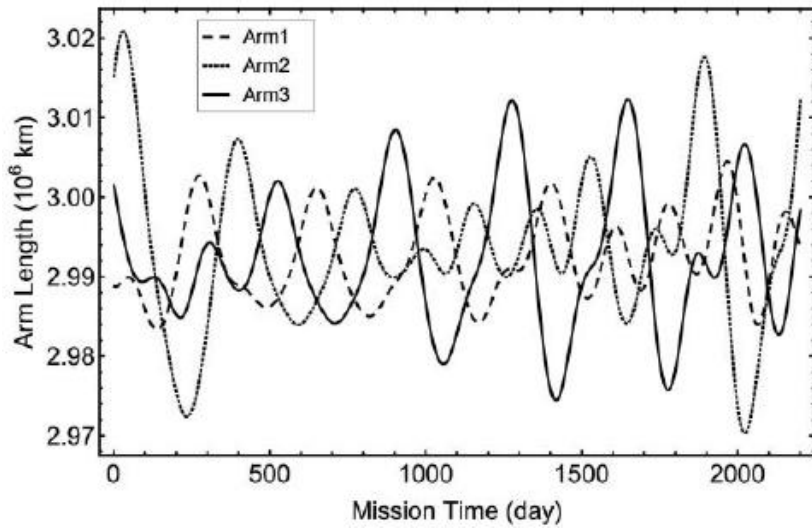
initial epoch: 2028-Mar-22nd 12:00:00 for 2200 days

		Initial choice of S/C initial states		Initial states of S/C after final optimization
S/C1 Position (AU)	X	-9.342358697598E-01	adjust to =>	-9.342355891858E-01
	Y	3.222028021891E-01		3.222027047288E-01
	Z	1.415510901823E-01		1.415510473840E-01
S/C1 Velocity (AU/day)	V _x	-6.020533666442E-03	=	-6.020533666442E-03
	V _y	-1.471303796371E-02		-1.471303796371E-02
	V _z	-6.532104563056E-03		-6.532104563056E-03
S/C2 Position (AU)	X	-9.422917194822E-01	=	-9.422917194822E-01
	Y	3.075956329521E-01		3.075956329521E-01
	Z	1.403200701890E-01		1.403200701890E-01
S/C2 Velocity (AU/day)	V _x	-5.875601408922E-03	=	-5.875601408922E-03
	V _y	-1.480936170059E-02		-1.480936170059E-02
	V _z	-6.319195852807E-03		-6.319195852807E-03
S/C3 Position (AU)	X	-9.335382669969E-01	=	-9.335382669969E-01
	Y	3.132742531958E-01		3.132742531958E-01
	Z	1.273476800288E-01		1.273476800288E-01
S/C3 Velocity (AU/day)	V _x	-5.949351791423E-03	=	-5.949351791423E-03
	V _y	-1.490443611747E-02		-1.490443611747E-02
	V _z	-6.410590762560E-03		-6.410590762560E-03

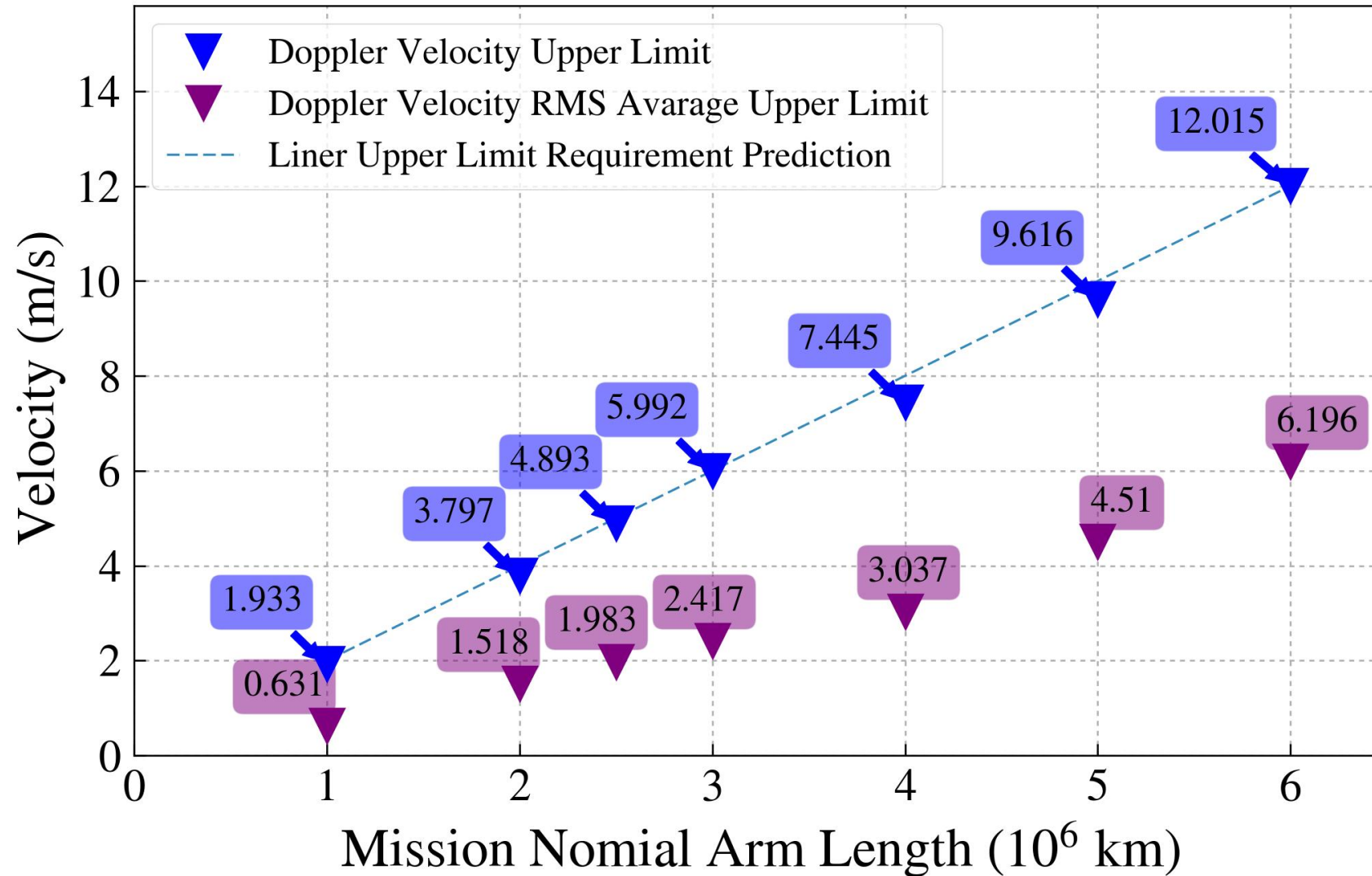
Variations of the arm lengths and the velocities in the line of sight direction in 2200 days for the LISA S/C configuration with initial condition adjustment



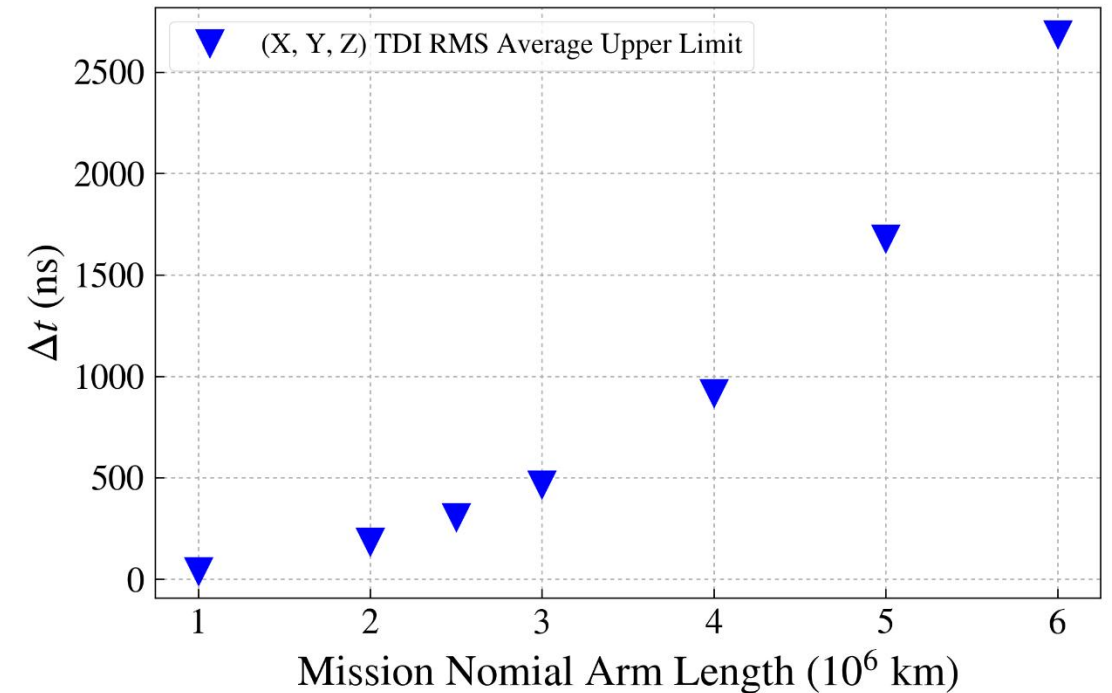
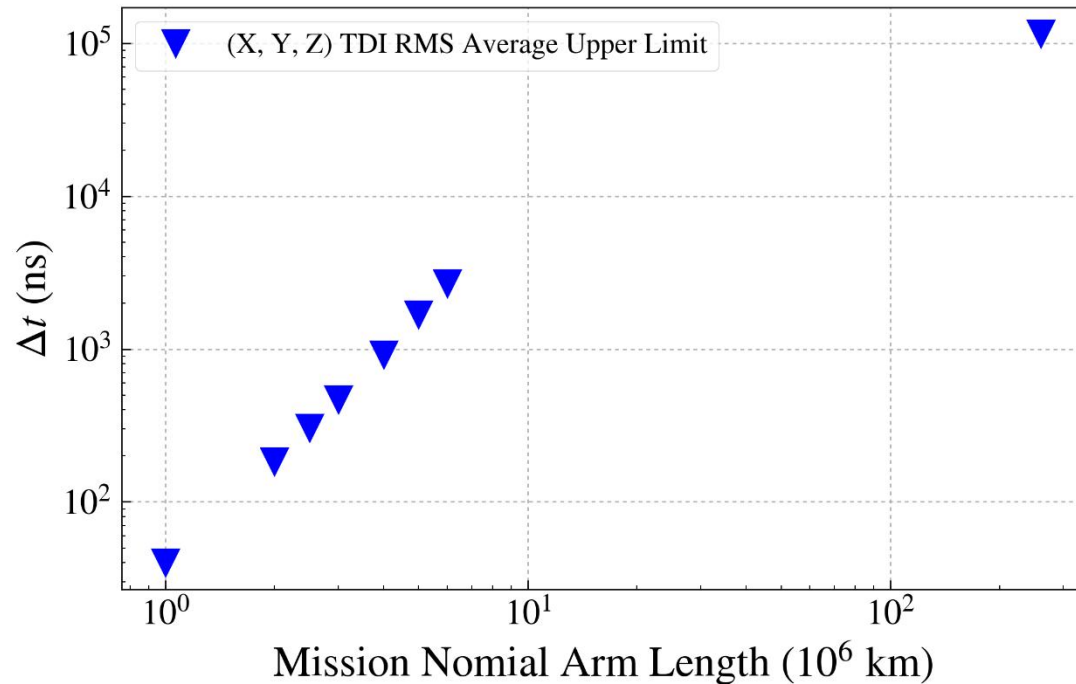
Variations of the arm lengths and the velocities in the line of sight direction in 2200 days for the TAIJI S/C configuration with initial condition adjustment



A comparison of cases for different arm lengths (G Wang & WTN)



(X, Y, Z)TDI time-delay difference vs. epoch



Comparison the resulting path length differences for the X, Y, Z, X+Y+Z and TDI Sagnac configurations from different arm lengths for various mission proposals: 1 Gm (eLISA), 2 Gm (an NGO-LISA-type mission with this nominal arm length), 2.5 Gm (new LISA), 3 Gm (TAIJI), 4 Gm, 5 Gm (original LISA), 2 Gm, and 260 Gm (ASTROD-GW).

1 st generation TDI configuration	TDI path difference ΔL							
	eLISA/NGO [ns] max, min, rms average	NGO-LISA-type with 2 Gm arm length [ns]	New LISA [ns] max, min, rms average	TAIJI [ns] max, min rms average	LISA-type with 4 Gm arm length max, min, rms average	LISA-type with 5 Gm arm length max, min, rms average	LISA-type with 6 Gm arm length max, min, rms average	ASTROD-GW [μ s] (Wang and Ni, 2015)
X	-119 to 99, 40	-487 to 454, 184	-799 to 737, 306	-1221 to 1084, 467	-2020 to 1748, 812	-3286 to 2967, 1417	-5032 to 4466, 2285	-194 to 182, 111
Y	-84 to 100, 38	-434 to 359, 176	-708 to 537, 289	-1039 to 740, 431	-2009 to 1837, 917	-3543 to 3262, 1680	-5438 to 5201, 2686	-190 to 196, 113
Z	-90 to 106, 37	-339 to 405, 152	-558 to 665, 248	-887 to 1030, 380	-2156 to 1894, 826	-3724 to 3096, 1471	-5985 to 4902, 2434	-200 to 194, 115
X+Y+Z	[-0.074, 0.777], 0.243	[-0.826, 2.910], 0.953	[-1.754, 4.466], 1.410	[-3.273, 6.243], 1.949	[-6.555, 7.909], 3.564	[-15.693, 8.743], 8.757	[-31.632, 7.665], 19.397	<i>[-58, 24], 23</i>
Sagnac- α	-1965 to -1857, 1906	-7865 to -7401, 7623	-12309 to -11551, 11911	-17759 to -16623, 17151	-31490 to -29650, 30494	-49273 to -46213, 47644	-71096 to -66426, 68601	-257627 to -257438, 257531
Sagnac- β	-1948 to -1855, 1907	-7838 to -7434, 7626	-12262 to -11624, 11915	-17666 to -16749, 17156	-31512 to -29626, 30496	-49466 to -46101, 47649	-71437 to -66137, 68602	-257626 to -257430, 257529
Sagnac- γ	[-1952, -1853], 1906	[-7799, -7428], 7620	[-12199, -11593], 11906	[-17611, -16661], 17145	[-31610, -29581], 30474	[-49581, -46142], 47610	[-71723, -66184], 68546	[-257629, -257433], 257530

Relay-U	[-79, 77], 32	[-298, 297], 137	[-502, 467], 222	[-781, 657], 333	[-1978, 1331], 773	[-3479, 2322], 1412	[-5584, 3511], 2295	[-175, 168], 100
Relay-V	[-102, 80], 34	[-415, 348], 144	[-689, 545], 238	[-1069, 776], 367	[-1895, 1480], 678	[-3128, 2507], 1175	[-4908, 3973], 1940	[-156, 172], 96
Relay-W	[-79, 96], 35	[-405, 375], 164	[-666, 596], 271	[-987, 879], 407	[-1809, 1265], 762	[-3167, 1933], 1370	[-4865, 2941], 2176	[-176, 167], 98
Beacon-P	[-60, 49], 20	[-245, 226], 92	[-401, 368], 153	[-612, 541], 233	[-1010, 876], 406	[-1639, 1490], 708	[-2505, 2247], 1141	[-97, 91], 56
Beacon-Q	[-43, 50], 19	[-218, 178], 89	[-356, 267], 145	[-521, 367], 216	[-1005, 921], 459	[-1770, 1637], 841	[-2711, 2613], 1344	[-95, 98], 57
Beacon-R	[-46, 53], 19	[-171, 202], 76	[-278, 332], 124	[-442, 514], 190	[-1076, 948], 413	[-1856, 1552], 736	[-2981, 2462], 1218	[-100, 97], 58
Monitor-E	[-49, 60], 20	[-226, 245], 92	[-368, 401], 153	[-541, 612], 233	[-876, 1010], 406	[-1490, 1639], 708	[-2247, 2505], 1141	[-91, 97], 56
Monitor-F	[-50, 43], 19	[-178, 218], 89	[-267, 356], 145	[-367, 521], 216	[-921, 1005], 459	[-1637, 1770], 841	[-2613, 2711], 1344	[-98, 95], 57
Monitor-G	[-53, 46], 19	[-202, 171], 76	[-332, 278], 124	[-514, 442], 190	[-948, 1076], 413	[-1552, 1856], 736	[-2462, 2981], 1218	[-97, 100], 58
Nominal arm length	1 Gm (1 Mkm)	2 Gm	2.5 Gm	3 Gm	4 Gm	5 Gm	6 Gm	260 Gm
Mission duration	2200 days	2200 days	2200 days	2200 days	2200 days	2200 days	2200 days	10 years
Requirement on ΔL	10 m (33 ns)	20 m (67 ns)	25 m (83 ns)	30 m (100 ns)	40 m (133 ns)	50 m (167 ns)	60 m (200 ns)	500 m (1670 ns)

[abba,baab]-1	[-0.01, 0.01], 0.002	[-0.02, 0.01], 0.002	[-0.02, 0.01], 0.003	[-0.02, 0.01], 0.003	[-0.02, 0.01], 0.004	[-0.02, 0.02], 0.005	[-0.03, 0.02], 0.007	[-0.91, 9.99], 0.50
[abba,baab]-2	[-0.011, 0.010], 0.002	[-0.018, 0.011], 0.002	[-0.012, 0.009], 0.002	[-0.011, 0.010], 0.002	[-0.016, 0.012], 0.003	[-0.021, 0.014], 0.004	[-0.027, 0.019], 0.006	[-0.69, 8.02], 0.50
[abba,baab]-3	[-0.010, 0.013], 0.002	[-0.013, 0.012], 0.002	[-0.013, 0.009], 0.002	[-0.017, 0.012], 0.002	[-0.017, 0.012], 0.003	[-0.022, 0.014], 0.005	[-0.027, 0.018], 0.007	[-19.39, 1.04], 0.60
Sagnac-Type α_{12-1}	[-0.17, 0.18], 0.07	[-1.3, 1.5], 0.7	[-2.7, 3.0], 1.3	[-4.8, 5.2], 2.2	[-11.6, 11.5], 5.4	[-23.2, 22.8], 11.2	[-42.0, 39.8], 20.6	[-92, 97], 57
Sagnac-Type α_{12-2}	[-0.06, 0.05], 0.02	[-0.5, 0.5], 0.2	[-0.9, 1.0], 0.4	[-1.7, 1.6], 0.8	[-3.9, 3.8], 1.8	[-7.9, 7.7], 4.0	[-15.1, 13.8], 7.5	[-41, 40], 25
Sagnac-Type α_{12-3}	[-0.06, 0.05], 0.02	[-0.5, 0.4], 0.2	[-1.0, 0.8], 0.4	[-1.8, 1.4], 0.8	[-4.1, 3.5], 1.8	[-8.5, 7.1], 3.9	[-15.5, 12.9], 7.4	[-41, 40], 26
Nominal arm length	1 Gm (1 Mkm)	2 Gm	2.5 Gm	3 Gm	4 Gm	5 Gm	6 Gm	260 Gm
Mission duration	2200 days	10 years						
Requirement on ΔL	10 m (33 ns)	20 m (67 ns)	25 m (83 ns)	30 m (100 ns)	40 m (133 ns)	50 m (167 ns)	60 m (200 ns)	500 m (1670 ns)

2nd Generation TDI configuration	TDI path difference ΔL							
	eLISA/NGO [ps] max, min, rms average	NGO-LISA-type with 2 Gm arm length [ps]	New LISA [ps] max, min, rms average	TAII [ps] max, min rms average	LISA-type with 4 Gm arm length max, min, rms average	LISA-type with 5 Gm arm length max, min, rms average	LISA-type with 6 Gm arm length max, min, rms average	ASTROD-GW [ns] (Wang and Ni, 2015)
[ab,ba]-1	[-0.51, 0.45], 0.187	[-4.4, 3.3], 1.6	[-8.9, 6.5], 3.2	[-15.8, 11.6], 5.7	[-35.3, 28.5], 13.5	[-72, 60], 28	[-130, 113], 51	[-252, 244], 152
[ab,ba]-2	[-0.44, 0.45], 0.179	[-3.6, 3.8], 1.6	[-7.3, 7.4], 3.1	[-12.8, 12.6], 5.4	[-35.4, 26.6], 13.9	[-76, 53], 30	[-140, 89], 55	[-248, 258], 156
[ab,ba]-3	[-0.44, 0.48], 0.182	[-3.5, 3.8], 1.5	[-7.1, 7.3], 3.0	[-13.0, 12.6], 5.2	[-35.0, 30.0], 13.3	[-73, 62], 28	[-135, 111], 52	[-255, 256], 155
[aabb,bbaa]-1	[-4.1, 3.6], 1.5	[-35, 26], 13	[-71, 52], 26	[-126, 93], 45	[-282, 228], 107	[-576, 479], 222	[-1033, 898], 404	[-2011, 1949], 1209
[aabb,bbaa]-2	[-3.5, 3.5], 1.4	[-29, 30], 12	[-58, 59], 24	[-102, 101], 43	[-283, 213], 111	[-607, 421], 237	[-1115, 712], 435	[-1977, 2063], 1248
[aabb,bbaa]-3	[-3.4, 3.8], 1.5	[-28, 30], 12	[-56, 58], 23	[-103, 101], 41	[-279, 239], 106	[-578, 494], 221	[-1075, 881], 409	[-2038, 2043], 1240
[abab,baba]-1	[-2.1, 1.8], 0.8	[-18, 13], 6	[-36, 26], 13	[-63, 46], 23	[-141, 114], 54	[-288, 239], 111	[-517, 449], 202	[-1006, 975], 605
[abab,baba]-2	[-1.7, 1.8], 0.7	[-14, 15], 6	[-29, 30], 12	[-51, 50], 21	[-141, 106], 55	[-304, 210], 118	[-557, 356], 218	[-989, 1032], 624
[abab,baba]-3	[-1.7, 1.9], 0.7	[-14, 15], 6	[-28, 29], 12	[-52, 50], 21	[-140, 120], 53	[-289, 247], 111	[-538, 440], 204	[-1019, 1022], 620

Discussion and Outlook

- All the first-generation TDIs violate their respective requirements.
- For **eLISA** of arm length 1 Gm, the deviation for X, Y, and Z TDIs could be up to a factor of **3.6**;
- for the case of **2 Gm** arm length, a factor of **6.8**;
- for the new LISA case of 2.5 Gm arm length, a factor of 9.6;
- for the TAIJI case of **3 Gm** arm length, a factor of **12.5**;
- for the case of **4 Gm** arm length, a factor of **15.2**;
- for the original LISA of **5 Gm**, a factor of **22.3**;
- for the case of **6 Gm** arm length, a factor **29.9**.
- If X, Y, and Z TDIs are used for the GW analysis, **either the TDI requirement needs to be relaxed** by the same factor **or laser frequency stability requirement needs to be strengthened** by the same factor.
- All the second-generation TDIs in Table 2 for eLISA/NGO of arm length 1 Gm, for the case of 2 Gm arm length and for the **new LISA case of 2.5 Gm arm length satisfy their respective requirements**.

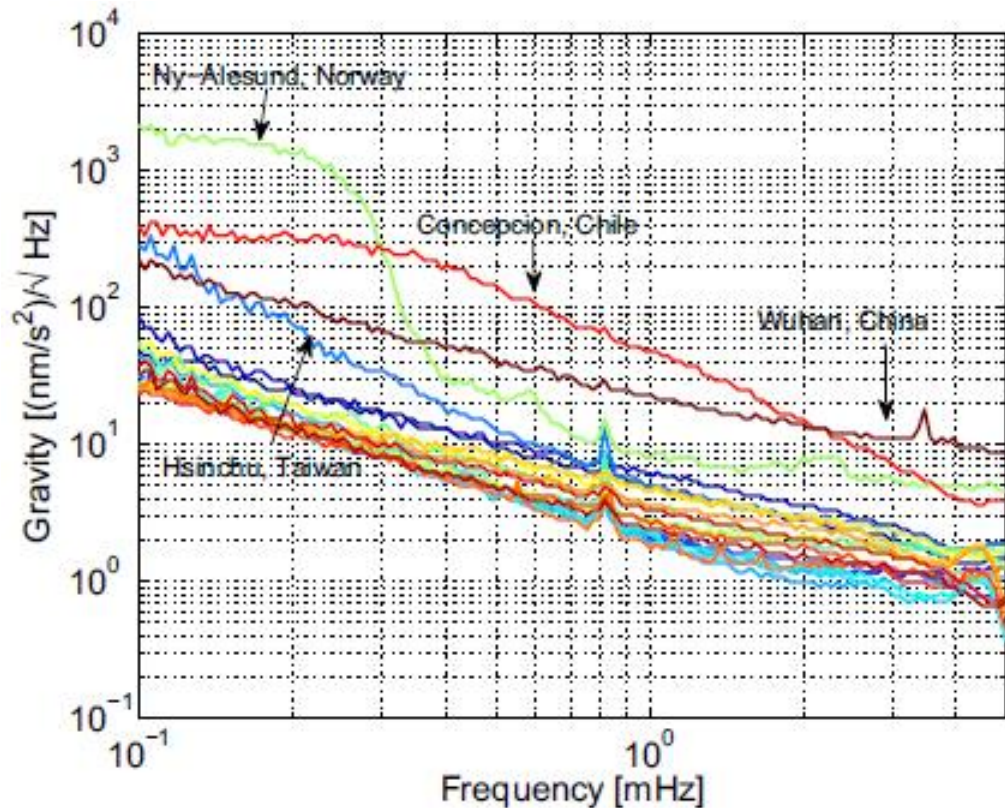
Estimated delta-V and propellant mass ratio for solar transfer of S/C (Deployment)

AM Wu & WTN

° ahead of Earth in solar orbit	Transfer orbit	Transfer time	Solar transfer delta-V after injection from LEO to solar transfer orbit	Solar transfer propellant mass ratio (Isp = 320 s)
180° (near L3)	Venus flyby transfer	1.3–1.5 year	2.2–2.5 km/s	0.50–0.55
60° (near L4)	Inner Hohmann, 2 Revolutions	1.833 year	1.028 km/s	0.280
300° (–60°) (near L5)	Outer Hohmann, 1 Revolutions	1.167 year	2 km/s	0.47
0–60°	Inner Hohmann, ≤ 2 Revolutions	Less than 1.833 year	Less than 1.028 km/s	Less than 0.280
60°–300°	Venus flyby transfer	1.3–1.5 year	2.2–2.5 km/s	0.50–0.55
300°–360°	Outer Hohmann, 1 Revolutions	Less than 1.167 year	Less than 2 km/s	Less than 0.47

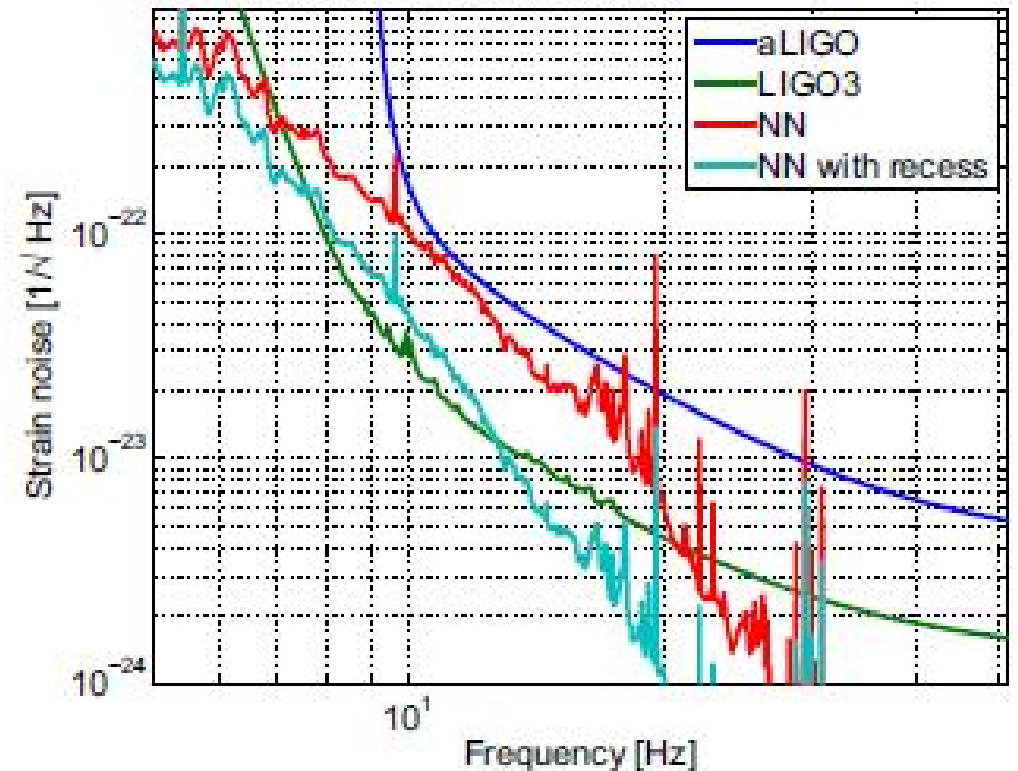
Constraints on Earth-Based GW detectors to extend to middle-frequency range (0.1-10 Hz)

- Vibration-seismic noise (can be tackled)
- Major Constraint -- Gravity-Gradient Noise has to be measured and separated
- Median spectra of superconducting gravimeters of the GGP. Image from Coughlin and Harms (2014b) **GGP: Global Geodynamics Project**



n space

Ref
Harms
Living
Review
In
Relativit
2019



Newtonian Noise — seismic and atmospheric NN would have to be reduced by large factors to achieve sensitivity goals with respect of NN

It is uncertain whether sufficiently sensitive seismic and infrasound sensors can be provided. It will be very challenging to achieve sufficient NN subtraction. A suppression of the NN by about 4 or 5 orders of magnitude at 0.1 Hz would be needed to make it comparable to the instrument noise limit. **A larger number of more sensitive sensors will be required.**

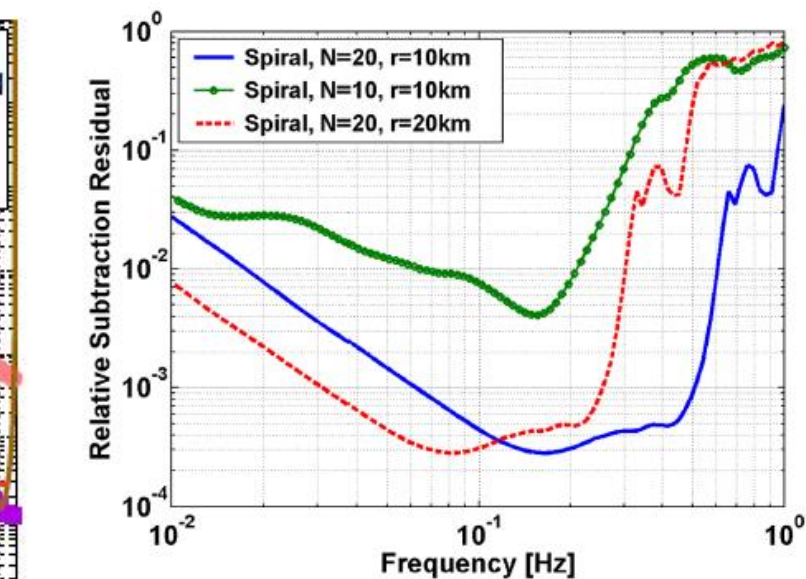
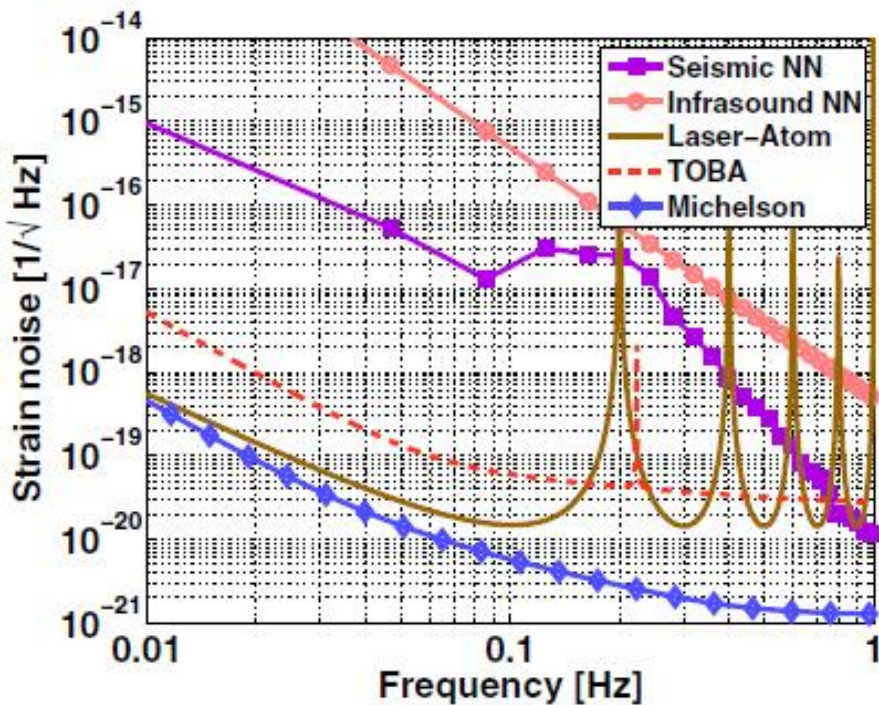


FIG. 10 (color online). Residuals of Rayleigh-wave gradient NN subtraction for double-wound spiral arrays using seismometers with SNR = 1000. Results are presented for different numbers N of seismometers and different array radii r .

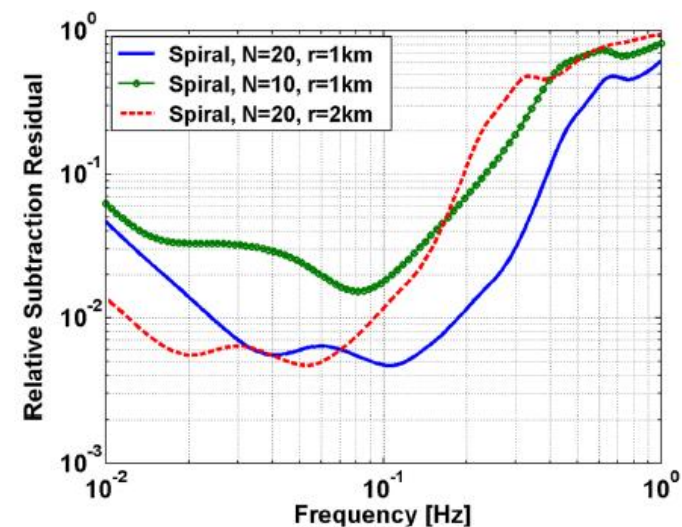


FIG. 11 (color online). Residuals of infrasound gradient NN subtraction for double-wound spiral arrays using microphones with SNR = 1000. Results are presented for different numbers N of microphones and different array radii r .

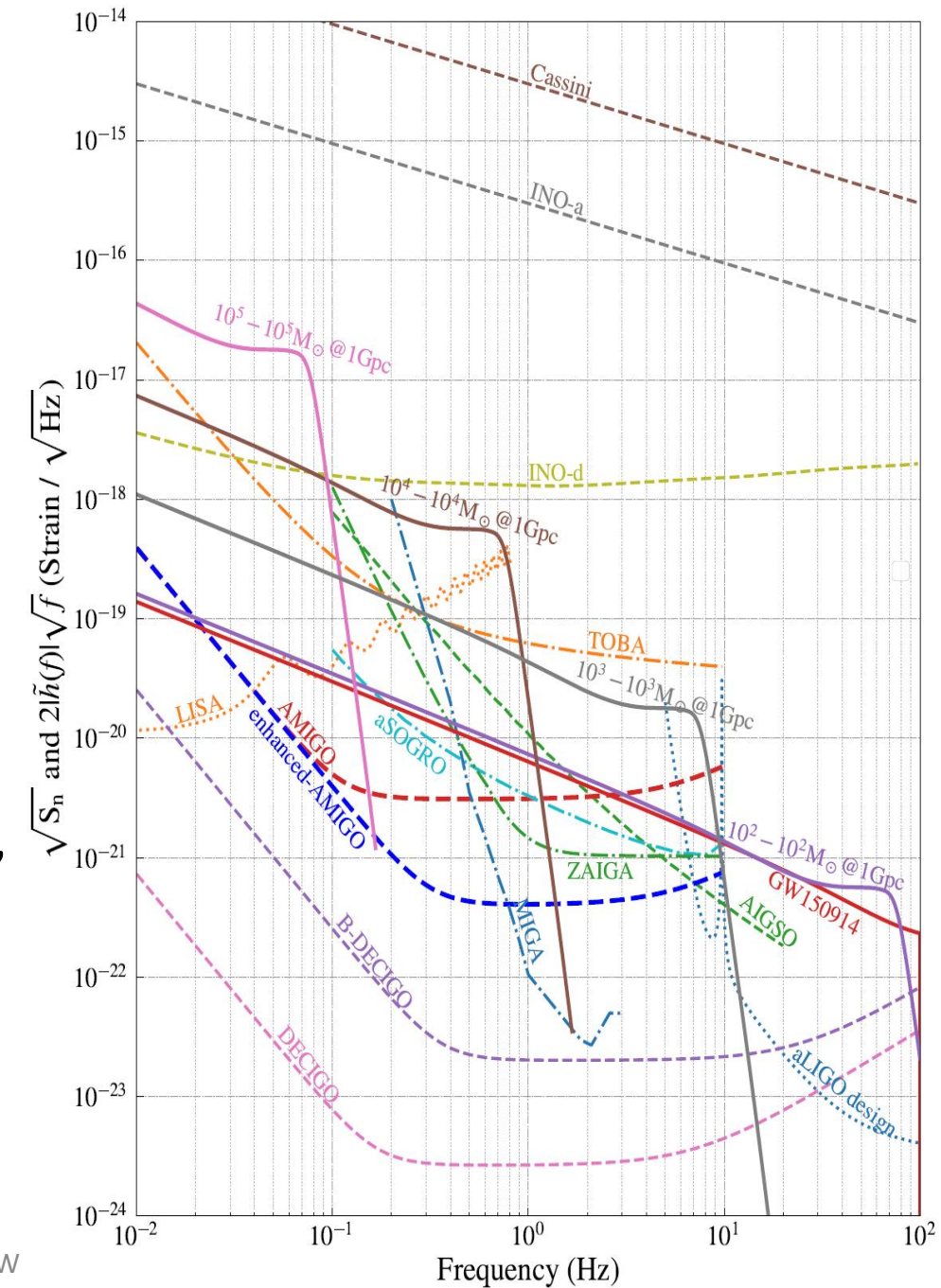
MG16 GW2 Session, 7 July, 2021: arxiv 2111.09715

Mid-frequency GWs (0.1-10 Hz): Sources & Detection Methods

	668 - Outlook of the Mid-frequency GW Detection and AMIGO	Wei-Tou Ni
	965 - Generation, propagation and detection of gravitational waves in inhomogeneous universe	Mr Bowen Liu
07:00	474 - Direct Determination of Supermassive Black Hole Properties with Gravitational-Wave Radiation from Surrounding Stellar-Mass Black Hole Binaries	Dr Hang-Yang
	761 - Fundamental Cosmology & Multi-band, Multi-messenger Astrophysics from the Moon	Dr Karan Jani
	181 - Lunar Gravitational-Wave Antenna	Jan Harms
08:00	174 - A cryogenic & superconducting inertial sensor for the Lunar Gravitational Wave Antenna and for... selenophysics	Francesca Badaracco
	460 - TOBA: a Ground-Based Mid.-Frequency Gravitational-Wave Antenna	Masaki Ando
	929 - Recent progress on ZAIGA	Dongfeng Gao
09:00	615 - AION and AEDGE: Gravitational physics with atom interferometry	Marek  kl
	276 - Space gravitational wave antenna DECIGO and B-DECIGO	Prof. Seiji Kawamura

Middle-Freq. GW Mission Concepts

- Cassini (completed mission),
- INOa,b,c,d ((Interplanetary Network of Optical Lattice Clocks),
- TOBA (Torsion Bar),
- aSOGRO (Superconducting Omni-directional Gravitational Radiation Observatory),
- MIGA (Matter-wave Interferometer G Antenna),
- ZAIGA (Zhaoshan Atom Interfer. G Antenna),
- AMIGO, DO (Deci-Hz Observatory)
- TIANGO (sky or space GW Obs.), B-DECIGO, DECIGO



DECIGO & B-DECIGO

- DECIGO was conceived in 2001 with the main scientific target to directly measure the acceleration of the Universe. The design has been elaborated with laser Fabry-Perot arm cavities. DECIGO consists of four clusters with each cluster having three differential Fabry-Perot interferometers with three drag-free spacecraft forming an equilateral triangle of nominal arm cavity length 1000 km. Lasers illuminating the cavity have power 10 W and wavelength 515 nm. The current design has main mirrors with diameter 1 m and mass 100 kg forming cavities of finesse 10. The four clusters also form a nearly equilateral triangle in the heliocentric orbits with two clusters in Earth-trailing orbits. The other two clusters are separated from each other and from the near-Earth clusters by 120 degrees in the heliocentric orbits. The DECIGO team recognized that “. . . analysis based on the observations by the Planck satellite lowered the upper limit of GW to 1×10^{-16} Omega-critical. As a result, *the DECIGO sensitivity became no longer good enough to detect the primordial gravitational waves*". **Nevertheless, with target sensitivity the best among all the present mid-frequency concepts (Table 1), it may still bring us some clues on the very early universe, e.g. revealing the thermal history after the inflation^{52,53} etc.**
- The design of B-DECIGO is down-scaled from DECIGO, consisting of one cluster with three spacecraft separated from each other by **100 km**. The arm cavity mirrors have diameter of 0.3 m with mass of 30 kg, and cavity finesse of 100. The laser wavelength is 515 nm and laser power 1 W. With target strain psd amplitude about one order higher than DECIGO, it serves as a pathfinder for DECIGO, and with the noise sensitivity well enough, it is also a good probe to the many mid-frequency GW sources discussed in section 2. **DECIGO team aim to launch B-DECIGO at the earliest in 2032.**

AMIGO: Astodynamical Middle-frequency Interferometric Gw Observatory)

Wei-Tou Ni,^{1, 2, 3} Gang Wang⁴ & An-Ming Wu⁵

¹*National Astronomical Observatories, Chinese Academy of Sciences*

²*Innovation Academy of Precision Measurement Science and Technology (APM),
Chinese Academy of Sciences, Wuhan*

³*Department of Physics, National Tsing Hua University, Hsinchu,*

⁴*Shanghai Astronomical Observatory, Chinese Academy of Sciences, Shanghai*

⁵*National Space Organization (NSPO), Hsinchu*

Ref. WTN, G Wang & A-M Wu, IJMPD 29 (2020) 1940007; WTN, 1709.05659

AMIGO: Astrodynamical Middle-frequency Interferometric GW Observatory

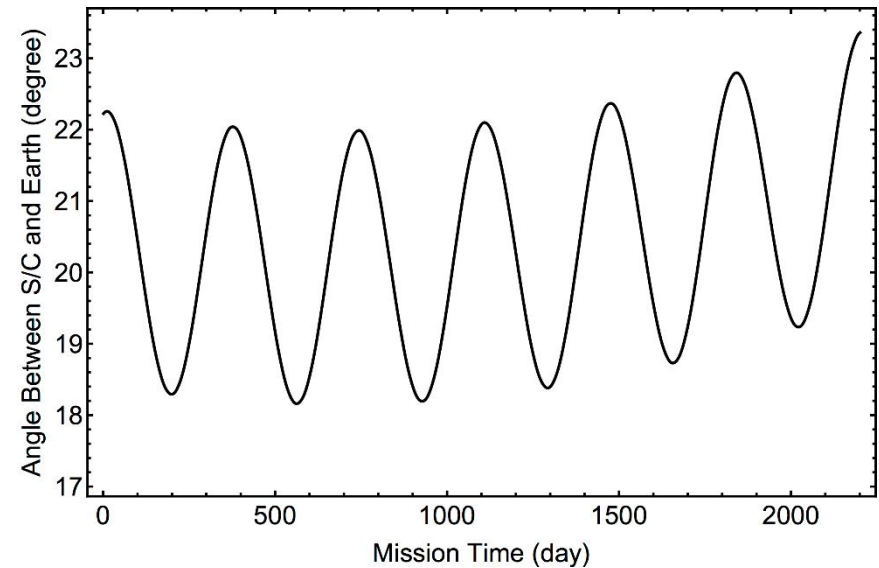
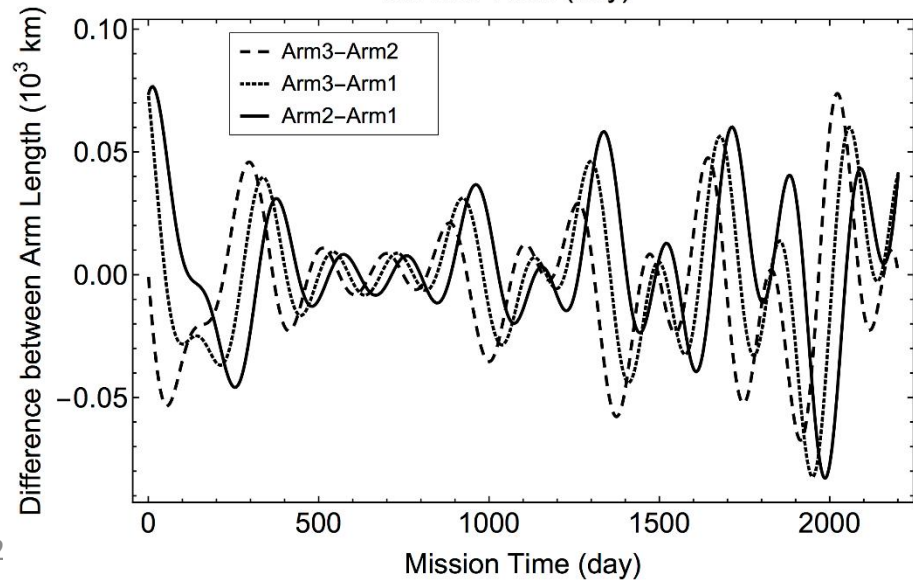
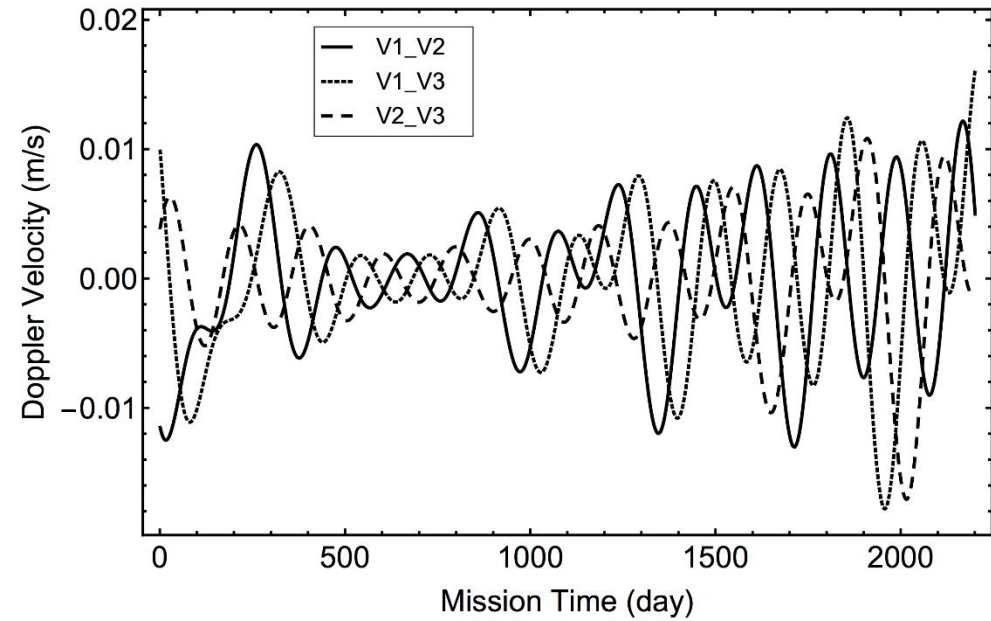
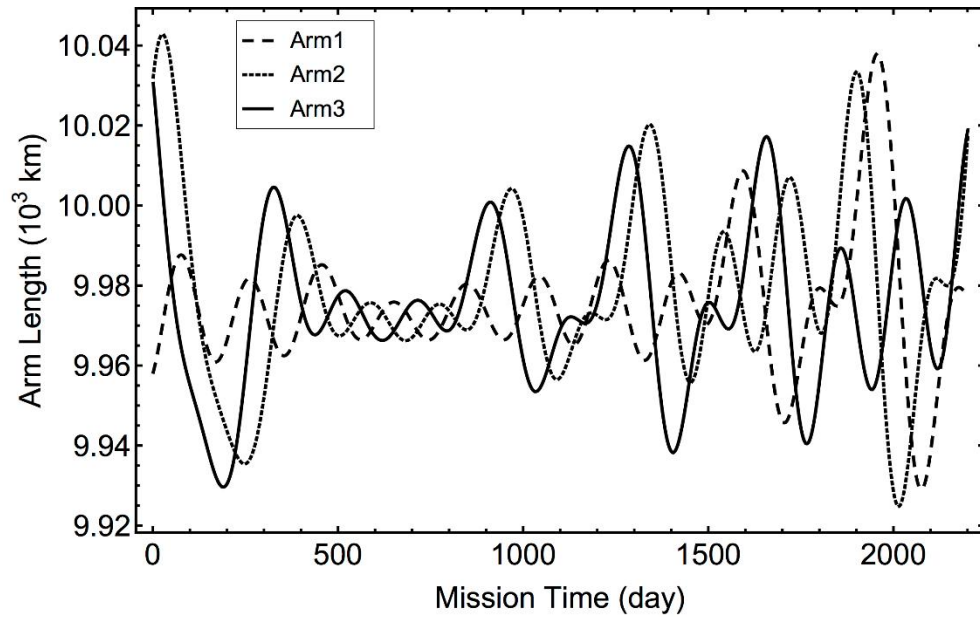
(Ni, Wang & Wu)

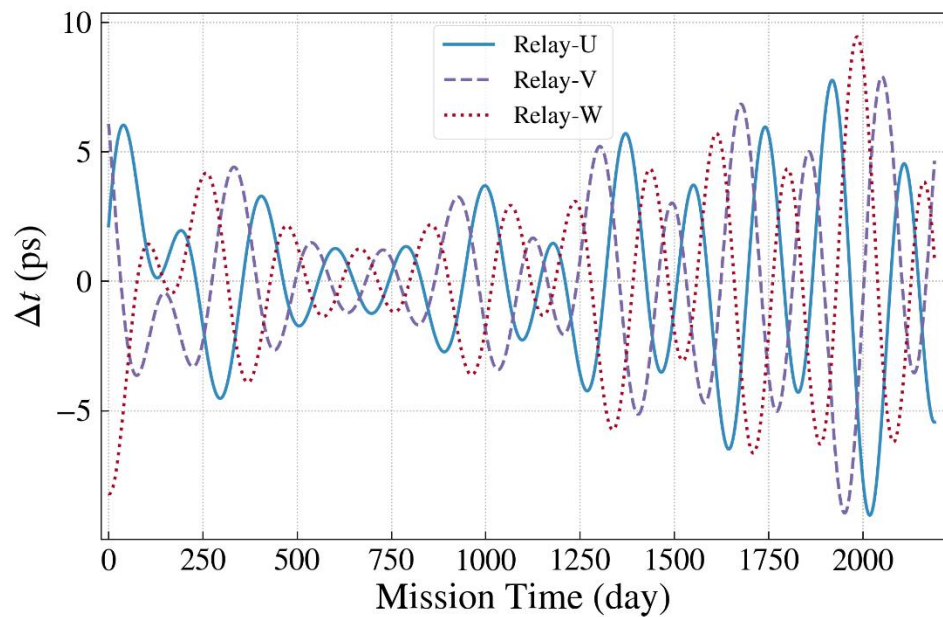
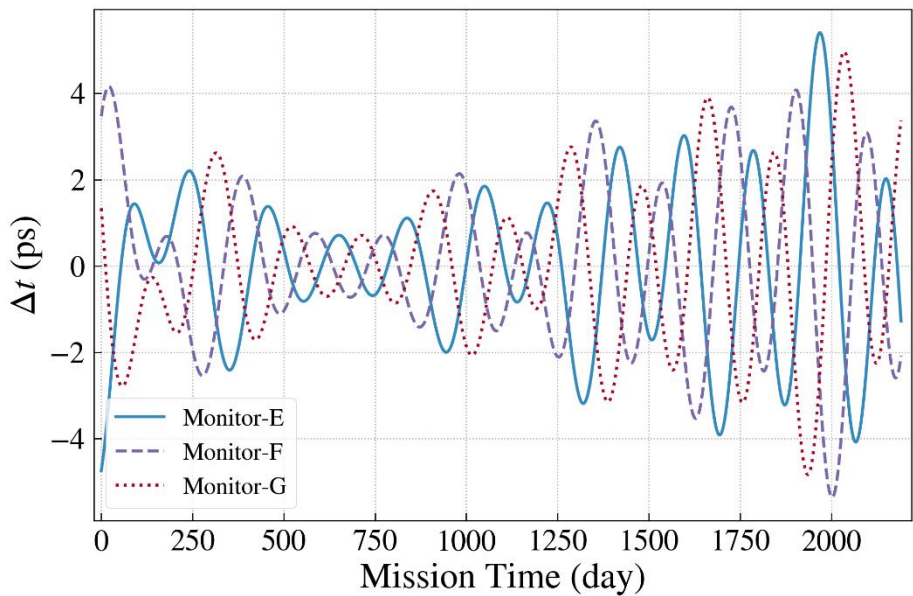
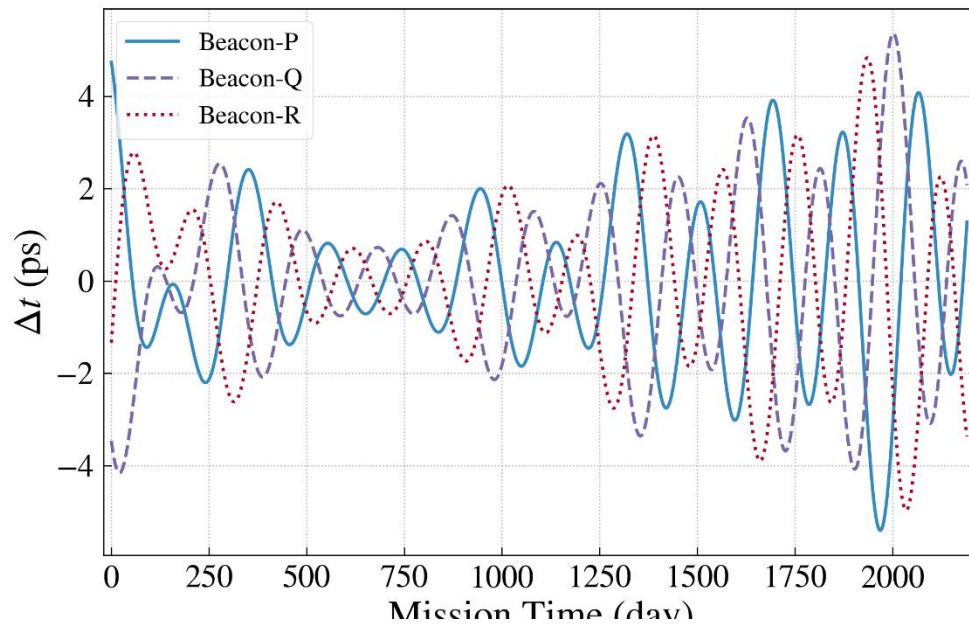
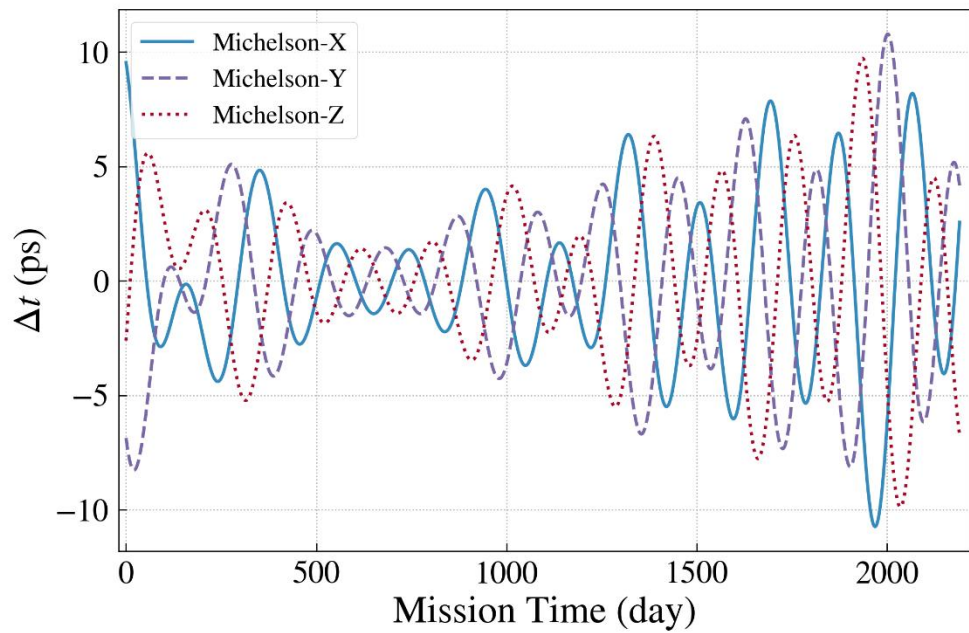
- Arm length: 10,000 km (or a few times)
- Laser power: 2-10 W (or more)
- Acceleration noise: assuming LPF noise
- Orbit: 4 options (all LISA-like formations):
 - (i) Earth-like solar orbit (3-20 degrees behind the Earth orbit)
 - (ii) 660,000 km high orbits around the
 - (iii) 100,000 km-250,000 high orbits around the Earth
 - (iv) near Earth-Moon L4 and L5 orbits
- **Scientific Goal:** to bridge the gap between high-frequency and low-frequency GW sensitivities. Detecting intermediate mass BH coalescence. Detecting inspiral phase and predict time of binary black hole coalescence for ground interferometers. *A new paper by YT Zhao, YJ Lu et al will be out soon.*

Outline

- AMIGO Mission Concept
- AMIGO Orbit Design & TDI
- Noise Spectral Density & Sensitivity
- Constant Arm vs Geodesic Options
- Discussion on Technology Development steps

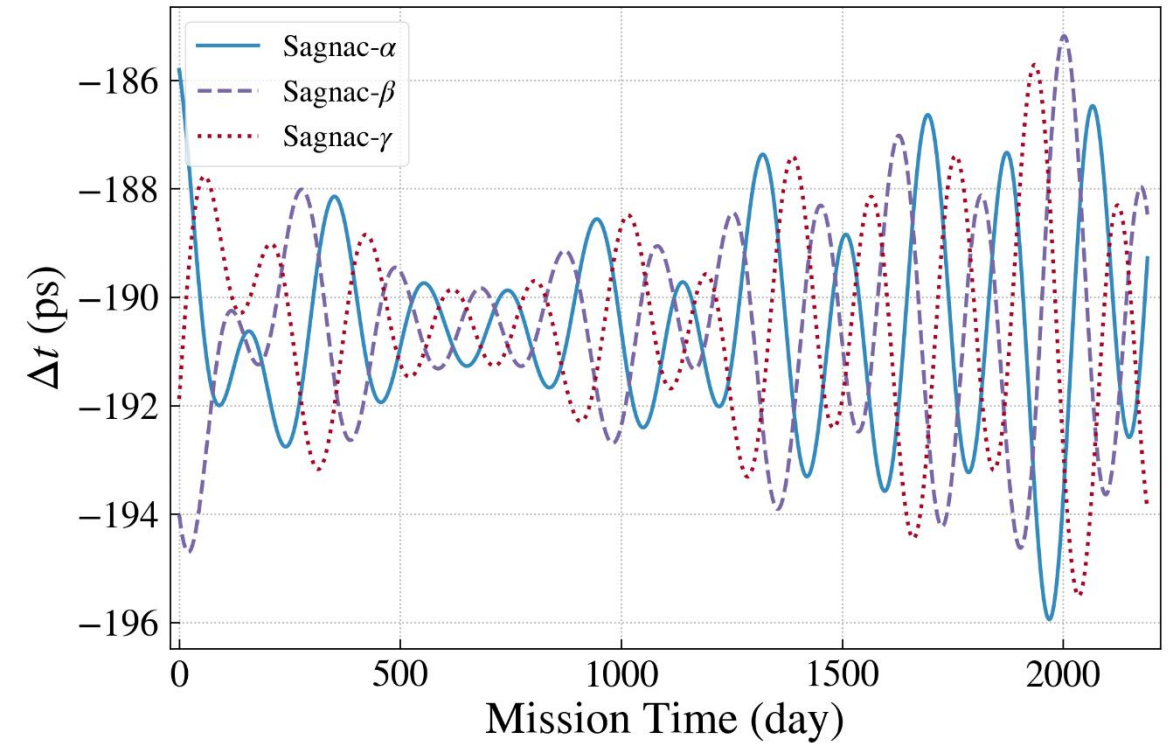
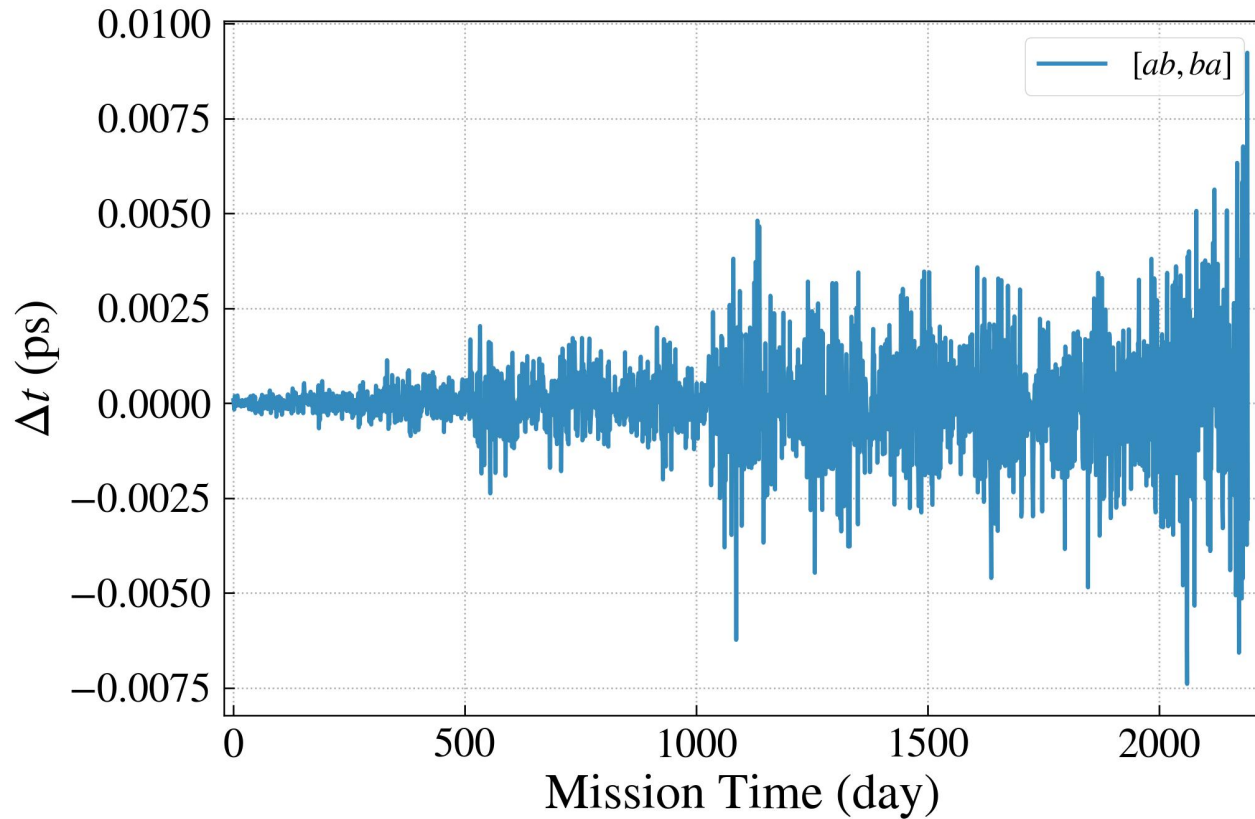
AMIGO Orbit design: Earth-like solar orbits





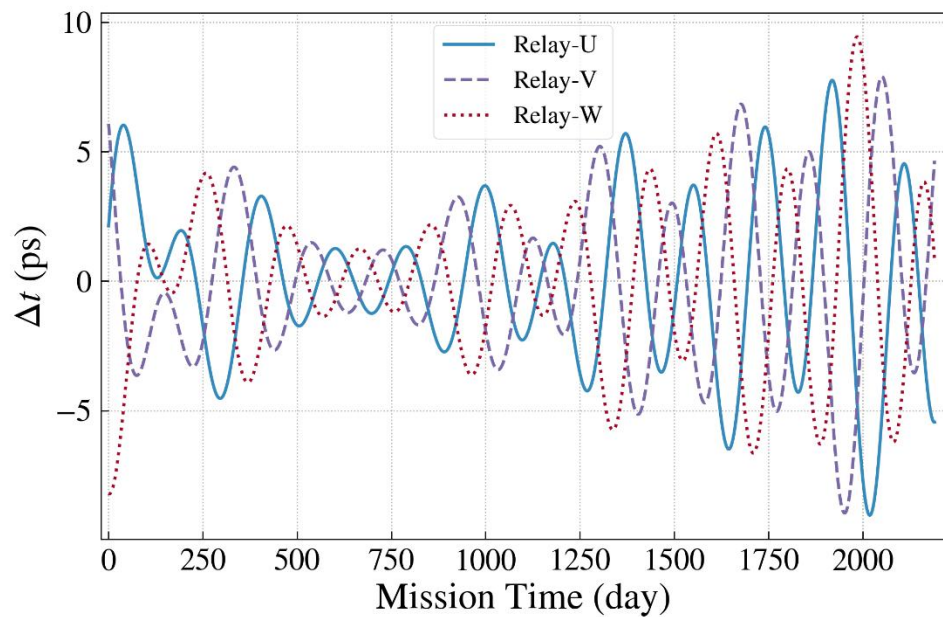
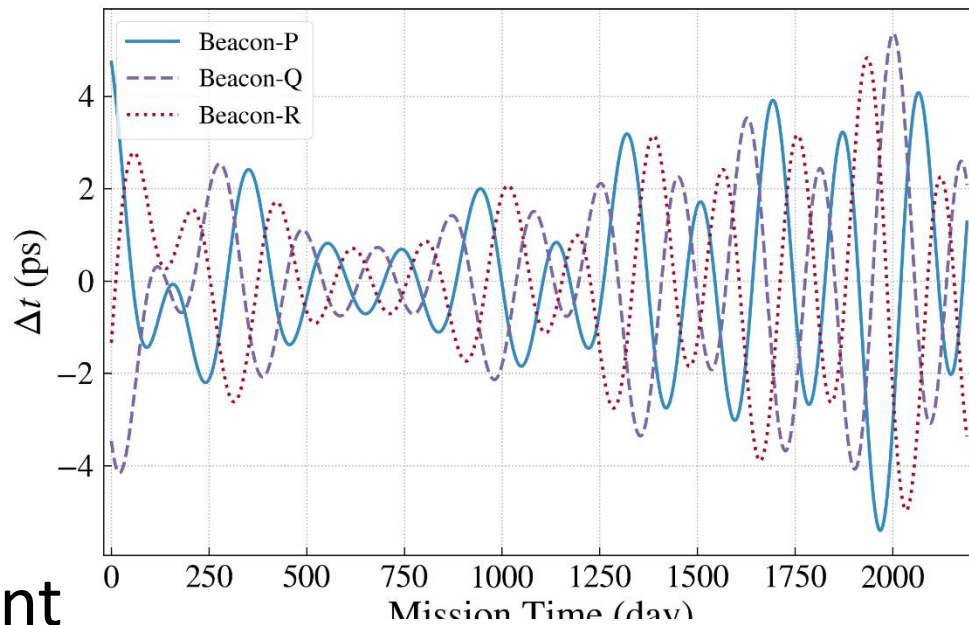
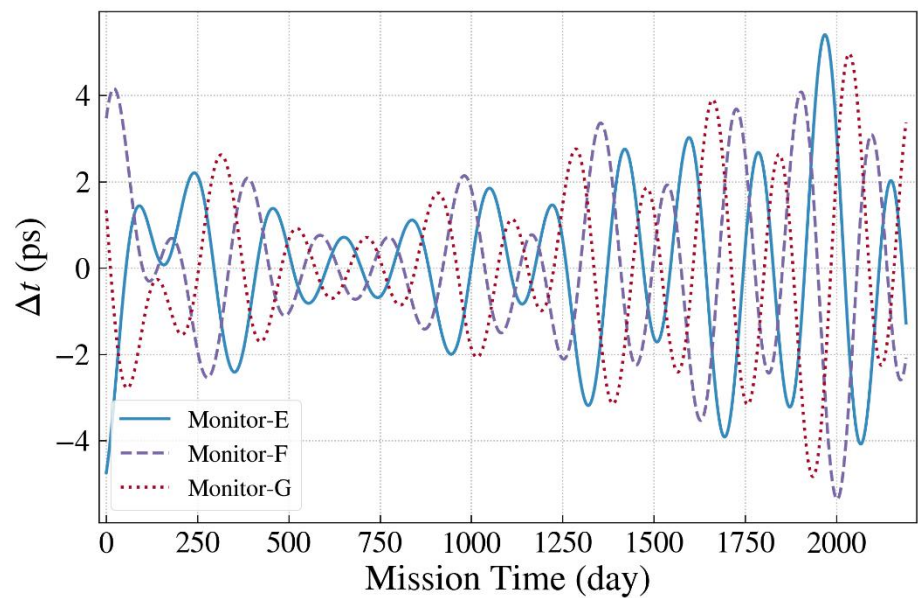
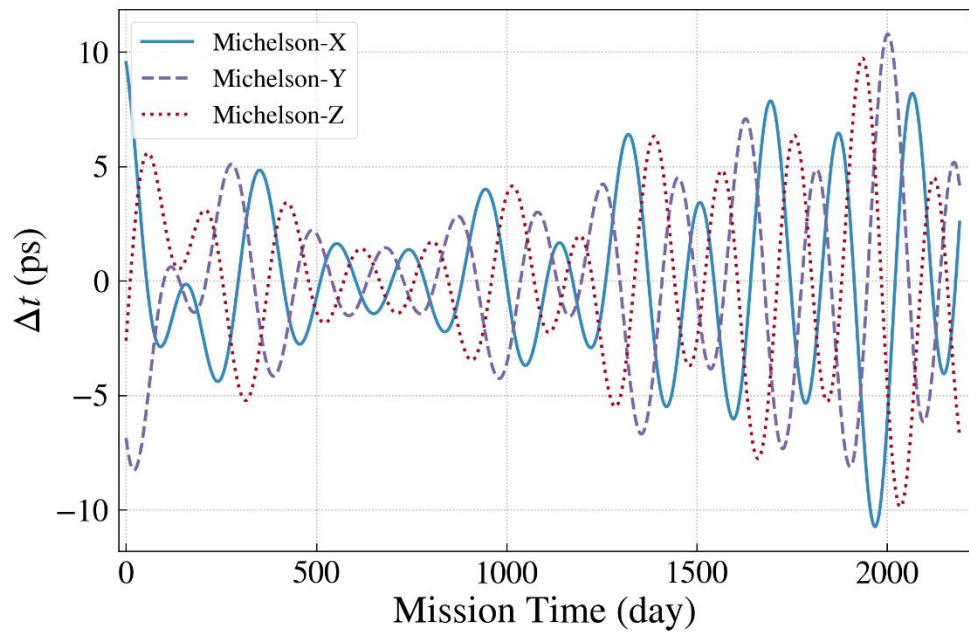
T
D
I

Time Delay Interferometry



TDI or Equal-Arm Interferometry

- Suppose laser frequency noise density is $30 \text{ Hz}/\text{Hz}^{1/2}$, converted to frequency instability, $10^{-13}/\text{Hz}^{1/2}$ at a particular detection frequency f_{GW} . If the two interfering beams are separated by $\Delta L \sim 30 \text{ m}$ (or 300 ns) at the emitting source, they pick up the frequency noise of $100 \text{ m} \times 10^{-13}/\text{Hz}^{1/2}$ at the particular detection frequency f_{GW} . If we take the total optical path to convert it to strain, say TAIJI arm length $3 \times 10^9 \text{ m}$, the strain sensitivity would be $30 \text{ m} \times 10^{-13}/\text{Hz}^{1/2} / (3 \times 10^9 \text{ m}) = 10^{-21}/\text{Hz}^{1/2}$. Ah Ha, it does not prevent GW sensitivity!!!
- If the two paths of a TAIJI TDI is different by less than 30 m, the laser frequency noise is less than the core noises (acceleration noise \propto length metrology noise).
- *For AMIGO, the baseline is 10^7 m , we have to shrink the ΔL to $\sim 10 \text{ cm}$*
- Is this possible? LLR (pulse ranging) and CW laser ranging can all do this.
- *LISA, TAIJI can do this; AMIGO can do this.*



T
D
I

Requirement

0.1 m
or
330 ps

All first generation TDIs satisfy the requirement

Table 5. Comparison of the resulting path length differences for the first-generation TDI's listed in Ref. 36 (i.e. X, Y, Z, X + Y + Z, Sagnac, U, V, W, P, Q, R, E, F and G TDI configurations) for AMIGO-S (AMIGO-S-8-12deg, AMIGO-S-2-6deg, AMIGO-S-2-4deg), for AMIGO-E1 and for AMIGO-EM, all of nominal arm lengths 10,000 km.

First generation TDI configuration	TDI path length difference ΔL				
	AMIGO-S-8-12deg [ps] [min, max], rms average	AMIGO-S-2-6deg [ps] [min, max], rms average	AMIGO-S-2-4deg [ps] [min, max], rms average	AMIGO-E1.0 [ns] [min, max], rms average	AMIGO-EM-L4 [ns] [min, max], rms average
X	[-19, 14], 7	[-34, 1], 14	[-48, 34], 33	[-40, 48], 15	[-30, 31], 13
Y	[-15, 14], 6	[-13, 20], 9	[-20, 83], 40	[-43, 41], 16	[-22, 30], 12
Z	[-12, 16], 6	[-7, 38], 13	[-56, 25], 22	[-46, 40], 16	[-29, 25], 12
X + Y + Z	[-0.01, 0.12], 0.06	[-0.2, 0.8], 0.2	[-0.03, 2], 0.6	[-3, 2], 2	[-7, 27], 9
Sagnac- α	[-202, -185], 193, 4 ^a	[-209, -191], 197, 5	[-208, -166], 193, 14	[-44, -1], 21, 9	[-19, 7], 6, 6
Sagnac- β	[-200, -185], 192, 3 ^a	[-199, -182], 191, 4	[-194, -143], 176, 18	[-46, -4], 20, 9	[-14, 7], 5, 5
Sagnac- γ	[-198, -183], 192, 3 ^a	[-195, -173], 189, 6	[-212, -171], 185, 11	[-48, -3], 21, 9	[-25, 10], 9, 8
Relay-U	[-10, 13], 5	[-11, 26], 8	[-69, 17], 28	[-42, 38], 14	[-28, 19], 11
Relay-V	[-15, 11], 6	[-33, 2], 13	[-30, 31], 20	[-37, 37], 13	[-27, 30], 12
Relay-W	[-12, 16], 6	[-2, 24], 10	[-22, 56], 35	[-42, 32], 13	[-17, 24], 8
Beacon-P	[-10, 7], 4	[-18, 1], 7	[-69, 17], 28	[-28, 17], 8	[-19, 7], 6
Beacon-Q	[-8, 7], 3	[-7, 10], 5	[-30, 31], 20	[-29, 17], 8	[-12, 5], 4
Beacon-R	[-6, 8], 3	[-4, 19], 7	[-22, 56], 35	[-28, 17], 8	[-28, 13], 10
Monitor-E	[-7, 10], 4	[-1, 18], 7	[-17, 25], 17	[-17, 28], 8	[-7, 19], 6
Monitor-F	[-7, 8], 3	[-10, 7], 5	[-41, 10], 20	[-17, 29], 8	[-5, 12], 4
Monitor-G	[-8, 6], 3	[-19, 4], 7	[-13, 29], 12	[-17, 28], 8	[-13, 28], 10
Mission duration	600 days	250 days	80 days	180 days	180 days
Requirement on ΔL	0.1 m (330 ps)	0.1 m (330 ps)	0.1 m (330 ps)	0.1 m (330 ps)	0.1 m (330 ps)

Note: ^aRoot mean square deviation from the mean.

References

1. W.-T. Ni, G. Wang, and A.-M. Wu, Astrodynamical middle-frequency interferometric gravitational wave observatory AMIGO: Mission concept and orbit design, *Int. J. Mod. Phys. D* 29, (2020) 1940007, arXiv:1909.04995 [gr-qc].
2. G. Wang, W.-T. Ni, and A.-M. Wu, Orbit design and thruster requirement for various constant-arm space mission concepts for gravitational-wave observation, *Int. J. Mod. Phys. D* 28, 1940006 (2020), arXiv:1908.05444 [gr-qc].
3. A.-M. Wu, W.-T. Ni and G. Wang, Deployment Simulation for LISA Gravitational Wave Mission, IAC-17-A2.1.4, 68th International Astronautical Congress, 25-29 September 2017, Adelaide, Australia (2017).
4. A.-M. Wu and W.-T. Ni, *Int. J. Mod. Phys. D* 22, 1341005 (2013), arXiv:1212.1253 [gr-qc].
5. W.-T. Ni, Gravitational Wave (GW) Classification, Space GW Detection Sensitivities and AMIGO (Astrodynamical Middle-frequency Interferometric GW Observatory), Proceedings of Joint Meeting of 13th International Conference on Gravitation, Astrophysics and Cosmology, and 15th Italian-Korean Symposium on Relativistic Astrophysics, Ewha Womans University, Seoul, Korea, July 3-7, 2017, EPJ Web of Conferences 168, 01004 (2018); arXiv:1709.05659 [gr-qc].
6. W.-T. Ni, Mid-Frequency Gravitational Wave Detection and Sources, *Int. J. Mod. Phys. D* 29, 1902005 (2020), arXiv:2004.05590 [gr-qc].

GW Sensitivities of AMIGO

- **Baseline Sensitivity: 2 W** emitting laser power, **300 mm ϕ telescope**
- $S_{AMIGOn}^{1/2}(f) = (20/3)^{1/2} (1/L_{AMIGO}) \times [(1 + (f/(1.29f_{AMIGO}))^2)]^{1/2} \times [(S_{AMIGOp} + 4S_a/(2\pi f)^4)]^{1/2} \text{ Hz}^{-1/2}$,
- over the frequency range of $20 \mu\text{Hz} < f < 1 \text{ kHz}$. Here $L_{AMIGO} = 0.01 \times 10^9 \text{ m}$ is the AMIGO arm length, $f_{AMIGO} = c/(2\pi L_{AMIGO})$ is the AMIGO arm transfer frequency, $S_{AMIGOp} = 1.424 \times 10^{-28} \text{ m}^2 \text{ Hz}^{-1}$ is the (white) position noise level due to laser shot noise which is $16 \times 10^{-6} (=0.004^2)$ times that for new LISA. $S_a(f)$ is the same colored acceleration noise level in (2)
- **Design Sensitivity: 10/2.688 W** emitting laser power, **360/500 mm ϕ telescope**
 - Shot noise for strain to gain a factor of 10 [$\approx (10\text{W}/2\text{W}) \times (360\text{mm}/300\text{mm})^4$]
 - AMIGO solid curve by using $S_{AMIGOp} = 0.1424 \times 10^{-28} \text{ m}^2 \text{ Hz}^{-1}$.
- **Enhanced sensitivity: 1 m SiC & 10 W laser \rightarrow 7.7 fold improvement**

In this subsection, we set the noise requirement for AMIGO. For the acceleration noise requirement, we set

$$S_a^{1/2}(f) \leq 3 \times 10^{-15} [1 + (f/0.3 \text{ Hz})^4]^{1/2} \text{ m s}^{-2} \text{ Hz}^{-1/2}, \quad (10 \text{ Hz} > f > 10 \text{ mHz}), \quad (5)$$

N.B. LISA LPF has already demonstrated in Feb 2017,

$$S_a(f) \leq 9 \times 10^{-30} [1 + (10^{-4} \text{ Hz}/f)^2 + 16 (2 \times 10^{-5} \text{ Hz}/f)^{10}] \text{ m}^2 \text{ s}^{-4} \text{ Hz}^{-1}, \quad (20 \text{ } \mu\text{Hz} - 0.03 \text{ Hz}) \quad (6)$$

For laser metrology noise, we set:

$$\text{Baseline (b-AMIGO): } S_{\text{AMIGOp}} \leq 1.4 \times 10^{-28} \text{ m}^2 \text{ Hz}^{-1}, \\ S_{\text{AMIGOp}}^{1/2} \leq 12 \text{ fm Hz}^{-1/2}, \quad (10 \text{ Hz} > f > 10 \text{ mHz})$$

LISA Pathfinder already
Achieved **35 fm Hz^{-1/2}**
60mHz to 5Hz (7)

$$\text{Design Goal (AMIGO): } S_{\text{AMIGOp}} \leq 0.14 \times 10^{-28} \text{ m}^2 \text{ Hz}^{-1}, \quad (8) \\ S_{\text{AMIGOp}}^{1/2} \leq 3.8 \text{ fm Hz}^{-1/2}, \quad (10 \text{ Hz} > f > 10 \text{ mHz})$$

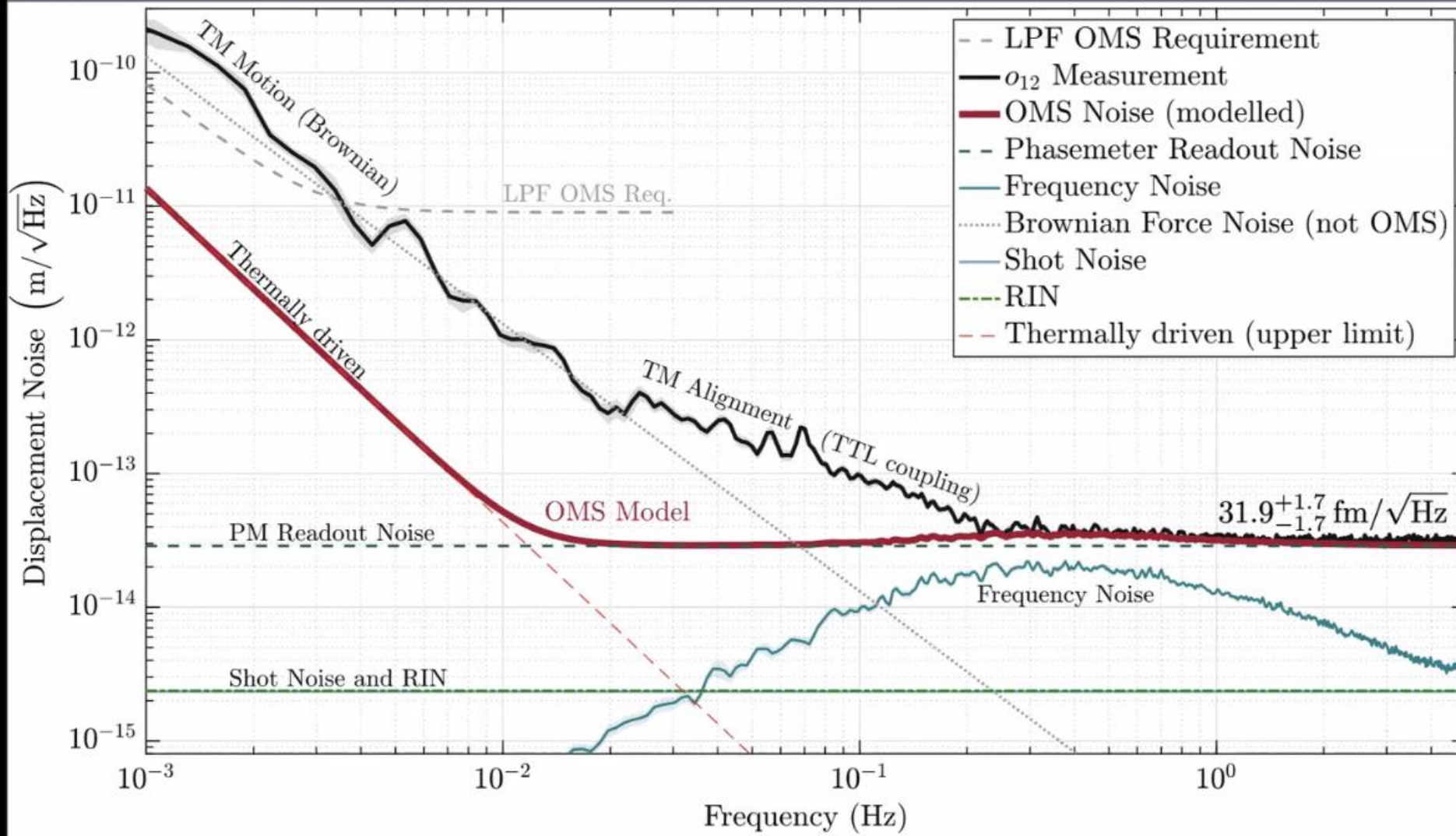
$$\text{Enhanced Goal (e-AMIGO): } S_{\text{AMIGOp}} \leq 0.0025 \times 10^{-28} \text{ m}^2 \text{ Hz}^{-1}, \quad (9) \\ S_{\text{AMIGOp}}^{1/2} \leq 0.5 \text{ fm Hz}^{-1/2}, \quad (10 \text{ Hz} > f > 10 \text{ mHz})$$



Differential TM displacement noise: June 1st 2016



lisa pathfinder



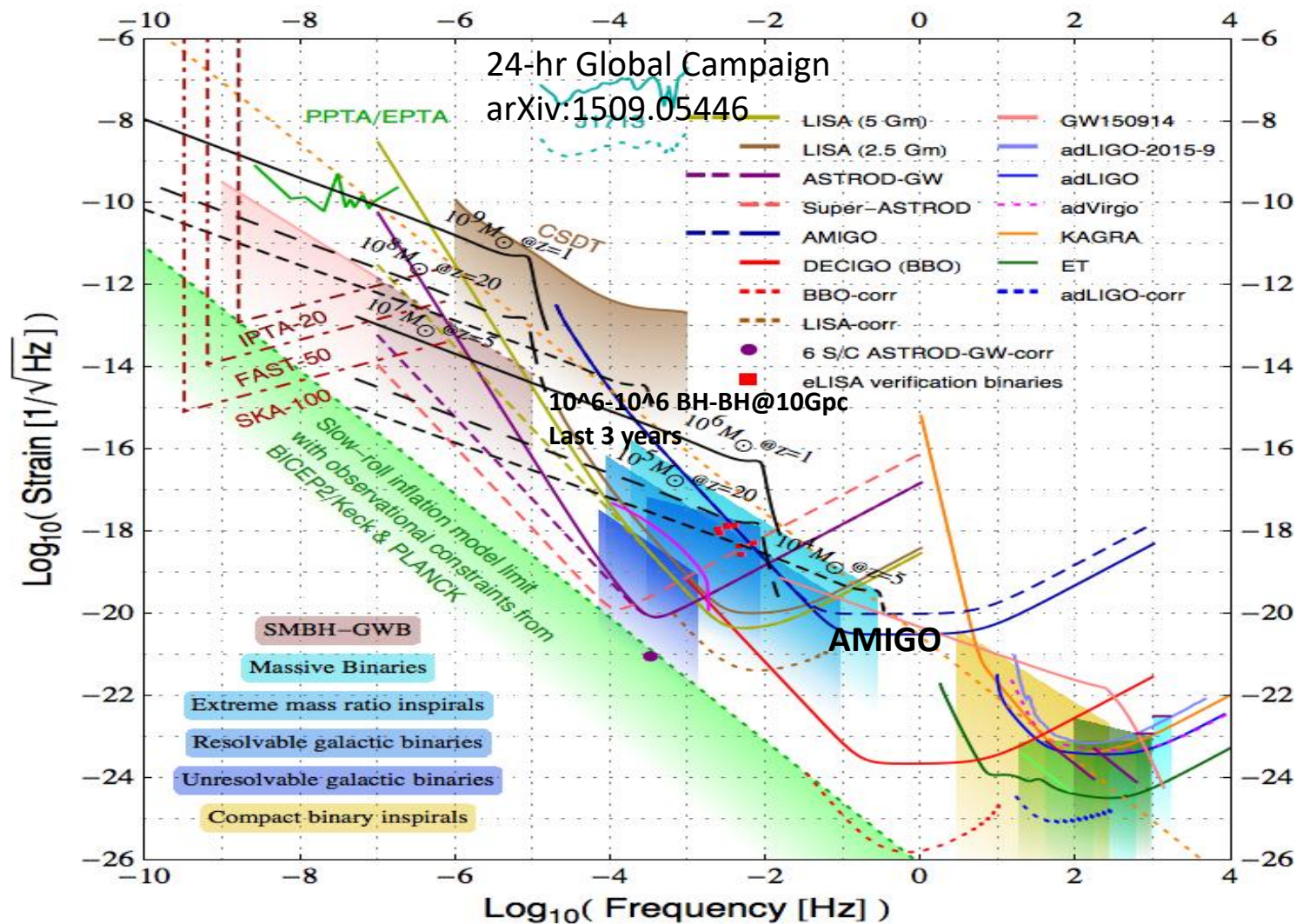
Laser metrology, TTL coupling, and requirements

- (i) After 3-month operation time since the start of scientific operations on March 1 2016, the LISA Pathfinder Team reported that readout **noise above 60 mHz to 5 Hz is 35 fm Hz^{-1/2}, two-order below the required 9 pm Hz^{-1/2}**
- (ii) Sensor noise in LISA Pathfinder of 2020 LISA Symposium by Gudrun Wanner: the differential TM (Test Mass) displacement noise: June 1st 2016. Between 0.2 Hz to 5 Hz, **31.9±1.7 fm Hz^{-1/2}** agree to Optical Metrology model (OMS). The OMS model contains shot noise, relative intensity noise, frequency noise, TM Readout noise, and thermally driven noise. Below 0.2 Hz, the excess noise includes TM Brownian motion, and TM alignment (**TTL [tilt-to-length] coupling**) noise.
- (iii) LISA Pathfinder TTL coupling: a bulge in the acceleration noise appeared in the 20-200 mHz frequency region. This bulge was due to S/C motion coupling into the longitudinal readout. **Wanner et al.** showed that this **TM alignment noise could be subtracted out.**
- (iv) **GRACE Follow-On (GRACE-FO)**, launched in May 2018. GRACE-FO has a Laser Ranging Interferometer (LRI) to measure the 200 km separation of 2 S/C, but with higher accuracy compared with K/Ka band range, and serves as a technology demonstrator for future geodesy missions and space GW detection missions like LISA. **Wegener et al.: TTL couplings of LRI within 200 μm/rad and meet the requirements.**
- (v) Chwalla, Danzmann, Alvarez et al. made a lab demonstration of reduction of TTL coupling by introducing two- and four-lens imaging systems. TTL coupling factors **below ±25 μm/rad** (i.e., **±1 pm/40 nrad**) for beam tilts within ±300 μrad of the system. Compensation of the additional TTL coupling due to lateral-alignment errors of the imaging system by introducing lateral shifts of the detector. **These results help validate the noise-reduction technique for the LISA or other long-arm interferometer. For AMIGO, the TTL coupling should be kept smaller by one more order of magnitude and the alignment noise should also be kept smaller by one order.**

Laser Length Metrology

- For the arm metrology, both LISA and AMIGO, in their respective best performance frequencies, require that the noise is basically limited by shot noise. This means that the length measurement noise is inversely proportional to the square root of power received, i.e. inversely proportional to $D_e D_r L$ with D_e the diameter of the emitting telescope, D_r the diameter of the receiving telescope and L the arm length.
- **LISA Pathfinder** showed in the frequency range between 0.2 Hz to 5 Hz, the measured displacement noise is $(31.9 \pm 1.7) \text{ fm Hz}^{-1/2}$ agreeing to their OMS model. This is roughly one order above the shot noise and RIN (Relative Intensity Noise). LISA requires about $10 \text{ pm Hz}^{-1/2}$ at 2 mHz for their arm length measurement at 2 mHz. In the thermally driven OMS Model this is achieved if their Brownian motion is accounted for. In addition, LISA need to reach this with lower power of incoming light, i.e. shot noise limit should be basically reached.
- For **basic AMIGO**, the $12 \text{ fm Hz}^{-1/2}$ laser metrology readout noise is 3 times more stringent and needs demonstration; (ii) For **AMIGO**, the $3.8 \text{ fm Hz}^{-1/2}$ laser metrology readout noise is 10 times more stringent and needs demonstration; (iii) In addition, in the arm measurement, shot noise needs to be basically reached with **AMIGO** power budget.

Strain power spectral density (psd) amplitude vs. frequency for various GW detectors and GW sources. [CSDT: Cassini Spacecraft Doppler Tracking; SMBH-GWB: Supermassive Black Hole-GW Background.]



Constant Arm Option Seems Viable

Table 6. The thruster and propellant requirement for various AMIGO mission orbit options assuming the total mass including fuel of the S/C is 1000 kg.

Mission concept (arm length 10^4 km)	Required acceleration (max)	Thruster requirement (max)	Propellant requirement for 1 yr by numerical integration (kg)	
			$I_{sp} = 300$ s	$I_{sp} = 1000$ s
AMIGO-E1	2.0 mm/s^2	2.0 N	999.8	922.0
AMIGO-EML4	2.5 mm/s^2	2.5 N	863.0	449.2
AMIGO-S-2-4deg	500 nm/s^2	$500 \mu\text{N}$	1.54	0.464
AMIGO-S-2-6deg	50 nm/s^2	$50 \mu\text{N}$	0.15	0.045
AMIGO-S-8-12deg	15 nm/s^2	$15 \mu\text{N}$	0.05	0.016

- From: LTP Team, LISA Pathfinder Performance Confirmed in an Open-Loop Configuration: Results from the Free-Fall Actuation Mode, PHYSICAL REVIEW LETTERS 123, 111101 (2019),
- The technology seems to be ripe for the solar orbit of AMIGO: 1 nm/s^2 in actuation mode

Summary

- Currently, a number of detection methods are proposed and under active research to bridge the middle-frequency band gap between Earth-based and space-borne GW observations with important science goals. In this band, technical limits will be extremely challenging to overcome for Earth-based due to Newtonian noises. In this paper, **we propose a first-generation middle-frequency mission concept AMIGO with 10,000 km arm length. The technical readiness level is high. The sensitivity is good to reach science goals considered in the last section.**
- **If a pathfinder mission is desired with 2-spacecraft demonstration of ranging in the solar-system for a LISA-like mission, the case with 2-5 degrees lagging behind the Earth orbit-choice could be considered.** Just take one arm of this AMIGO case, it would be good to test many things in the solar system: deployment, both radio and laser communications, noise budget, and drag-free system together with a concentrated effort on distance metrology. It might be simpler than go to L1 or L2 Sun-Earth Lagrange point.

Constant Equal-Arm Interferometry

- Many space GW detection proposals need to use constant/equal arm configurations [21]. To name a few, they are AEDGE [9], AIGSO [13, 14]; DECIGO/B-DECIGO [43, 44], ELGAR [18] etc. AIGSO has 10 km arm length, the shortest arm length among these mission proposals. In [21], we calculated that the actuation acceleration needed to maintain such orbits for AIGSO is around 10 pm s^{-2} .
- In the mission of LISA Pathfinder, different levels of force and torque authority were implemented, from the nominal configuration with x-force authority (on the sensitive line-of-sight axis) of 1100 pm s^{-2} to the URLA configuration levels, with x-force authority of 26 pm s^{-2} [45]. The published LPF differential acceleration noise floor is established by measurements in this configuration. Specifically, LISA Pathfinder demonstrated that when a constant out of the loop force with amplitude of 11.2 pN was applied to the sensitive axis of TM1 (Test Mass 1) for reducing the gravitational imbalance between the TMs, this force does not introduce significant noise or calibration errors [45]. Basically the accelerometer part of the constant-arm technology is already demonstrated by LISA Pathfinder for AIGSO in effect.
- B-DECIGO has a nominal arm length of 100 km, DECIGO 1,000 km, and AMIGO 10,000 km. The actuation accelerations needed are respectively 10, 100, and 1000 times more than AIGSO. While the actuation accelerations needed for constant arm implementation of b-DECIGO and DECIGO is still basically in the LISA Pathfinder nominal configuration range, the actuation accelerations for constant arm AMIGO is one order larger. On what noise level could the actuation accelerations be done needs to be studied and demonstrated carefully for AMIGO. A suggestion is to use an additional test mass (i.e. a pair) to alternate with the original one [7].

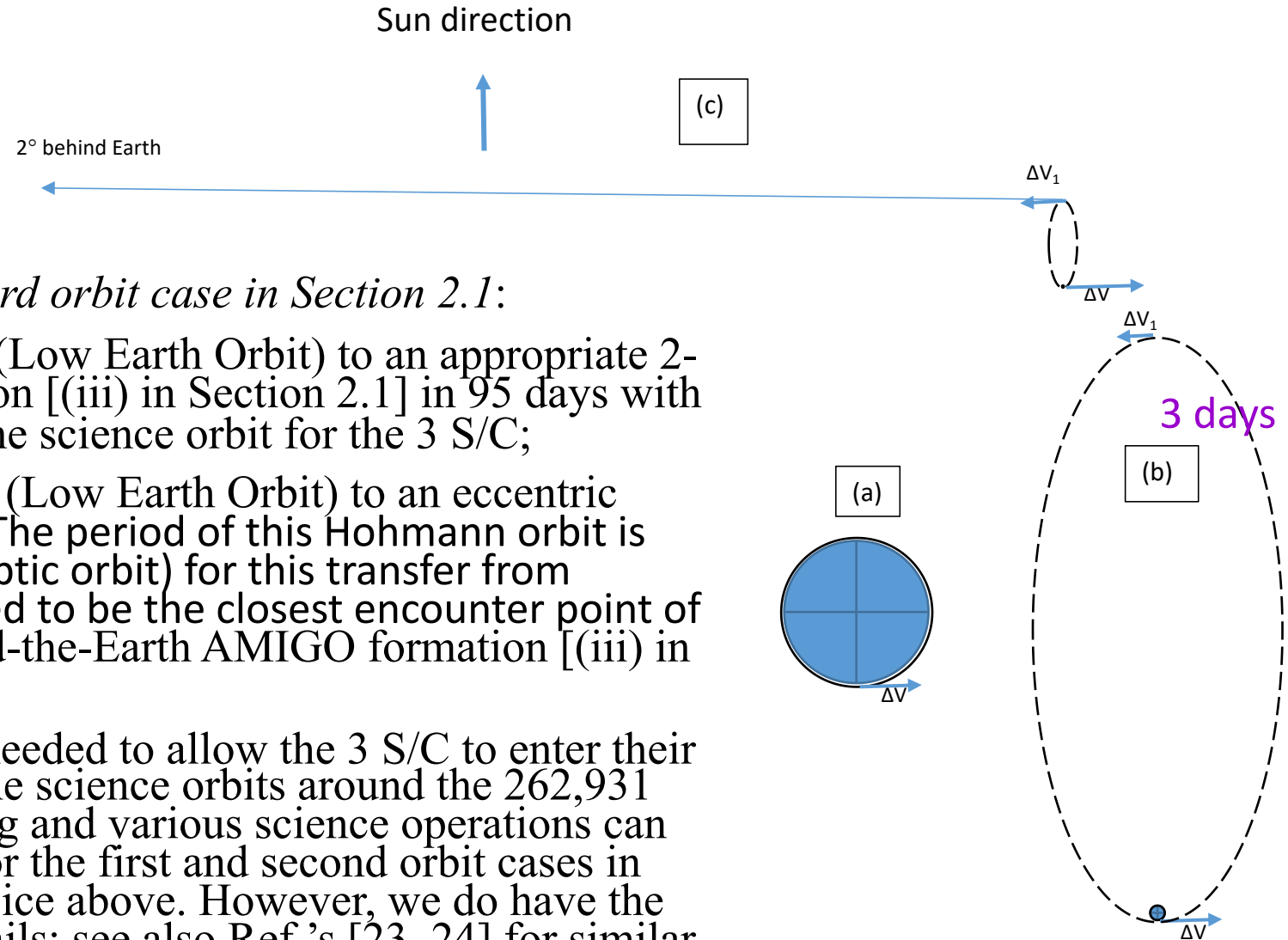
- There will be two pathfinder technology demonstration missions with 2 spacecraft/satellites planned in the near future (~ 2025): Taiji-2 and Tianqin-2. Constant arm space interferometry mode could be tested in some stages of the missions (together with the geodetic mode) if adopted.

AMIGO-5

- One aim of the mid-frequency GW space missions is to bridge the sensitivity gap between the current/planned Earth-based GW detectors and the mHz space GW detectors under implementation. The optimal arm length would be dependent on the projected sensitivities and the technology that could be achieved at the time of manufacture. So is for AMIGO. In our previous work, we have mentioned that 1×10^7 m or a few times of this. In the following, we illustrate the noise requirement by a **50,000 km AMIGO termed AMIGO-5**:
- For the acceleration noise requirement, we set
- $S_a^{1/2}(f) \leq 3 \times 10^{-15} [1 + (f/0.3 \text{ Hz})^4]^{1/2} \text{ m s}^{-2} \text{ Hz}^{-1/2}$, ($10 \text{ Hz} > f > 10 \text{ mHz}$), (5)
- same as AMIGO before.
- For laser metrology noise, we set:
- Baseline (b-AMIGO-5): $S_{\text{AMIGOp}}^{1/2} \leq 60 \text{ fm Hz}^{-1/2}$ ($10 \text{ Hz} > f > 10 \text{ mHz}$), (7)'
- Design Goal (AMIGO-5): $S_{\text{AMIGOp}}^{1/2} \leq 19 \text{ fm Hz}^{-1/2}$ ($10 \text{ Hz} > f > 10 \text{ mHz}$), (8)'
- Enhanced Goal (e-AMIGO-5): $S_{\text{AMIGOp}}^{1/2} \leq 2.5 \text{ fm Hz}^{-1/2}$ ($10 \text{ Hz} > f > 10 \text{ mHz}$). (9)'
- The sensitivity curves in the strain power spectral density amplitude vs. frequency plot for AMIGOs of different arm lengths would just have their flat bottoms shifted to the left in frequency in proportional to the ratio of arm lengths. In our considered frequency range of 10 mHz-10 Hz, the astrophysical confusion limit of LISA/TAIJI/TIANQIN does not play a role.

Deployment

- There are two desirable options for the *third orbit case in Section 2.1*:
 - (i) A last-stage launch from 300 km LEO (Low Earth Orbit) to an appropriate 2-degree-behind-the-Earth AMIGO formation [(iii) in Section 2.1] in 95 days with a Δv of about 80 m/s in the end to reach the science orbit for the 3 S/C;
 - (ii) A last-stage launch from 300 km LEO (Low Earth Orbit) to an eccentric Hohmann orbit with apogee 262931 km (The period of this Hohmann orbit is about 6 days.). It takes 3 days (half an elliptic orbit) for this transfer from perigee to apogee. This apogee is designed to be the closest encounter point of the center of mass of the 2-degree-behind-the-Earth AMIGO formation [(iii) in Section 2.1].
- From here, a Δv 's of about 1.6 km/s are needed to allow the 3 S/C to enter their respective science orbits. After entering the science orbits around the 262,931 km apogee, the calibration, commissioning and various science operations can be started [7, 22]. As to the deployment for the first and second orbit cases in Section 2.1, we don't have the second choice above. However, we do have the first choice. Ref. [22] will present the details; see also Ref.'s [23, 24] for similar deployments in the cases for LISA and ASTROD-GW.



Deployment
in a week

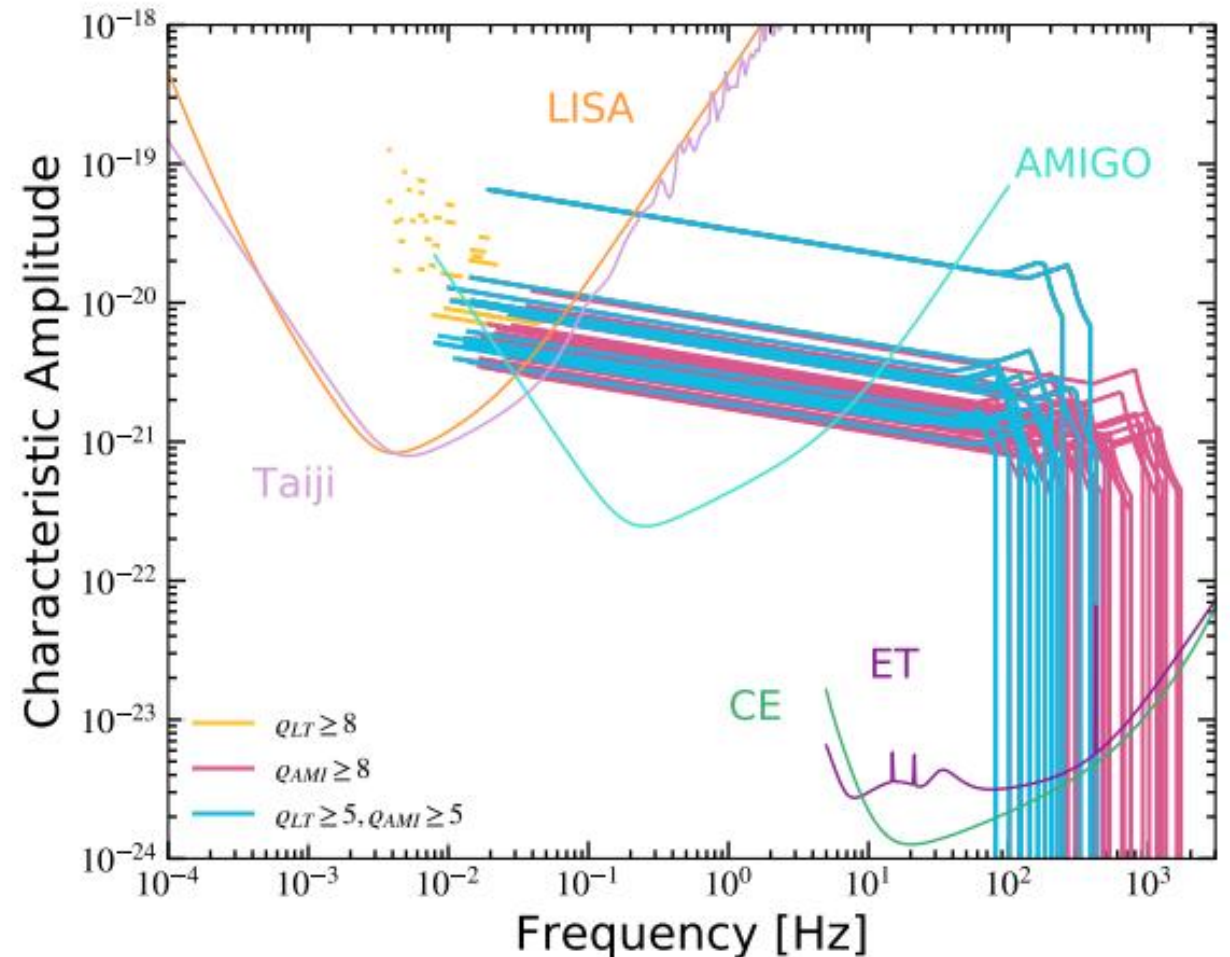
Outlook and Opportunities

- Taiji-1 [46] and Tianqin-1 [47, 48] have achieved their pathfinder demonstration goals in 2019. After the Taiji-2 and Tianqin-2 pathfinder demonstrations in ~2025 and before the mHz space GW mission launches in 2034, if needed or desired, there could possibly be another pathfinder demonstration or a mid-frequency space GW mission call. Then AMIGO might be a candidate choice for the mission concepts.
-
- The AMIGO-S-8-12deg orbits for 600 days could be an earlier geodetic GW mission option with the orbits worked out starting at a suitable epoch. If a 10-year geodetic mission is desired, it has to go to about 20° behind/leading the Earth orbit. The AMIGO-S-2-6deg orbits for 250 days and the AMIGO-S-2-4deg (for 80 days in the geodetic option; for 300 days or more for the constant equal-arm option) could be a pathfinder mission with one arm (two S/C); they are closer to Earth and takes less days (less than a week to reach the technological demo orbit) and less power for deployments [22].

GWTC-3 model (observationally constrained model from LVK collaboration) and EMBS (evolution of massive binary stars) model

Evolution tracks of characteristic amplitudes for the mock BBHs which are detectable by **LT-AMIGO** (i.e., $\diamondsuit_{LT} \geq 5$ and $\diamondsuit_{AMI} \geq 5$, **blue**), by **LT** (i.e., $\diamondsuit_{LT} \geq 8$, **yellow lines**), by **AMIGO** (i.e., $\diamondsuit_{AMI} \geq 8$, **magenta lines**).

Observed for a continuous period of 4 years.



Expected number of detectable **BBH** events from different models by 4 years' observations of LISA, Taiji, **LT**, and AMIGO, and **those of multiband BBH events by joint observations of detectors in the low-frequency and middle-frequency bands.** [adapted from Zhao et al.]

GWDetector	GWTC-3 Model	lowR $\cdot\cdot$	midR $\cdot\cdot$	EMBS Model	lowR $\cdot\cdot$	midR $\cdot\cdot$	highR $\cdot\cdot$
LISA	3	9+3-4	15	3	9+3-3	16	
Taiji	5	14+4-3	24	5	15+5-4	27	
AMIGO	23	51+8-6	83	21	47+6-7	76	
LT	15	32+6-5	52	15	34+6-5	57	
LISA-AMIGO	0	3+1-2	6	1	3+2-2	7	
Taiji-AMIGO	3	10+3-4	19	3	10+3-3	19	
LT-AMIGO	6	18+4-5	32	7	18+5-4	33	

Note: first column denotes the GW detector name or different combinations of them, here 'LT' represents the LISA-Taiji network. Second column shows the 16th detectable number ranking from small to large of BBHs for GWTC-3 model with $R_{\cdot\cdot} = 10.6 \text{ Gpc}^{-3} \text{ yr}^{-1}$ labeled as low $R_{\cdot\cdot}$. Third column shows the median value and 68% confidence interval of the numbers among 100 realizations of BBHs for GWTC-3 model with $R_{\cdot\cdot} = 19.1 \text{ Gpc}^{-3} \text{ yr}^{-1}$ labeled as mid $R_{\cdot\cdot}$. Fourth column shows the 84th detectable number for GWTC-3 model with $R_{\cdot\cdot} = 27.5 \text{ Gpc}^{-3} \text{ yr}^{-1}$ labeled as high $R_{\cdot\cdot}$. The fifth to seventh columns show the corresponding results for the EMBS model, respectively.

Y. Zhao, Y. Lu, C. Yan, Z. Chen and W.-T. Ni, **Multiband** Gravitational Wave Observations of Stellar Binary Black Holes **at the Low to Middle and High Frequencies**, MNRAS, 522, 2951-2966 (2023).

Table 3. Median values and 68% confidence intervals of the distributions of parameter estimation uncertainties for multiband BBHs

GW Detector	low	$\Delta\Omega_{90\%}$ median	high	low	σ_{d_L}/d_L median	high	low	σ_{M_c}/M_c median	high	low	σ_{η} median	high
LT	1.6×10^{-1}	1.6×10^0	1.6×10^1	1.6×10^{-2}	1.6×10^{-1}	1.6×10^0	4.8×10^{-7}	4.7×10^{-6}	4.7×10^{-5}	7.9×10^{-4}	7.8×10^{-3}	7.7×10^{-2}
AMIGO	2.3×10^0	2.2×10^1	2.2×10^2	1.1×10^{-2}	1.1×10^{-1}	1.0×10^0	6.4×10^{-8}	6.4×10^{-7}	6.3×10^{-6}	6.8×10^{-5}	6.7×10^{-4}	6.6×10^{-3}
ET-CE	9.0×10^{-3}	8.9×10^{-2}	8.8×10^{-1}	2.6×10^{-4}	2.5×10^{-3}	2.5×10^{-2}	7.2×10^{-5}	7.1×10^{-4}	7.0×10^{-3}	1.8×10^{-4}	1.8×10^{-3}	1.7×10^{-2}
LT-AMIGO	1.1×10^{-1}	1.1×10^0	1.1×10^1	8.3×10^{-3}	8.2×10^{-2}	8.1×10^{-1}	2.2×10^{-8}	2.2×10^{-7}	2.1×10^{-6}	4.2×10^{-5}	4.2×10^{-4}	4.1×10^{-3}
LT-ET-CE	7.3×10^{-3}	7.2×10^{-2}	7.1×10^{-1}	1.9×10^{-4}	1.9×10^{-3}	1.8×10^{-2}	6.1×10^{-9}	6.0×10^{-8}	5.9×10^{-7}	1.9×10^{-5}	1.9×10^{-4}	1.8×10^{-3}
AMIGO-ET-CE	3.5×10^{-4}	3.5×10^{-3}	3.5×10^{-2}	1.7×10^{-4}	1.7×10^{-3}	1.6×10^{-2}	3.4×10^{-8}	3.4×10^{-7}	3.4×10^{-6}	1.1×10^{-5}	1.1×10^{-4}	1.1×10^{-3}
LT-AMIGO-ET-CE	3.3×10^{-4}	3.3×10^{-3}	3.2×10^{-2}	1.6×10^{-4}	1.6×10^{-3}	1.6×10^{-2}	4.2×10^{-9}	4.2×10^{-8}	4.1×10^{-7}	8.8×10^{-6}	8.7×10^{-5}	8.6×10^{-4}

Note: first column denotes the GW detector name or different combinations of them. Second, fourth and third columns show the low and high values of 68% confidence interval and the median value of the distribution of $\Delta\Omega_{90\%}$ among 100 realizations of multiband BBHs. The fifth to seventh columns, the eighth to tenth columns and the last three columns show the corresponding results for the σ_{d_L}/d_L distribution, the σ_{M_c}/M_c distribution, and the σ_{η} distribution, respectively.

OUTLOOK

- 2030-2050 will be the golden decades for space GW detection
- LISA-like missions will be launched
- Both first-generation middle-frequency and μHz space GW mission will be implemented
- It is a great decade to do multi-messenger astro cosmology
- An Example for future direction:
Cosmology to 0.1 % or below

